

1990

The Imidization of PMR-15 Aromatic Thermosetting Polyimide

Thomas Clifton Prettyman
College of William & Mary - Arts & Sciences

Follow this and additional works at: <https://scholarworks.wm.edu/etd>



Part of the [Materials Science and Engineering Commons](#), and the [Polymer Chemistry Commons](#)

Recommended Citation

Prettyman, Thomas Clifton, "The Imidization of PMR-15 Aromatic Thermosetting Polyimide" (1990). *Dissertations, Theses, and Masters Projects*. Paper 1539625591.
<https://dx.doi.org/doi:10.21220/s2-mrty-0r41>

This Thesis is brought to you for free and open access by the Theses, Dissertations, & Master Projects at W&M ScholarWorks. It has been accepted for inclusion in Dissertations, Theses, and Masters Projects by an authorized administrator of W&M ScholarWorks. For more information, please contact scholarworks@wm.edu.

THE IMIDIZATION OF PMR-15 AROMATIC
THERMOSETTING POLYIMIDE

A Thesis

Presented to

The Faculty of the Department of Chemistry
The College of William and Mary in Virginia

In Partial Fulfillment
Of the Requirements for the Degree of
Master of Arts

by

Thomas Prettyman

1990

APPROVAL SHEET

This thesis is submitted in partial fulfillment of the
requirements for the degree of

MASTER OF ARTS

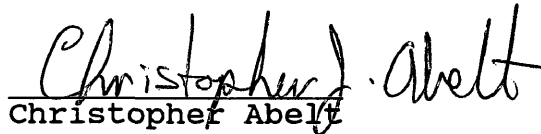


Thomas Clifton Prettyman

Approved, October 1990



David Kranbuehl



Christopher Abelt



Stephen Hudson

TABLE OF CONTENTS

	Page
LIST OF FIGURES.....	iv
LIST OF TABLES.....	viii
ABSTRACT.....	ix
PART 1. THE IMIDIZATION OF PMR-15 AROMATIC THERMOSETTING POLYIMIDE.....	1
CHAPTER I. AN INTRODUCTION TO PMR-15.....	2
CHAPTER II. ¹³ C-NMR STUDIES OF PMR-15 MONOMERS AND THEIR REACTIONS.....	10
CHAPTER III. KINETIC STUDIES OF PMR-15 BY THERMOGRAVIMETRIC ANALYSIS.....	36
CHAPTER IV. A COMPUTERIZED KINETIC MODEL OF THE PMR-15 IMIDIZATION REACTION.....	62
PART 2. RHEOLOGICAL STUDY OF THE RELATIONSHIP BETWEEN THE GLASS TRANSITION TEMPERATURE AND DEGREE OF CURE IN TWO EPOXY RESIN SYSTEMS.....	83

LIST OF FIGURES

Figure		Page
1.1	PMR-15 MONOMERS.....	2
1.2	PMR-15 POLYIMIDE PREPOLYMER FORMATION.....	3
1.3	REVERSE DIELS-ALDER CROSSLINKING OF NORBORNYL ENDGROUPS.....	4
1.4	DSC SCAN BY LAUVER OF PMR-15 REACTION.....	4
1.5	PMR-15 IMIDIZATION SCHEME I.....	5
1.6	PMR-15 IMIDIZATION SCHEME II.....	6
1.7	PMR-15 IMIDIZATION SCHEME III.....	7
2.1	¹³ C-NMR OF MDA.....	17
2.2	¹³ C-NMR OF NE.....	18
2.3	¹³ C-NMR OF NA.....	19
2.4	¹³ C-NMR OF NDA.....	20
2.5	¹³ C-NMR OF NDE.....	21
2.6	¹³ C-NMR OF BTDE.....	22
2.7	¹³ C-NMR OF BTDA.....	23
2.8	¹³ C-NMR OF BTTA.....	24
2.9	¹³ C-NMR OF BTTE.....	25
2.10	¹³ C-NMR OF PMR-15.....	26
2.11	¹³ C-NMR OF UNREACTED 2:1 NE/MDA.....	27
2.12	¹³ C-NMR OF 2:1 NE/MDA AFTER 10 MINUTES AT 100°C.....	28
2.13	¹³ C-NMR OF 2:1 NE/MDA AFTER 20 MINUTES AT 100°C.....	29
2.14	¹³ C-NMR OF 2:1 NE/MDA AFTER 60 MINUTES AT 100°C.....	30
2.15	¹³ C-NMR OF 2:1 NE/MDA AFTER 120 MINUTES AT 100°C.....	31
2.16	¹³ C-NMR OF 1:1 BTDE/MDA AFTER 10 MINUTES AT 120°C.....	32
2.17	¹³ C-NMR OF 1:1 BTDE/MDA AFTER 20 MINUTES AT 120°C.....	33
2.18	¹³ C-NMR OF 1:1 BTDE/MDA AFTER 45 MINUTES AT 120°C.....	34
3.1	FORMATION OF BISNADIMIDE FROM NE AND MDA....	37
3.2	2:1 NE/MDA: ALPHA VS. TIME.....	45
3.3	1:1 BTDE/MDA: ALPHA VS. TIME.....	45
3.4	ALPHA VS. TIME FOR NE/MDA, BTDE/MDA, AND PMR-15 AT 80°C.....	46

FIGURE		Page
3.5	ALPHA VS. TIME FOR NE/MDA, BTDE/MDA, AND PMR-15 AT 120°C.....	46
3.6	ALPHA VS. TIME FOR NE/MDA, BTDE/MDA, AND PMR-15 AT 160°C.....	47
3.7	NE/MDA REACTION ORDER DETERMINATION AT 80°C (#1).....	47
3.8	NE/MDA REACTION ORDER DETERMINATION AT 80°C (#2).....	48
3.9	NE/MDA REACTION ORDER DETERMINATION AT 120°C.....	48
3.10	NE/MDA REACTION ORDER DETERMINATION AT 140°C.....	49
3.11	NE/MDA REACTION ORDER DETERMINATION AT 160°C (#1).....	49
3.12	NE/MDA REACTION ORDER DETERMINATION AT 160°C (#2).....	50
3.13	BTDE/MDA REACTION ORDER DETERMINATION AT 80°C.....	50
3.14	BTDE/MDA REACTION ORDER DETERMINATION AT 105°C (#1).....	51
3.15	BTDE/MDA REACTION ORDER DETERMINATION AT 105°C (#2).....	51
3.16	BTDE/MDA REACTION ORDER DETERMINATION AT 120°C.....	52
3.17	BTDE/MDA REACTION ORDER DETERMINATION AT 140°C.....	52
3.18	BTDE/MDA REACTION ORDER DETERMINATION AT 160°C.....	53
3.19	NE/MDA AT 80°C (#1): 3rd ORDER RATE CONSTANT	53
3.20	NE/MDA AT 80°C (#2): 3rd ORDER RATE CONSTANT	54
3.21	NE/MDA AT 120°C: 3rd ORDER RATE CONSTANT....	54
3.22	NE/MDA AT 140°C: 3rd ORDER RATE CONSTANT....	55
3.23	NE/MDA AT 160°C (#1): 3rd ORDER RATE CONSTANT.....	55
3.24	NE/MDA AT 160°C (#2): 3rd ORDER RATE CONSTANT.....	56
3.25	BTDE/MDA AT 80°C: 3rd ORDER RATE CONSTANT...	56
3.26	BTDE/MDA AT 105°C (#1): 3rd ORDER RATE CONSTANT.....	57
3.27	BTDE/MDA AT 105°C (#2): 3rd ORDER RATE CONSTANT.....	57
3.28	BTDE/MDA AT 120°C: 3rd ORDER RATE CONSTANT..	58
3.29	BTDE/MDA AT 140°C: 3rd ORDER RATE CONSTANT..	58
3.30	BTDE/MDA AT 160°C: 3rd ORDER RATE CONSTANT..	59
3.31	2:1 NE/MDA: ln k VS. 1/RT.....	59
3.32	1:1 BTDE/MDA: ln k VS. 1/RT.....	60

Figure		Page
4.1	PMR-15 IMIDIZATION SIMULATION AT 80°C: CHAIN DISTRIBUTION VS. TIME.....	74
4.2	PMR-15 IMIDIZATION SIMULATION AT 120°C: CHAIN DISTRIBUTION VS. TIME.....	74
4.3	PMR-15 IMIDIZATION SIMULATION AT 160°C: CHAIN DISTRIBUTION VS. TIME.....	75
4.4	PMR-15 IMIDIZATION SIMULATION AT 200°C: CHAIN DISTRIBUTION VS. TIME.....	75
4.5	PMR-15 IMIDIZATION SIMULATION AT 80°C: CHAIN CONCENTRATION VS. TIME.....	76
4.6	PMR-15 IMIDIZATION SIMULATION AT 120°C: CHAIN CONCENTRATION VS. TIME.....	76
4.7	PMR-15 IMIDIZATION SIMULATION AT 160°C: CHAIN CONCENTRATION VS. TIME.....	77
4.8	PMR-15 IMIDIZATION SIMULATION AT 200°C: CHAIN CONCENTRATION VS. TIME.....	77
4.9	PMR-15 CHAIN DISTRIBUTION VS. ALPHA: k (NE/MDA)=2*k (BTDE/MDA).....	78
4.10	PMR-15 CHAIN DISTRIBUTION VS. ALPHA: k (NE/MDA)=k (BTDE/MDA).....	78
4.11	PMR-15 CHAIN DISTRIBUTION VS. ALPHA: 2*k (NE/MDA)=k (BTDE/MDA).....	79
4.12	PMR-15 CHAIN CONCENTRATION VS. ALPHA: k (NE/MDA)=2*k (BTDE/MDA).....	79
4.13	PMR-15 CHAIN CONCENTRATION VS. ALPHA: k (NE/MDA)=k (BTDE/MDA).....	80
4.14	PMR-15 CHAIN CONCENTRATION VS. ALPHA: 2*k (NE/MDA)=k (BTDE/MDA).....	80
4.15	PMR-15 AVERAGE IMIDIZATION VS. ALPHA FOR THE THREE CASES.....	81
5.1	DOW AT $\alpha = .5$ / VISCOSITY VS. TIME.....	88
5.2	DOW AT $\alpha = .6$ / VISCOSITY VS. TIME.....	88
5.3	DOW AT $\alpha = .7$ / VISCOSITY VS. TIME.....	89
5.4	DOW AT $\alpha = .8$ / VISCOSITY VS. TIME.....	89
5.5	DOW AT $\alpha = .9$ / VISCOSITY VS. TIME.....	90
5.6	DOW AT $\alpha = 1$ / VISCOSITY VS. TIME.....	90
5.7	SHELL AT $\alpha = .3$ / VISCOSITY VS. TIME.....	91
5.8	SHELL AT $\alpha = .4$ / VISCOSITY VS. TIME.....	91
5.9	SHELL AT $\alpha = .5$ / VISCOSITY VS. TIME.....	92
5.10	SHELL AT $\alpha = .6$ / VISCOSITY VS. TIME.....	92
5.11	SHELL AT $\alpha = .7$ / VISCOSITY VS. TIME.....	93
5.12	SHELL AT $\alpha = .8$ / VISCOSITY VS. TIME.....	93
5.13	SHELL AT $\alpha = .9$ / VISCOSITY VS. TIME.....	94
5.14	SHELL AT $\alpha = 1$ / VISCOSITY VS. TIME.....	94
5.15	DOW AT $\alpha = 0$ / ϵ' VS. TIME.....	95
5.16	SHELL AT $\alpha = 0$ / ϵ' VS. TIME.....	95

Figure		Page
5.17	DOW: T_g VS. ALPHA.....	96
5.18	SHELL: T_g VS. ALPHA.....	96

LIST OF TABLES

Table		Page
2a	MDA ¹³ C-NMR SPECTRUM.....	11
2b	NE ¹³ C-NMR SPECTRUM.....	11
2c	BTDE ¹³ C-NMR SPECTRUM.....	12
2d	CARBONYL CARBON ASSIGNMENTS FOR NA AND DERIVATIVES.....	13
2e	CARBONYL CARBON ASSIGNMENTS FOR BTDA AND DERIVATIVES.....	13
2f	2:1 NE/MDA CARBONYL CARBONS AT 100°C.....	15
3a	2:1 NE/MDA WEIGHT LOSS RESULTS.....	39
3b	1:1 BTDE/MDA WEIGHT LOSS RESULTS.....	39
3c	2:1 NE/MDA REACTION ORDERS.....	40
3d	1:1 BTDE/MDA REACTION ORDERS.....	40
3e	2:1 NE/MDA RATE CONSTANTS.....	43
3f	1:1 BTDE/MDA RATE CONSTANTS.....	43
3g	ARRHENNIUS PARAMETERS FOR THE TWO SYSTEMS...	44
4a	CHAIN CONCENTRATIONS FOR PMR-15 AT ALPHA=.98.....	68
5a	DOW 138/H41: MEASURED T _g 'S.....	86
5b	SHELL 1282/9470: MEASURED T _g 'S.....	86
5c	EMPIRICALLY DETERMINED DiBENEDETTO PARAMETERS.....	87

ABSTRACT

PMR-15 aromatic thermosetting polyimide is a widely used matrix resin for advanced composites. Though there exists a large database of its mechanical and physical properties, the chemistry of the reacting PMR-15 system is not well understood. This study is concerned with the mechanism and kinetics of the PMR-15 imidization reaction.

^{13}C -NMR and FTIR studies have led to the proposal of various imidization mechanisms. Principal among those are schemes which involve an amide or an anhydride intermediate. In this study ^{13}C -NMR spectra of reacting PMR-15 monomers showed no intermediates, and it was concluded that no stable intermediate is formed.

Thermogravimetric Analysis (TGA) has been performed on PMR-15, and rate constants and activation energies calculated. The following study used TGA to determine kinetic parameters for the two separate imidization reactions taking place in the system. The reactions were found to be third order or greater and third order rate constants were calculated. Contrary to earlier reports, the overall 1:1 BTDE/MDA reaction was found to be faster than the NE/MDA reaction at temperatures lower than 120°C .

To monitor polymer chain growth in the PMR-15 system, a computerized model was devised using the rate constants previously determined. Examination of the resultant chain distributions versus degree of reaction showed chain length and type to be dependent on the ratio of rates of the two reactions and therefore dependent on the cure temperature.

A separate section of this thesis presents a method of measuring the glass transition temperature (T_g) of epoxy resin systems. Rheology, in combination with Dynamic Dielectric Analysis, proved to be a simple and reliable method of relating T_g to degree of cure for two epoxy resin systems.

THE IMIDIZATION OF PMR-15 AROMATIC
THERMOSETTING POLYIMIDE

PART 1

CHAPTER I

AN INTRODUCTION TO PMR-15

The aromatic polyimide thermosetting resin PMR-15 (for "polymerization of monomer reactants" - formulated molecular weight 1500) is a frontrunner in the search for high temperature matrix resins for advanced composites. Epoxies used for aerospace applications are typically limited to use temperatures below 175°C, while graphite reinforced PMR-15 parts have been shown to be stable to 316°C. However, the difficulties in processing polyimide composites have limited their applications.¹

PMR-15 resin is composed of three monomer reactants: the dimethyl ester of 3,3',4,4'-benzophenone tetracarboxylic anhydride (BTDE), 4,4'-methylene dianiline (MDA), and the monomethyl ester of 5-norbornene-2,3-dicarboxylic anhydride (NE) (Figure 1.1). The molar ratios of the reactants, respectively, are n:(n+1):2, where n = 2.087.¹

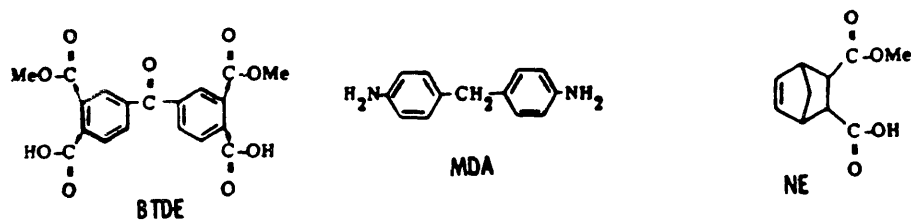


Figure 1.1. PMR-15 monomers.

The monomers are usually mixed in a 50/50 wt.% alkyl alcohol solution. The fibers are impregnated with resin and the low-boiling solvent driven off at low temperatures before reaction. There are two reaction stages. The first is the formation of the polyimide prepolymer at temperatures between room temperature and 200°C (Figure 1.2). The second is the crosslinking of the norbornyl endgroups at temperatures above 200°C through a reverse Diels-Alder reaction (Figure 1.3).^{1,2}

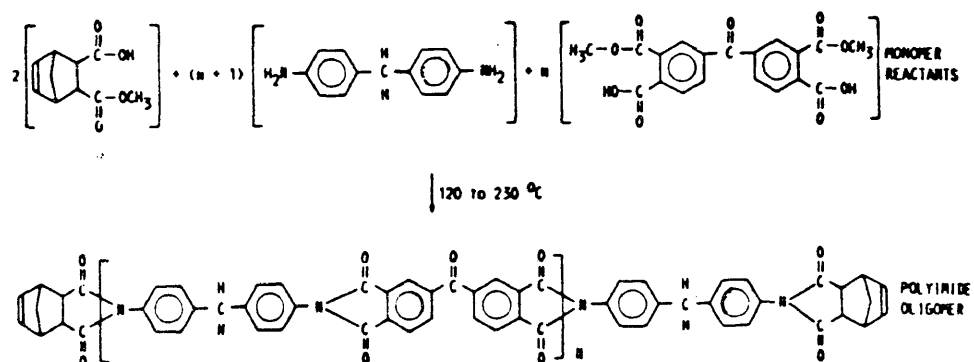


Figure 1.2. PMR-15 polyimide prepolymer formation.

Difficulties in processing arise in the first stage because the reaction involves the evolution of methanol and water. These volatiles create voids in composite parts which

can affect part performance.

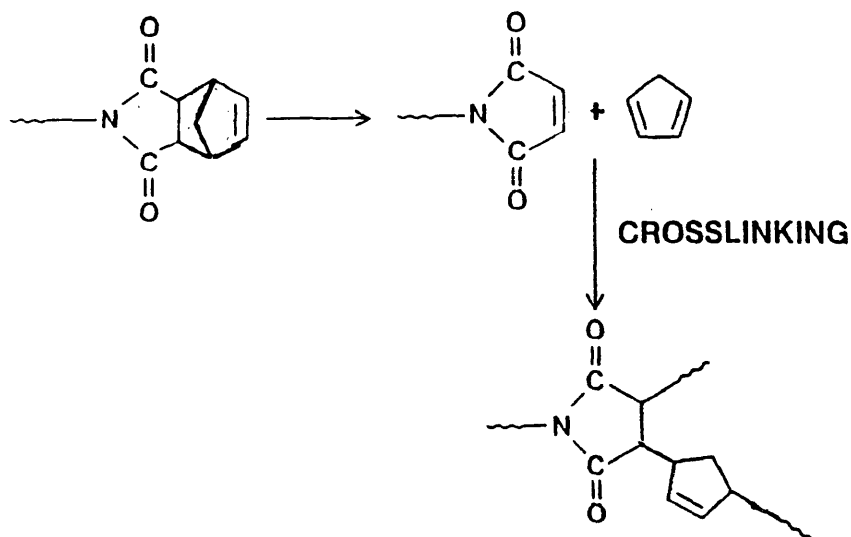


Figure 1.3. Reverse Diels-Alder crosslinking of norbornyl endgroups.

Differential Scanning Calorimetry by Lauver of the overall cure reaction of PMR-15 showed four thermal events (Figure 1.4), which Lauver explained as follows:³

- 1.) The endotherm below 100 C occurs due to monomer association in the melt phase.
- 2.) A second endotherm, centered around 140°C, is due to loss of volatiles during imidization.

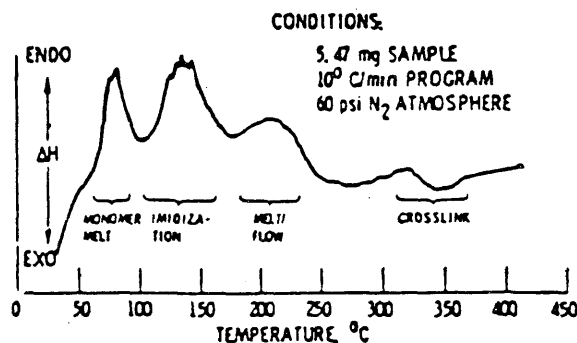


Figure 1.4. DSC scan by Lauver of PMR-15 reaction.

- 3.) The third endotherm is due to the melt and flow of the

polyimide prepolymer.

4.) The exotherm occurring above 300 C is attributable to the crosslinking reaction of the norbornyl end groups³. The crosslinking reaction will not be discussed in this study.

POSSIBLE MECHANISMS OF IMIDIZATION

The first attempts to explain the imidization of PMR-15 suggested two steps: 1) formation of the polyamic acid, and 2) cyclodehydration to the polyimide.

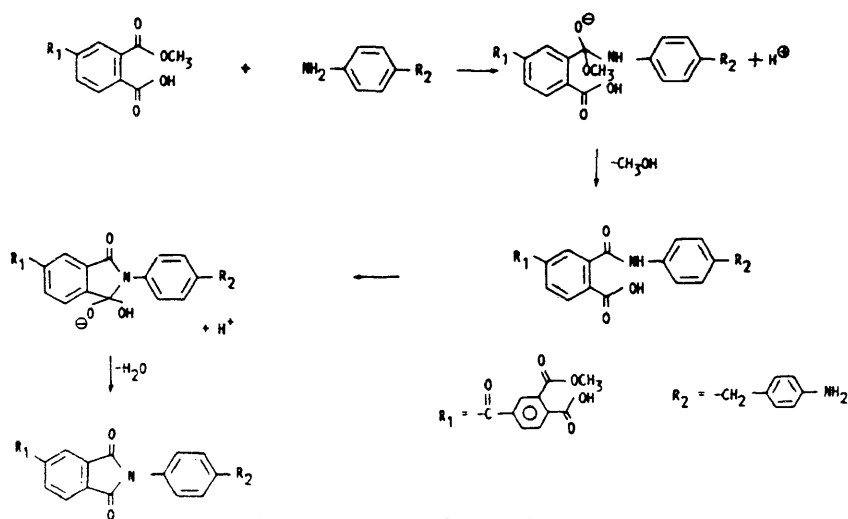


Figure 1.5. PMR-15 reaction scheme I.

Infrared spectroscopic studies on PMR-15 and related compounds suggested such a mechanism (Scheme I).⁴ Separate sets of absorption bands for amide and imide were reported, and by monitoring the intensity of these bands versus temperature it was concluded that Scheme I was the actual mechanism. Thus the ester would undergo nucleophilic attack by

the amine to displace methanol and form amide-acid. Also present were peaks which were attributed to cyclic anhydride formation. This anhydride was formed by reversion of the amic acid in the presence of free amine, which forms a salt with the acid. Disappearance of the anhydride at higher temperature was attributed to the lower probability of salt formation at those temperatures.

Later ^{13}C -NMR studies showed amic acid always accompanied by imide⁵. This is contrary to what would be expected with Scheme I, which should result in an initial appearance of amic acid peaks followed by their disappearance and the appearance of imide peaks. This discrepancy suggests that the amide is only a transient intermediate in imide formation and not a distinct isolable species and supports a mechanism of complete imidization in one step (Scheme II).

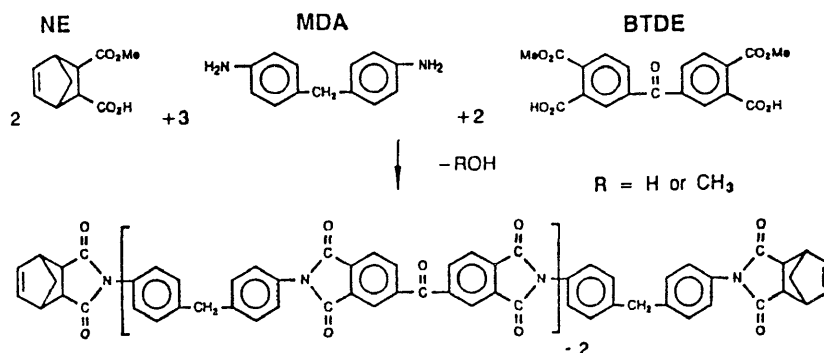


Figure 1.6. PMR-15 imidization scheme II.

Numerous carbon-13 NMR and FTIR studies have reported the presence of anhydride throughout the reaction.^{4,5,6} Initially this was explained as a competing side-reaction as in

Scheme I, but recently anhydride formation has been described as a distinct step in imidization (Scheme III): 1) the amine and acid form a salt, 2) the acid-ester salt reacts to yield cyclic anhydride and methanol, and 3) the anhydride reacts rapidly with the amine to form amic-acid.^{6,7} At the reaction temperatures used, the amic acid converts to imide at sufficiently high rate that anhydride formation is the rate-limiting step.

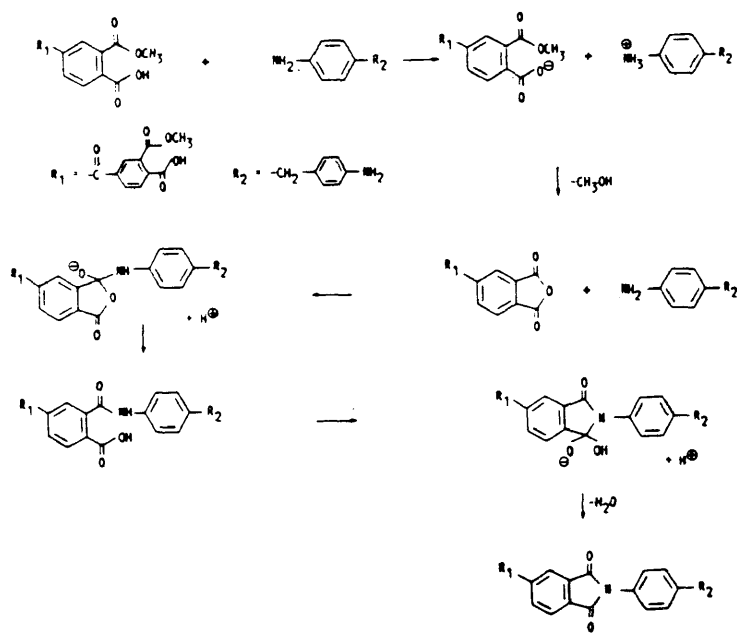


Figure 1.7. PMR-15 imidization scheme III.

Young and Chang reported a different scheme for anhydride formation through their FTIR work with LARC-160, a polyimide in the PMR family closely related to PMR-15 in molecular structure. Their study showed that after an initial buildup of polyamic acid, a large anhydride band appeared in the temperature range of 50-280°C with a maximum intensity at

about 180°C). They proposed that after initial formation of high molecular weight polyamic acid, the chains are cleaved at various points by degradation of some of the amide linkages to anhydride. Then upon further heating, final reaction occurs to the ultimate molecular weight of the polymer, coinciding with the disappearance of the FTIR anhydride band (Scheme IV).⁸

NOTES FOR CHAPTER I

1. T. Serafini, "PMR-15 Polyimide Composites for Aerospace Applications", in: Mittal, K.L. (Ed.), Polyimides, New York: Plenum Press, 1984; Vol. 2, pp. 957-975.
2. R. Clark, Master's Thesis. College of William and Mary, 1989.
3. R.W. Lauver, J. Polymer Sci. Polymer Chem. Ed., 17, 2529 (1979).
4. P.J. Dynes, R.M. Panos, and C.L. Hammermesh, J. Appl. Polymer Sci., 25, 1059 (1980).
5. S.E. Delos, R.K. Schellenberg, J.E. Smedley, and D.E. Kranbuehl, J. Appl. Polymer Sci., 27, 4295 (1982).
6. J.C. Johnston, M.A. Meador, and W.B Alston, J. Polymer Sci. Polymer Chem. Ed., 25, 2175 (1987).
7. D. Garcia, and T.T. Serafini, J. Polymer Sci. Polymer Phys. Ed., 25, 2275 (1987).
8. P.R. Young and A.C. Chang in 30th National SAMPE Symp., 30, 889 (1985).

CHAPTER II

¹³C-NMR STUDIES OF PMR-15 MONOMERS AND THEIR REACTIONS

Many researchers have reported the presence of anhydride during PMR-15 imidization. Johnston et al reported anhydride as a precursor to amide through FTIR studies on BTDE/MDA and analogous model compounds.¹ Garcia and Serafini made similar conclusions.² ¹³C-NMR studies at BP Research were inconclusive in regards to anhydride formation, but did report the presence of amide.³ This section describes a ¹³C-NMR study undertaken to shed further light on the PMR-15 imidization mechanism and to identify any amide or anhydride intermediates.

All measurements were made with a General Electric QE-300 NMR Spectrometer. DMSO-d₆ was the solvent. Spectra were taken on MDA; the acid/ester, anhydride, diacid, and diester forms of NA; the diacid/diester, anhydride, tetraacid, and tetraester forms of BTDA; and PMR-15. Thus we hoped to be able to accurately determine the identity of peaks in the PMR-15 spectrum. Figures 2.1 through 2.10 show these spectra.

Our peak assignments for the three PMR-15 monomers are listed in Tables 2a-c. The final entry for each peak gives the chemical shift reported by BP Research for the corresponding

Table 2a
MDA ^{13}C -NMR SPECTRUM

<u>peak no.</u>	<u>δ (ppm)</u>	<u>assignment</u>	<u>BP Research³</u>
1	114.16	C ₃ , C ₅	115.09
2	129.08 129.66	C ₂ , C ₆	129.13 129.21
3	146.39		*

* BP has no corresponding peak here.

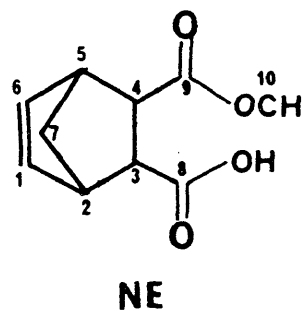
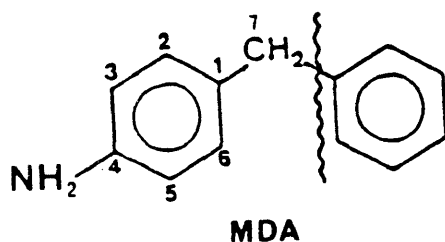


Table 2b
NE ^{13}C -NMR SPECTRUM

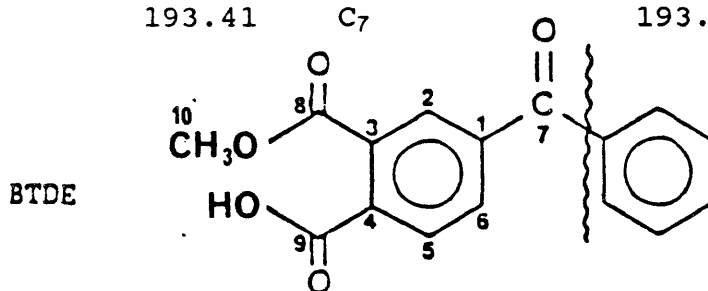
<u>peak no.</u>	<u>δ (ppm)</u>	<u>assignment</u>	<u>BP Research³</u>
1	45.88 46.08	C ₂ , C ₅ **	45.38
2	47.76 48.18	C ₃ , C ₄ **	44.85
3	52.59	C ₇	51.78
4	134.27 135.31	C ₁ , C ₆	134.53
5	172.62	C ₉ (ester)	***
6	173.26	C ₈ (acid)	***

** Our assignments for peaks 1 and 2 are tentative and may be opposite.

***BP assigns a single peak at 176.86 to NE C₈ and C₉. Another at 173.80 is assigned to reacted NE/MDA amide carbonyl.

Table 2c
BTDE ^{13}C -NMR SPECTRUM

<u>peak no.</u>	<u>δ (ppm)</u>	<u>assignment</u>	<u>BP Research³</u>
1	48.82 52.85	C ₁₀	52.85
2	128.1 129.87 132.35 132.45 137.48 138.03	aromatic carbons C ₁₋₆	123.94 (C _{2, C₅}) 131.93 (C ₄) 134.83 (C ₆) 135.87 (C ₃) 141.65 (C ₁)
3	167.11 167.18 167.73 167.92 167.96 168.65	C _{8, C₉}	166.40
5	193.41	C ₇	193.50



carbon.³ (BP Research's assignments were made on reacted PMR-15, as opposed to isolated monomers.)

It is interesting to note that, though there are 5 kinds of carbons in MDA (C₁, C_{2/C₆}, C_{3/C₅}, C₇, and C₄), only 3 separate peaks appear in the MDA spectrum (Table 2a).

There are three possible configurations of the BTDE acid/esters; these would lead to eight possible types of carbonyl carbons. Figure 2.6 shows only six carbonyl carbon peaks.

Tables 2d and 2e list our carbonyl assignments for the NA

and the BTDA for their respective acid/ester, anhydride, all-acid, and all-ester adducts.

Though the two carbonyl carbons of a BTDA anhydride group are of different types, only one peak for those carbons appears in Figure 2.7.

Table 2d
CARBONYL ASSIGNMENTS FOR NA AND DERIVATIVES

<u>acid/ester</u>	<u>anhydride</u>	<u>diaacid</u>	<u>diester</u>
172.62	172.52	173.64	172.73
173.26		174.79	173.38

Table 2e
CARBONYL ASSIGNMENTS FOR BTDA AND DERIVATIVES

<u>acid/ester</u>	<u>anhydride</u>	<u>tetraacid</u>	<u>tetraester</u>
167.11	168.49	167.82	167.67
167.18		168.76	168.61
167.73			
167.92			
167.96			
168.65			

By determining the chemical shifts of the acid and ester carbonyl carbons from the fully acidified and the fully-esterified adducts, specific chemical shifts in the acid/esters could be assigned to acid and ester. The NDE carbonyl carbon peaks occur upfield from those of the NDA; hence, in Table 2b the upfield carbonyl peak (no. 5) is assigned as ester, while the downfield carbonyl peak (no. 6) is called acid.

Because there are several possible configurations for the BTDE acid/esters, there are many carbonyl peaks and acid and

ester peak differentiation is not attempted here.

2:1 NE/MDA and 1:1 BTDE/MDA were reacted to various degrees in order to detect any amide or anhydride in either case. Table 2f lists the carbonyl peak shifts and heights for NE/MDA aged to varying degrees at 100°C. The peaks at 172.64 and 173.29 are readily recognizable as ester and acid. According to a previous ¹³C-NMR study by Kranbuehl, the peaks at 176.83 and 176.88 are nadimide carbonyl carbons.⁴ The anhydride peak at 172.52 ppm that we assume would appear if anhydride was present does not in fact appear. BP Research identified a peak at 173.80 as an amide NE carbonyl, one at 141.86 as amide MDA C₁, and a peak at 119.78 as equivalent amide MDA C₃ and C₅ carbons, but these peaks do not appear in these spectra either. The results only serve to support a mechanism of complete imidization in one step (Chapter I, Scheme II). If anhydride or amide is an intermediate and the formation of one of these intermediates is the rate-controlling step, then all anhydride or amide formed must subsequently be converted to imide in such short time as to make it a non-isolable species.

The data presented in Table 2g also shows how ¹³C-NMR may be used as a qualitative means of monitoring the advancement of the imidization reaction. At t = 0 minutes only acid and ester are present, but with time one can monitor the gradual disappearance of the acid and ester carbonyl peaks and the

subsequent appearance and relative growth of the nadimide carbonyl peaks.

Spectra were also taken on 1:1 BTDE/MDA aged to various times at 120°C. Problems arose in making the less soluble cured samples concentrated enough to obtain clean spectra. The

Table 2f
2:1 NE/MDA carbonyl peaks at 100°C

time(min.)	acid/ester		nadimide	
	δ (ppm)	height	δ (ppm)	height
0	172.64	129	—	—
	173.29	186		
10	172.62	125	176.83	162
	173.27	170	176.88	131
20	172.62	38	176.81	146
	173.26	45	176.88	122
60	172.61	19	176.80	231
	173.24	15	176.87	47
120	—	—	176.81	80
			176.86	37

spectra obtained for those samples that were aged for an hour or more at 120°C were noisy and only the tallest peaks were distinguishable from noise. Figures 2.11 - 2.13 are the spectra for 1:1 BTDE/MDA cured at 120°C for 10, 20, and 45 minutes.

None of these spectra show the peak at 168.49 that would be characteristic of the BTDA anhydride carbonyl listed in Table 2e. Nor do any of the spectra contain a peak to match BP Research's peak at 141.86 labeled as MDA C₁ carbon. There is,

however, a peak at 119.79 in Figure 2.11 that would correspond to the peak at 119.78 that BP Research assigned as C₃ and C₅ carbons of MDA. This peak also appears in Figures 2.12 and 2.13. Scheme I, with amide as a precursor to imide, would be reasonable with regards to the BTDE/MDA imidization if this assignment were correct. However, it is curious that we do not see these peaks in the similar NE/MDA imidization; and the assignment should be regarded with skepticism.

CONCLUSIONS

Though several research teams have reported seeing anhydride at various stages of PMR-15 imidization, ¹³C-NMR results show no evidence of anhydride, either as intermediate or product of a side-reaction in the NE/MDA or BTDE/MDA imidization. The peaks at 172.52 and 168.49 corresponding, respectively, to the nadic and BTDA anhydride carbonyl carbons are not present at any stage of either reaction. Nor does ¹³C-NMR show evidence for the amide intermediate of Scheme I. Thus it must be concluded here that imidization takes place in a single step (Scheme II); any amide or anhydride formed during the reaction would be a short-lived transition state.

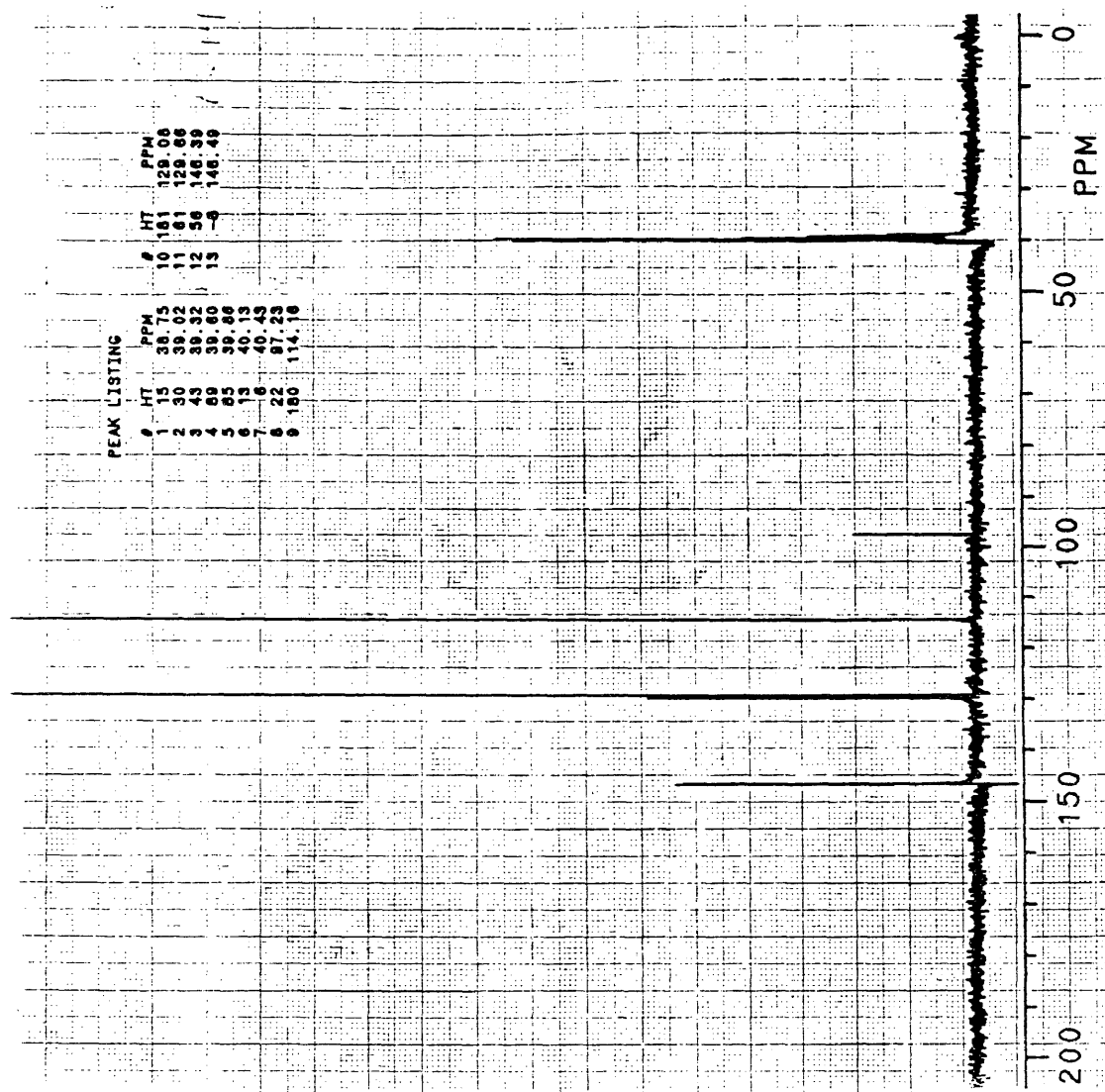
Figure 2.1: ^{13}C -NMR of MDA.

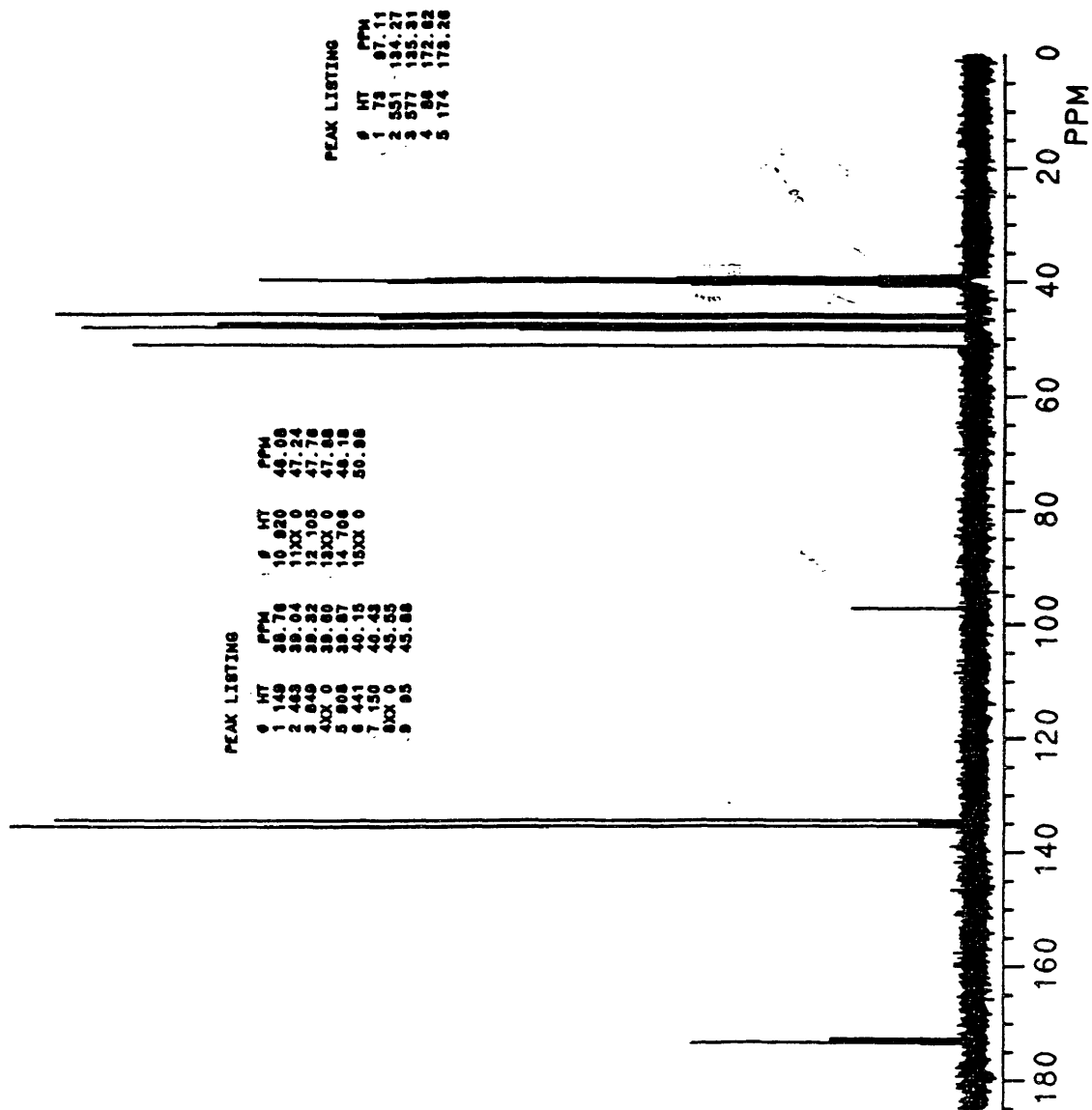
Figure 2.2: ^{13}C -NMR of NE.

Figure 2.3: ¹³C-NMR of NA.

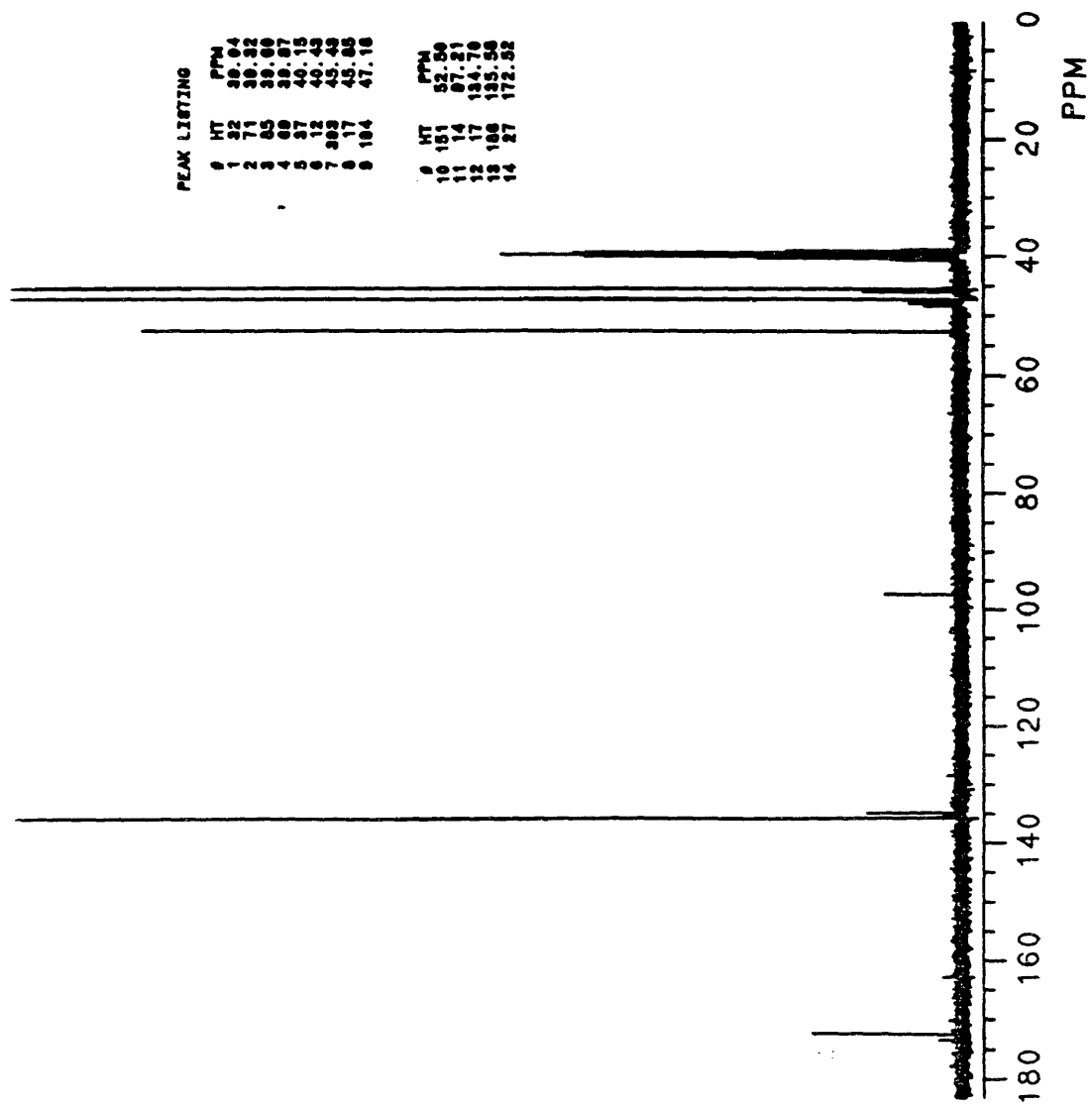


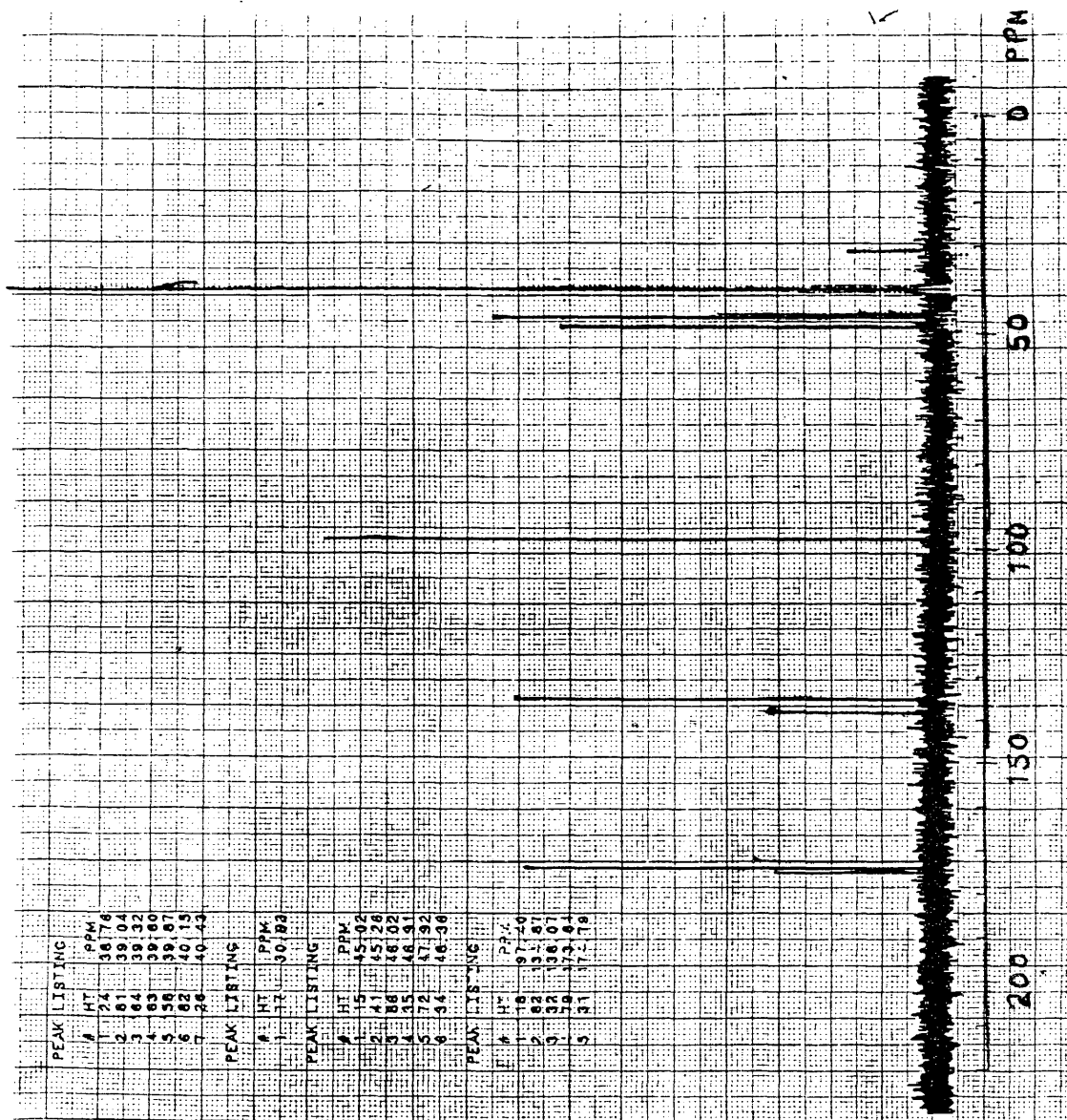
Figure 2.4: ^{13}C -NMR of NDA.

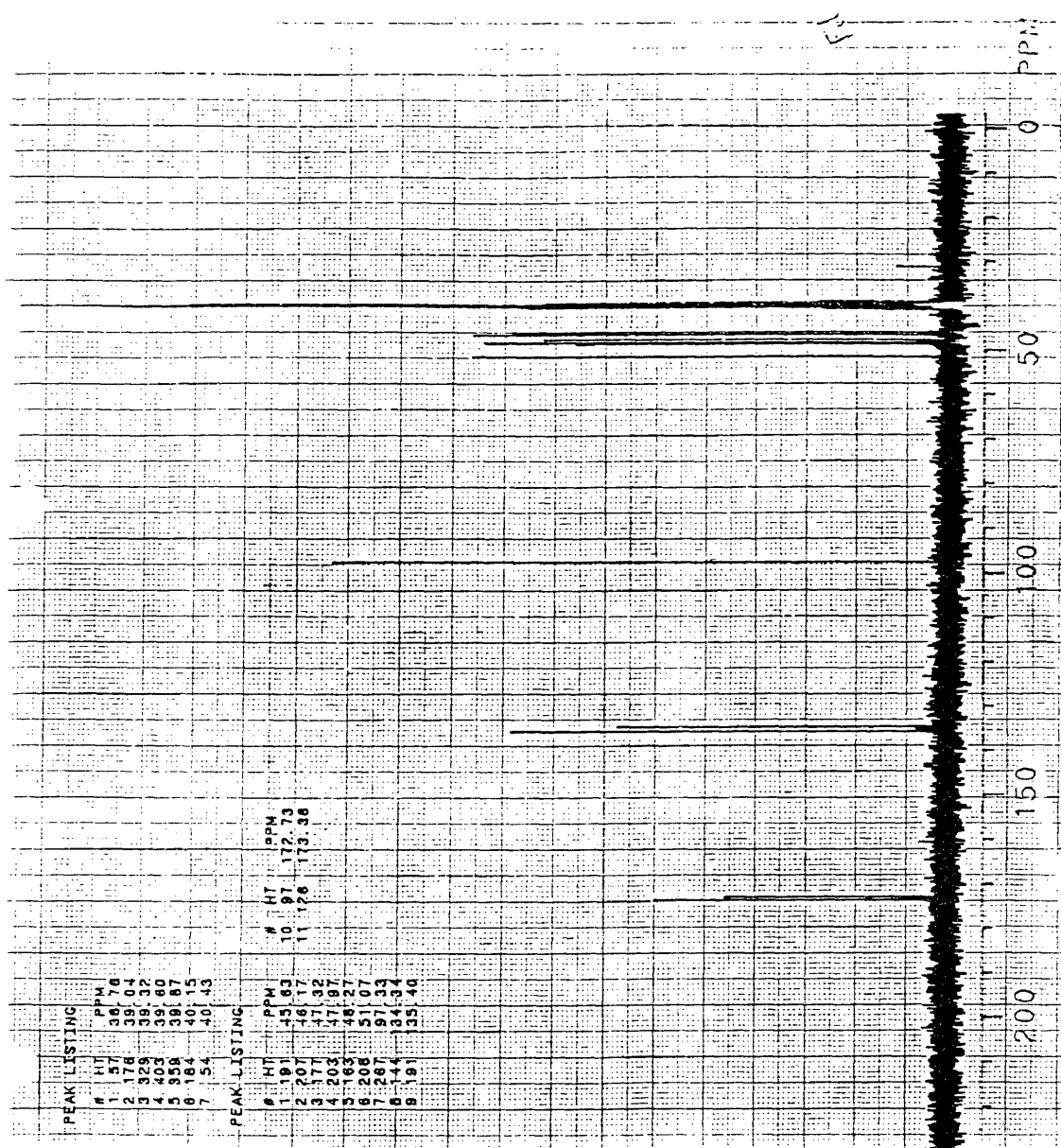
Figure 2.5: ^{13}C -NMR of NDE.

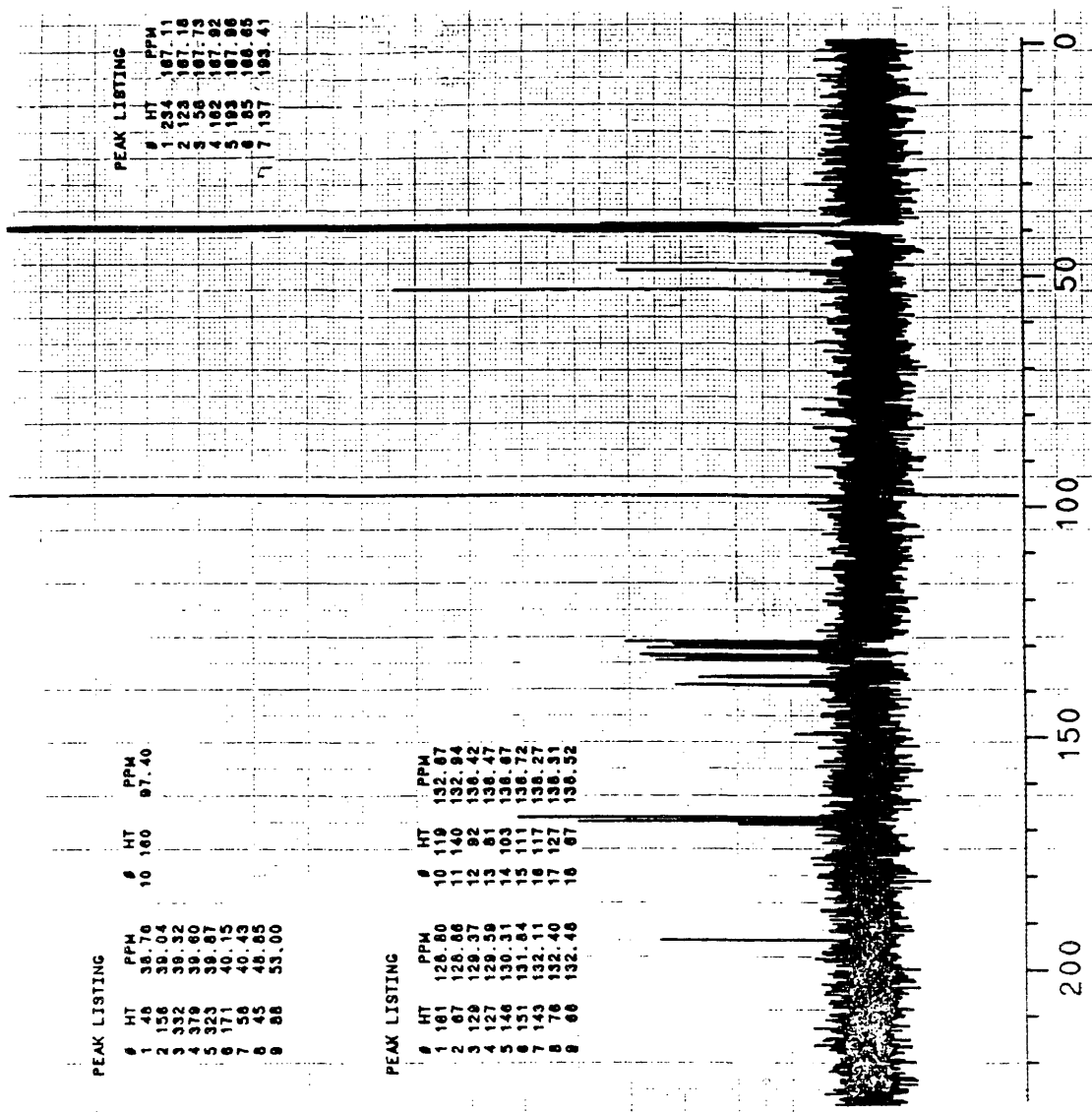
Figure 2.6: ^{13}C -NMR of BTDE.

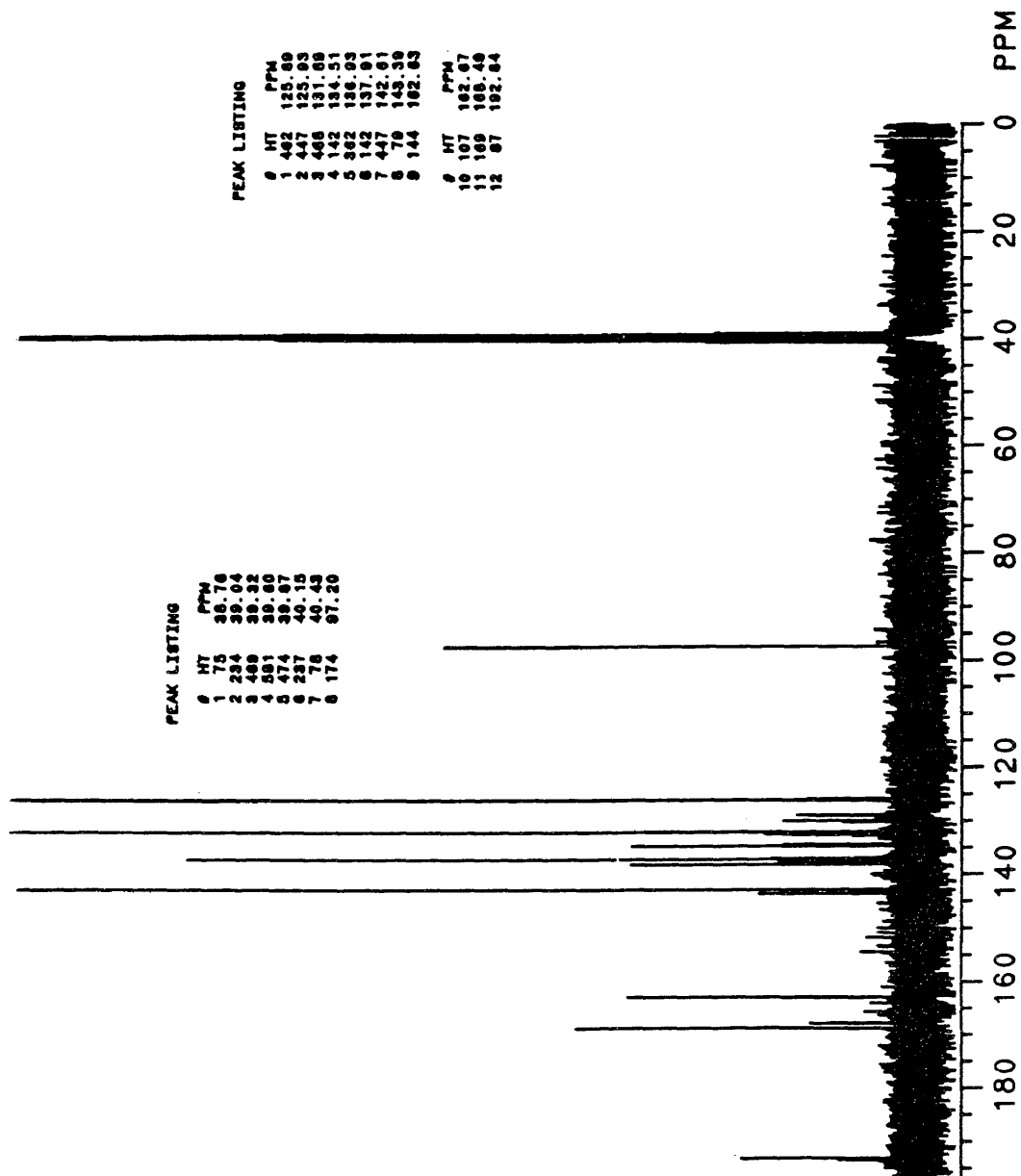
Figure 2.7: ^{13}C -NMR of BTDA.

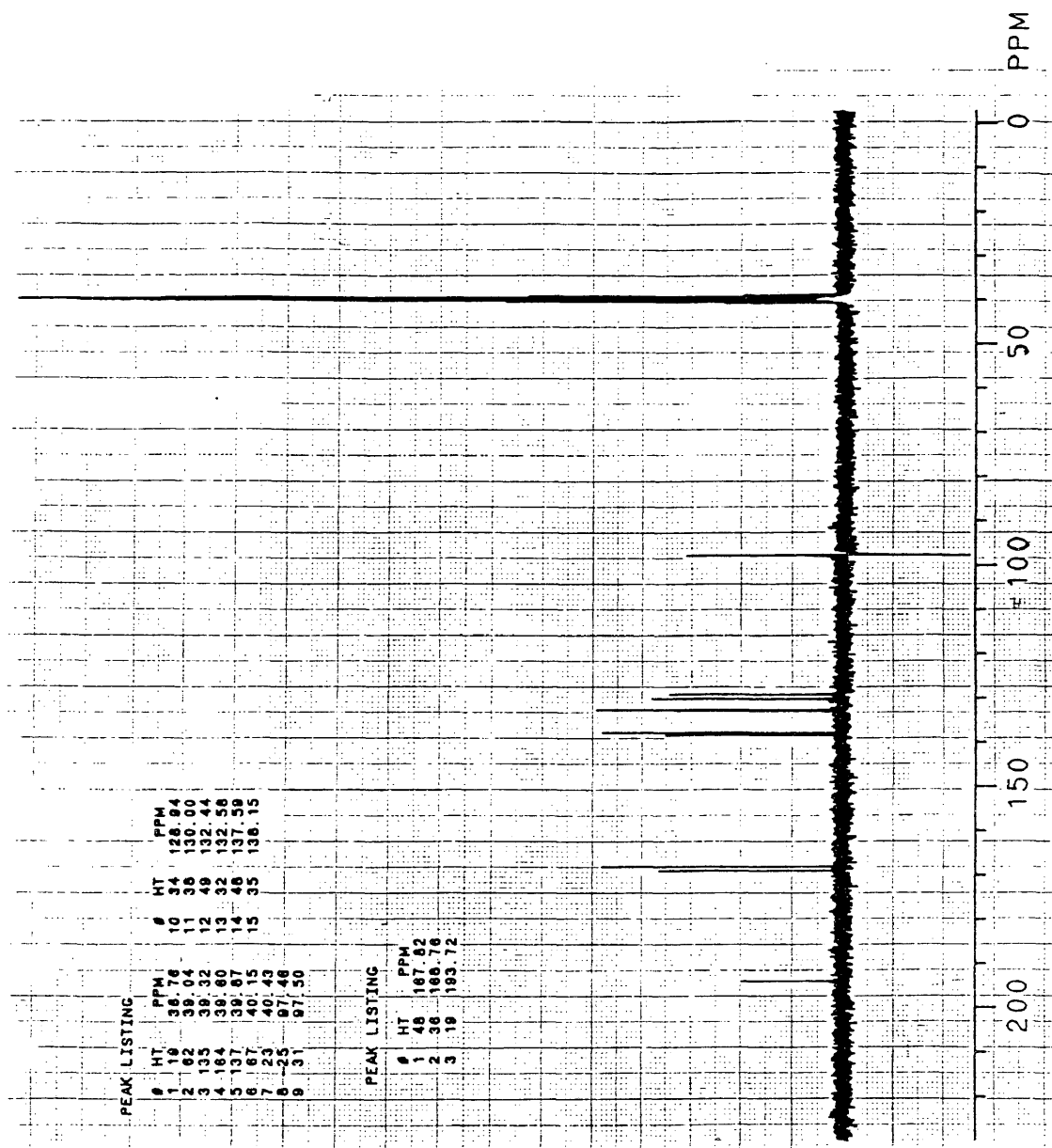
Figure 2.8: ^{13}C -NMR of BTTA.

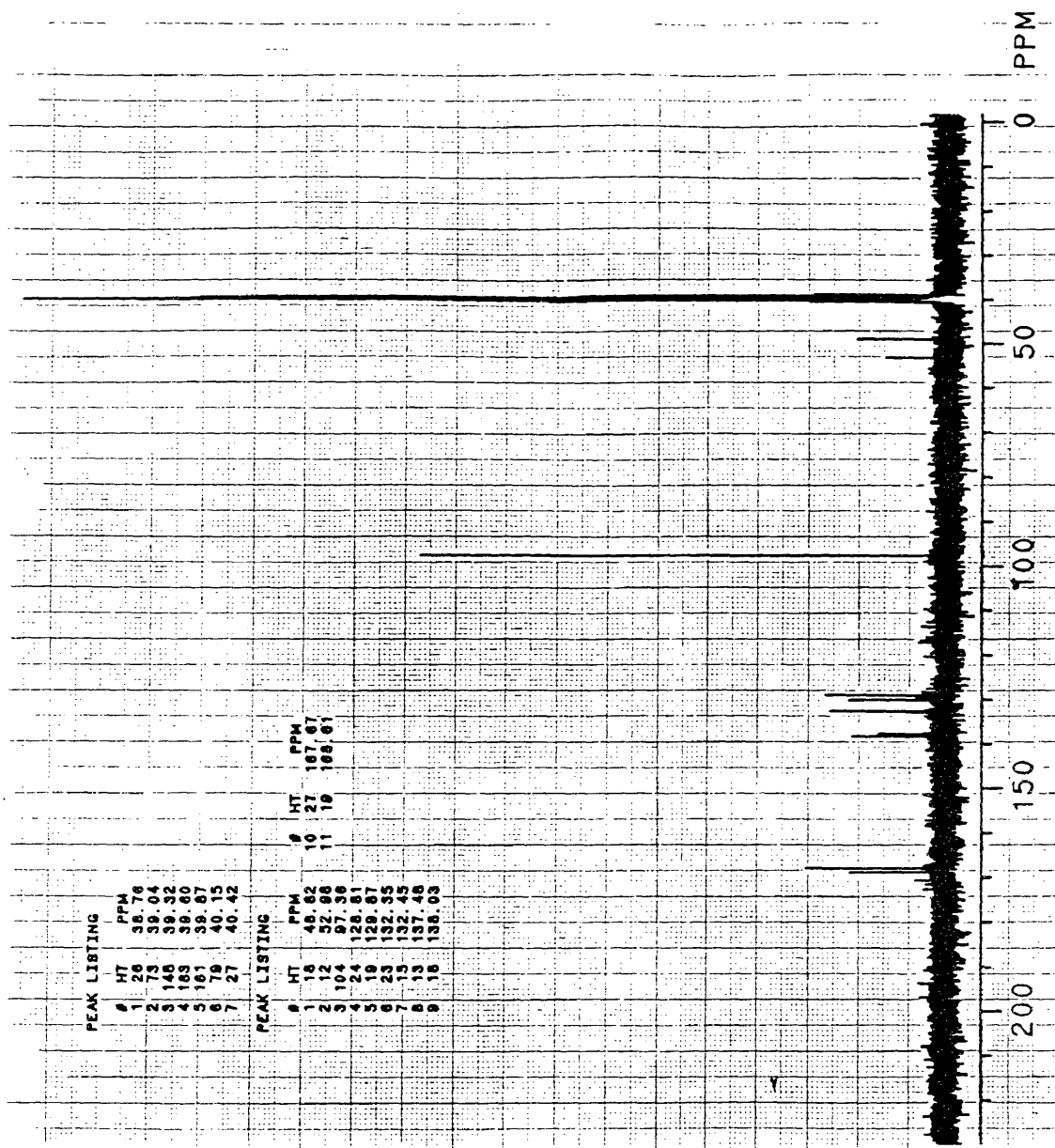
Figure 2.9: ^{13}C -NMR of BTTE.

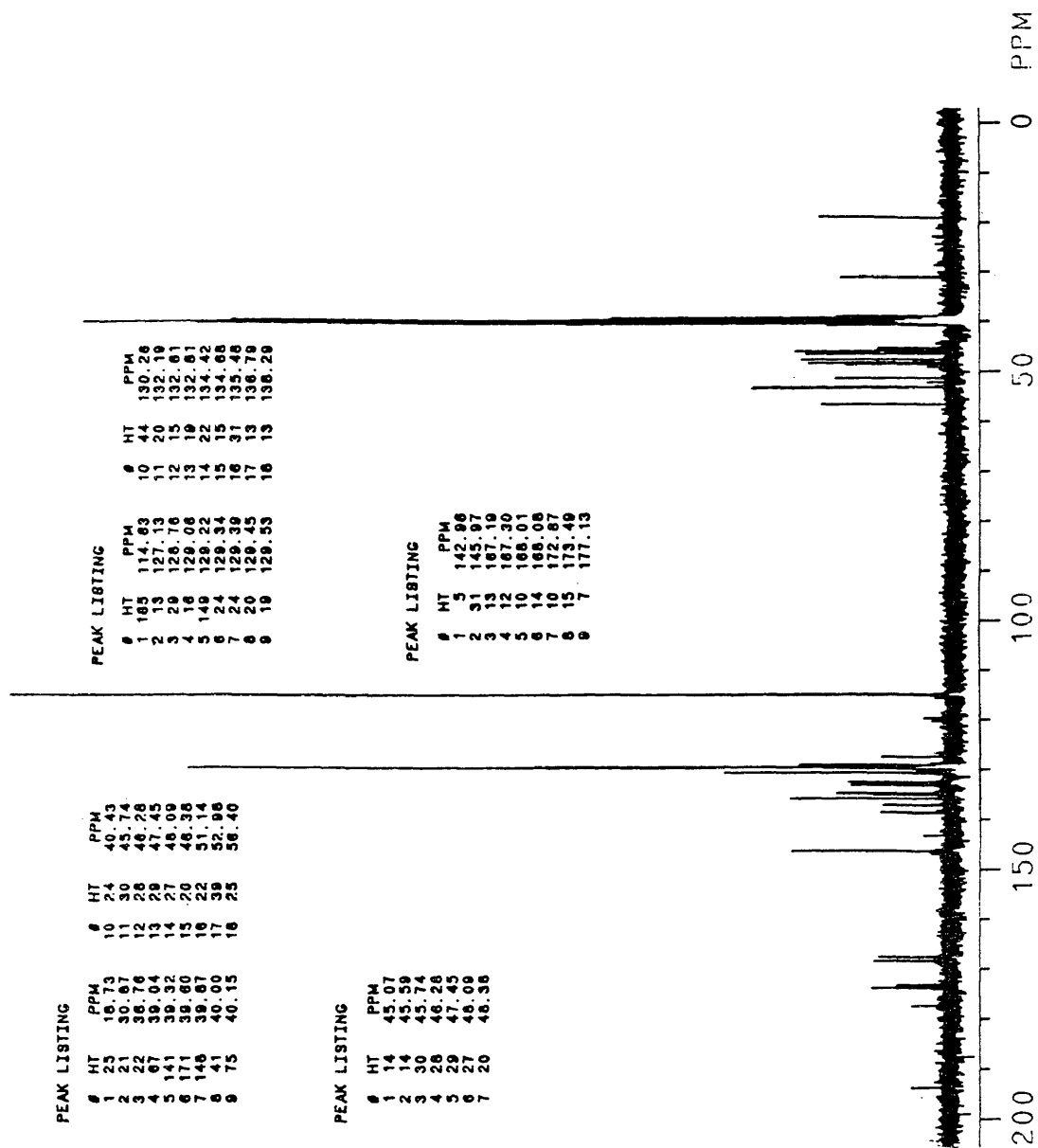
Figure 2.10: ^{13}C -NMR of PMR-15.

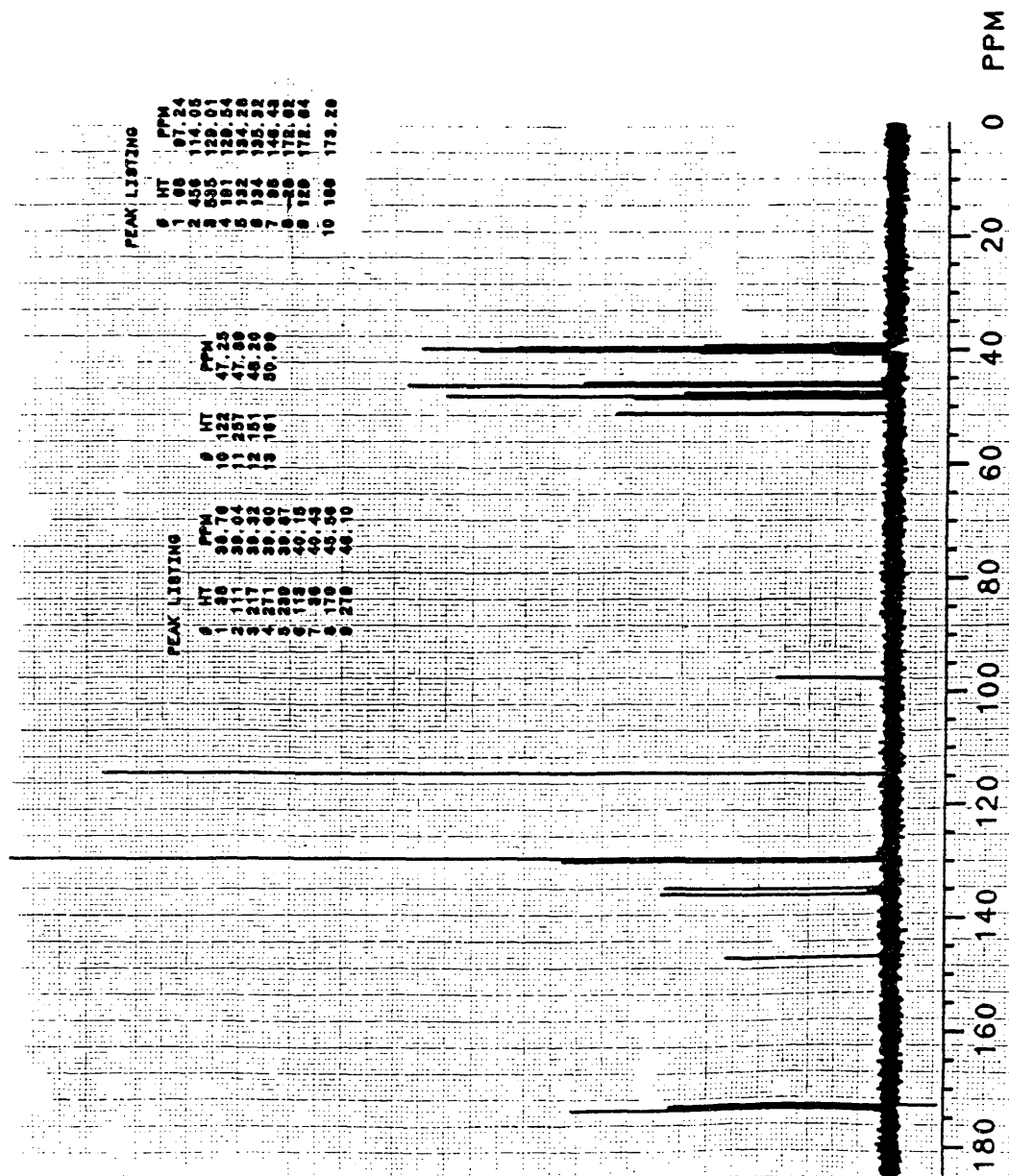
Figure 2.11: ^{13}C -NMR of unreacted 2:1 NE/MDA.

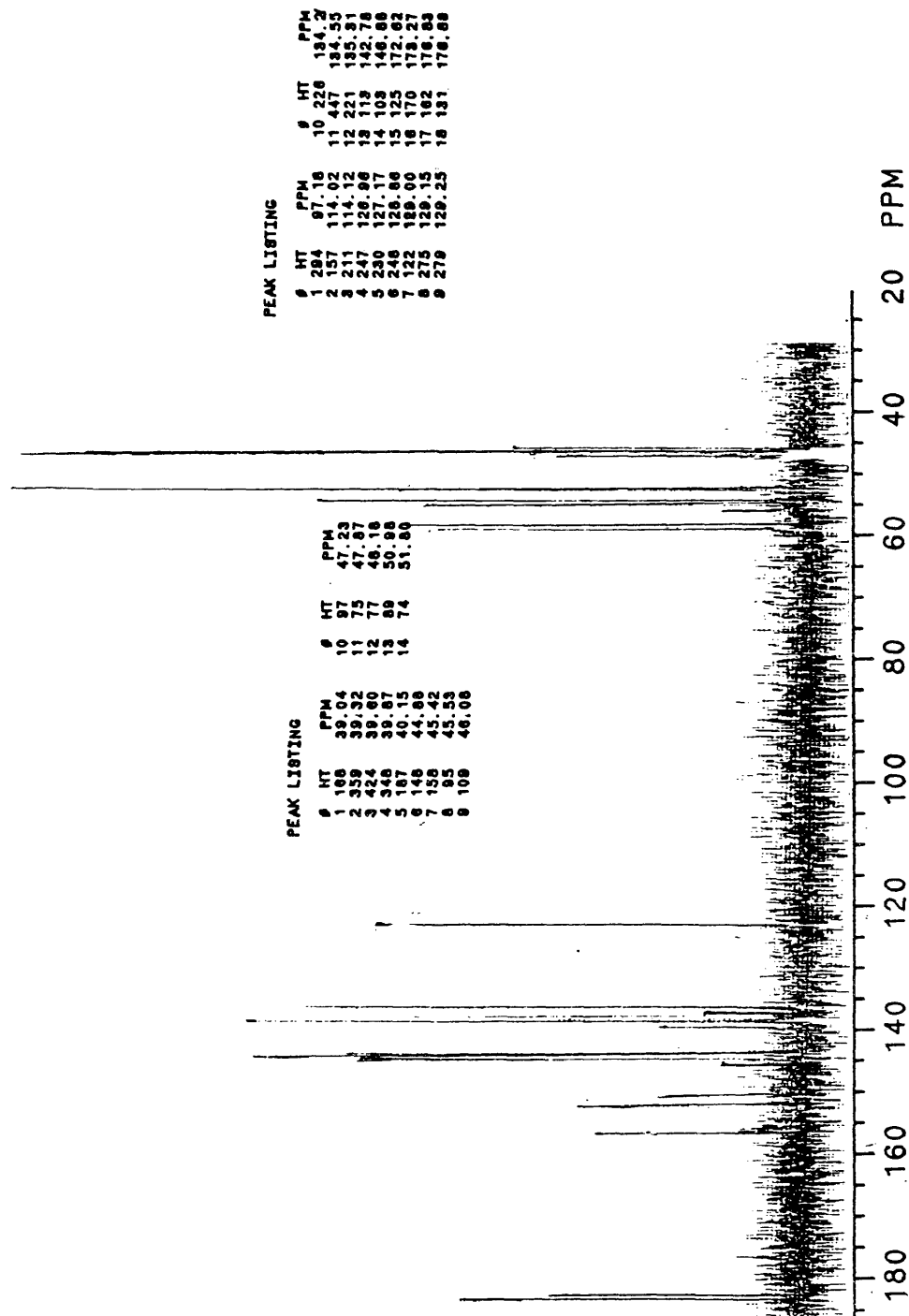
Figure 2.12: ^{13}C -NMR of 2:1 NE/MDA after 10 minutes at 100°C.

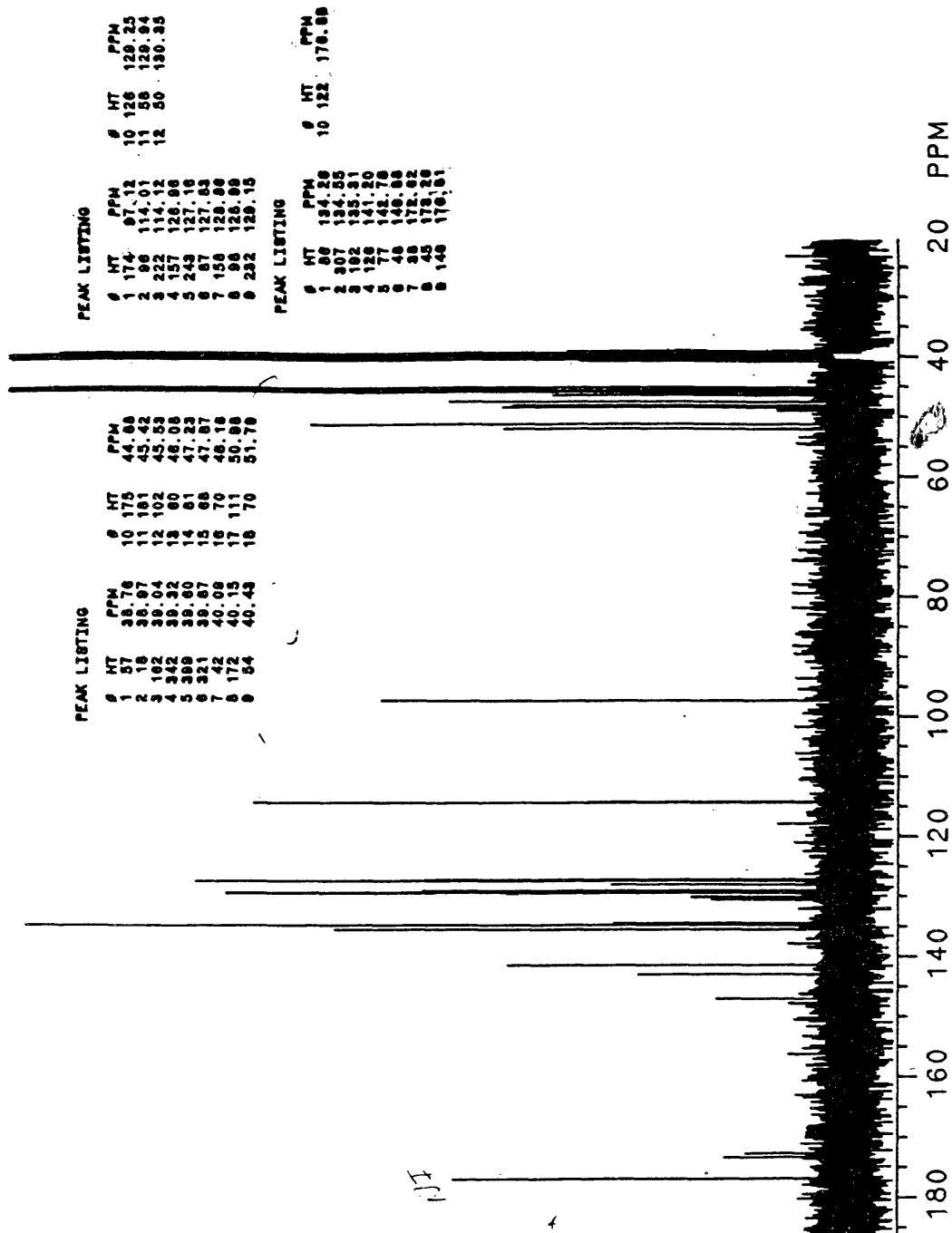
Figure 2.13: ^{13}C -NMR of 2:1 NE/MDA after 20 minutes at 100°C .

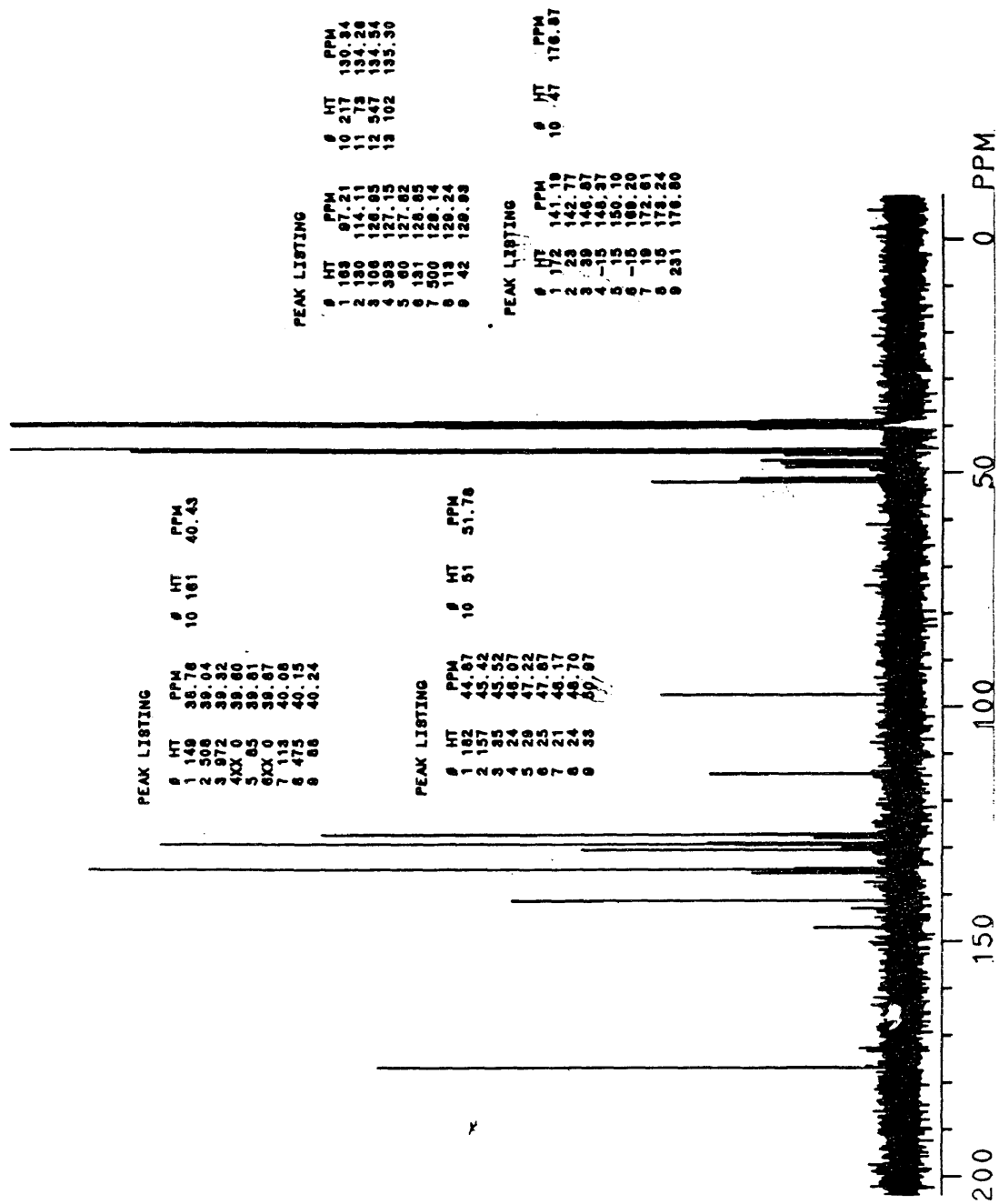
Figure 2.14: ^{13}C -NMR of 2:1 NE/MDA after 60 minutes at 100°C.

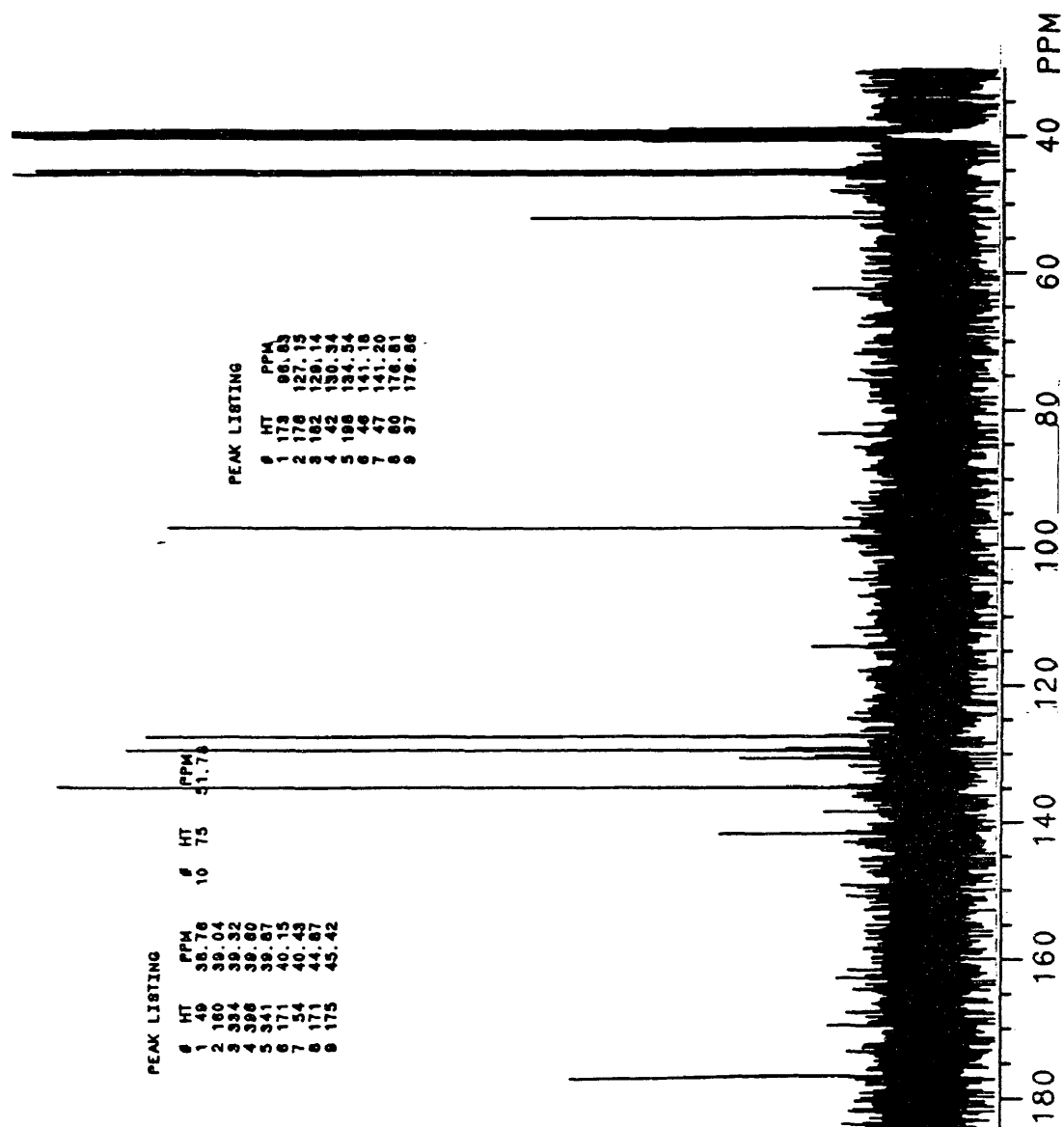
Figure 2.15: ^{13}C -NMR of 2:1 NE/MDA after 120 minutes at 100°C.

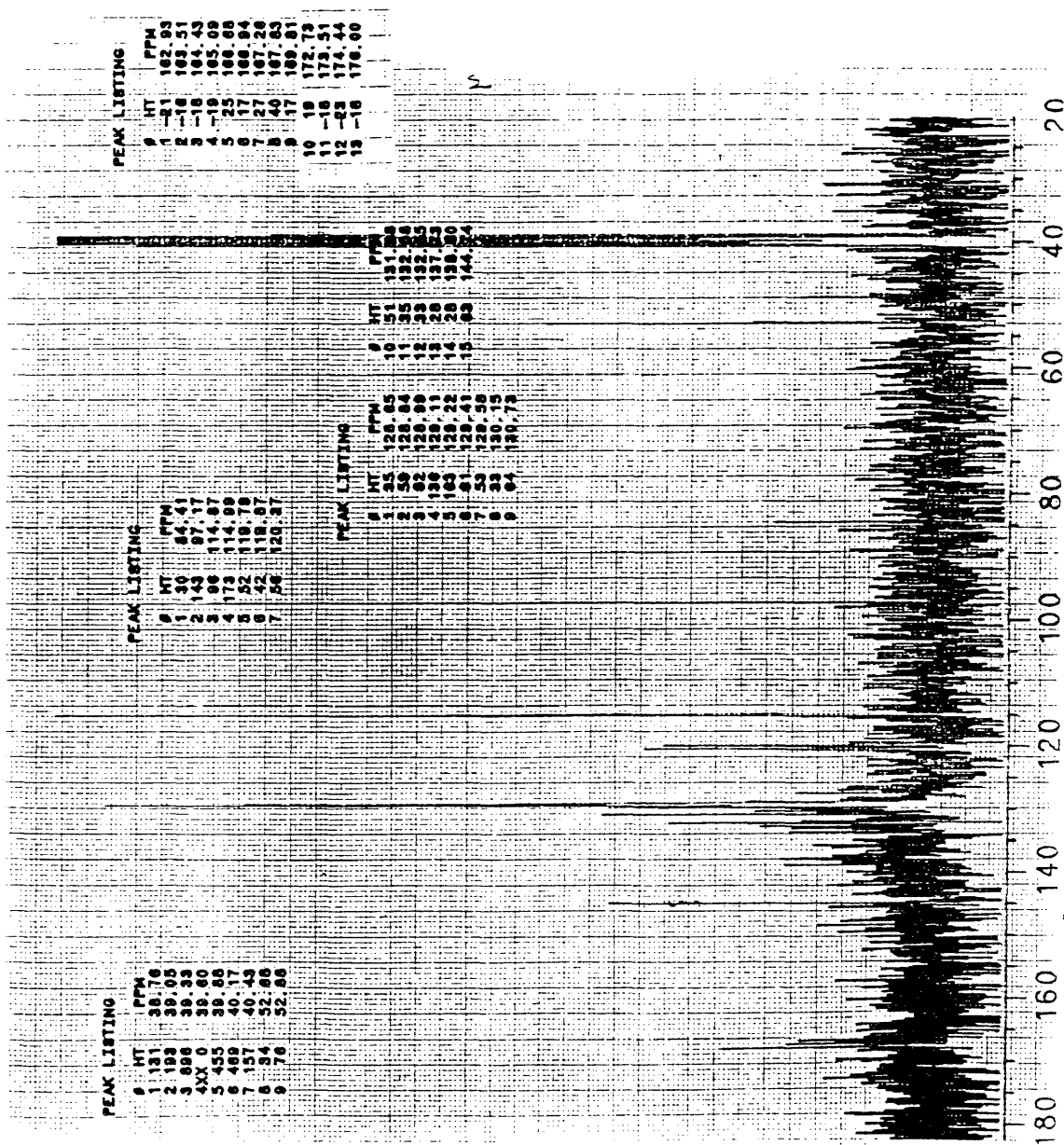
Figure 2.16: ^{13}C -NMR of 1:1 BTDE/MDA after 10 minutes at 120°C.

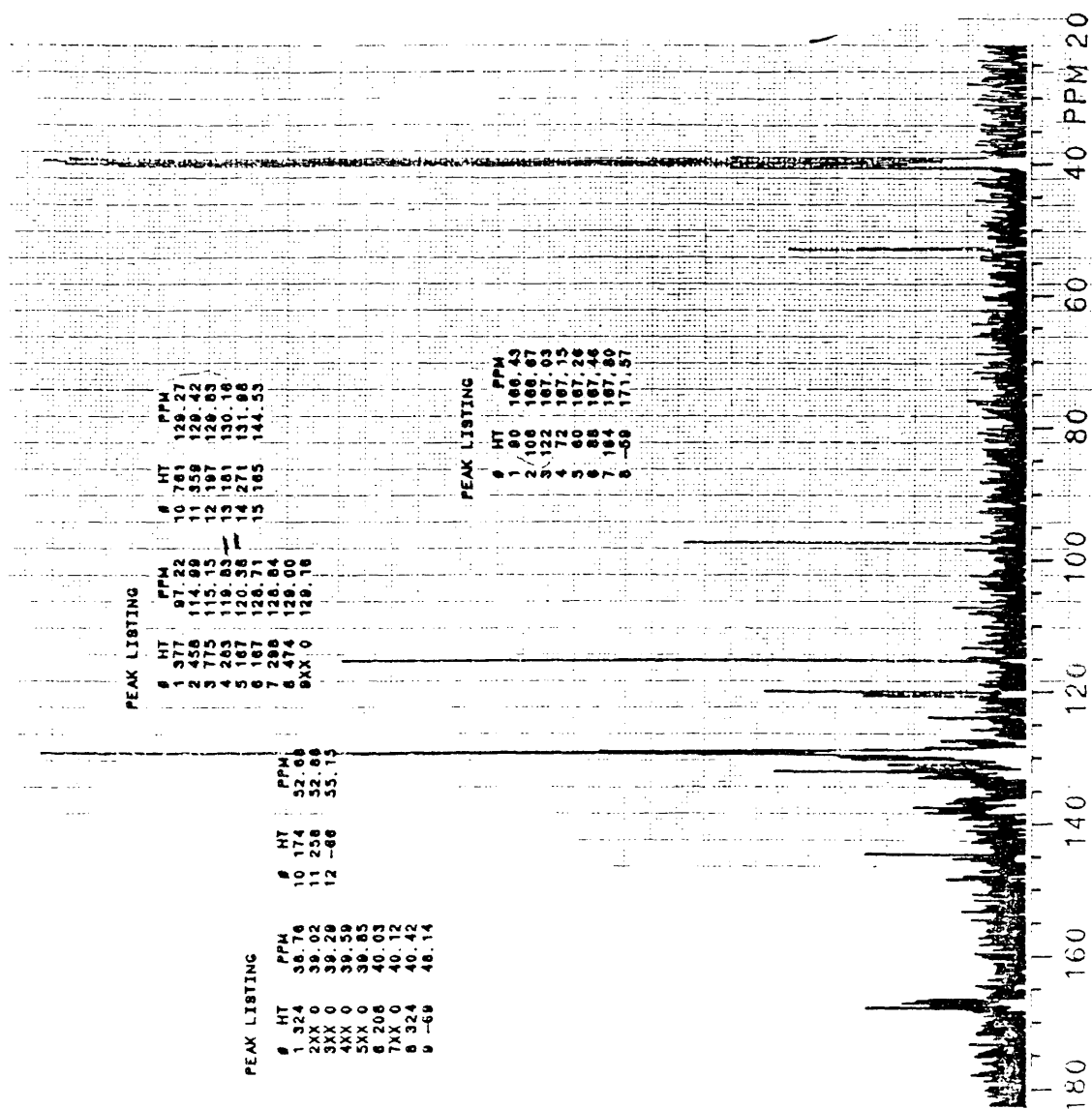
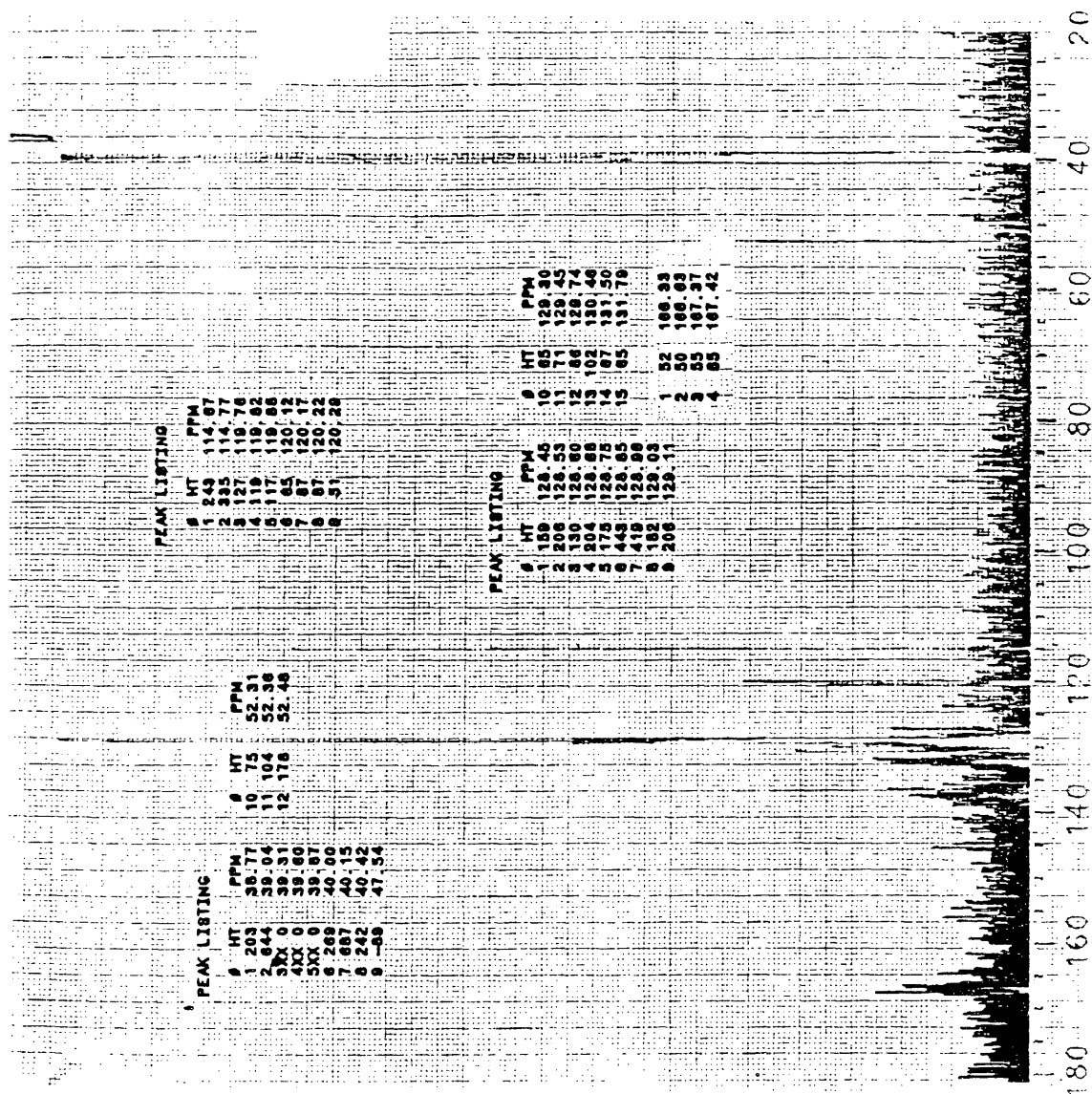
Figure 2.17: ^{13}C -NMR of 1:1 BTDE/MDA after 20 minutes at 120°C.

Figure 2.18: ^{13}C -NMR of 1:1 BTDE/MDA after 45 minutes at 120°C.

NOTES FOR CHAPTER II

1. J.C. Johnston, M.A. Meador , and W.B. Alston, J. Polymer Sci. Polymer Chem. Ed., 25, 2175 (1987).
2. D. Garcia and T.T. Serafini, J. Polymer Sci. Polymer Phys. Ed., 25, 2275 (1987).
3. J.N. Hay, J.D. Boyle, P.G. James, J.R. Walton, and D. Wilson, Polymerisation Mechanisms in PMR-15 Polyimide. Middlesex, England: BP Research Center. Unpublished Report.
4. D.E. Kranbuehl, S.E. Delos, E.C. Yi, and J.T. Mayer, "Dynamic Dielectric Analysis of the Cure Chemistry of PMR-15", in: K.L. Mittal (Ed.), Polyimides, New York: Plenum Press, 1984; Vol 1, pp. 469-491.

CHAPTER III

KINETIC STUDIES OF PMR-15 BY THERMOGRAVIMETRIC ANALYSIS

Thermogravimetric analysis (TGA) has been used by Kranbuehl in the past to study the PMR-15 imidization reaction.¹ The formation of the imide from acid/ester and amine liberates one methanol molecule and one water molecule per imide linkage formed. By monitoring the weight loss of a sample over time one should be able to determine the kinetic parameters of the reaction. Kranbuehl's studies determined the overall order of the PMR-15 reaction to be 3 or greater.¹

TGA was performed on samples in an aluminum foil cup suspended from a Perkin-Elmer AD2B Autobalance. The cup was hung inside a Delta Design 5900 forced-air oven. A separate steel chamber enclosed the cup and prevented the flow of air from the oven fans from affecting the balance. A thermocouple next to the sample cup monitored temperature. Data from the balance was taken through a Kiethley 179A TRMS Multimeter at one to two minute intervals by a Hewlett-Packard 9826 computer.

There are actually two different imidizations taking place, and one should be able to use TGA to study them independently. Each MDA has two amines, whereas the NE has only one acid/ester. Therefore a mixture of 2:1 NE/MDA should

theoretically react completely to bisnadimide (BNI) (Figure 3.1). The theoretical weight loss for such a mixture would be 16.7% if fully cured.

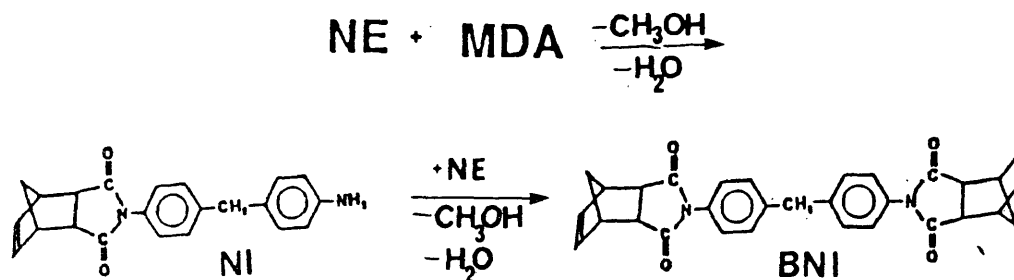


Figure 3.1. Formation of bisnadimide from NE and MDA.

Similarly, each BTDE molecule possesses two acid/esters, and a ratio of 1:1 BTDE/MDA would polymerize with a weight loss of 17.1%.

MDA is available commercially. The monomer NE was synthesized by Walton's method of refluxing 5-norbornene-2,3-dicarboxylic anhydride for 3 hours in a 50/50 weight percent solution with methanol². BTDE was prepared with the same procedure. PMR-15, 2:1 NE/MDA, and 1:1 BTDE/MDA were prepared by combining the monomers in the correct stoichiometric amounts, dissolving in methanol, and drying at room temperature with a vacuum pump. The dried mixtures were then stored under nitrogen at -10°C to prevent reaction. The PMR-15 and BTDE/MDA dried in a matter of hours, and it is assumed here that no reaction occurred during that time spent at room temperature. The samples used were no more than 3 months old, and earlier studies have indicated that unreacted PMR monomers are stable up to 6 months at -10°C .³

The NE/MDA, however, can take 3 or more days to dry completely. To avoid the imidization that might occur during this time spent at room temperature, the samples described here were dried for only one day. The resultant "gooey" mixture was assumed to contain a minimum of solvent (the mixture is a gum instead of powder); but this methanol should have evaporated early in the reaction (less than 5 minutes), and should not have introduced significant error into the weight loss measurements. The difference between average total percent weight loss and theoretical percent weight loss for the NE/MDA was only slightly higher than that for BTDE/MDA -- 2.3 versus 1.0 (Tables 3a and 3b). To avoid any reaction of the nadic group with residual methanol to form diesters, experiments with NE/MDA were performed on samples mixed no more than a week.

The resultant weight loss data for both systems is listed in Tables 3a and 3b. Figures 3.2 and 3.3 compare alpha (degree of cure) versus time data for the two systems at various temperatures . Figures 3.4, 3.5, and 3.6 compare the two reactions and the overall reaction of PMR-15 at 80, 120, and 160°C. One first notices that the the BTDE/MDA reacts faster than the NE/MDA at all three temperatures. This is seemingly contrary to earlier reports that characterized the nadic reaction as the faster reaction at the lower temperatures, and will be discussed later in this chapter. More consistent with the earlier view is the observation that the NE/MDA reacts to

higher alphas at the lower temperatures.

Table 3a

2:1 NE/MDA weight loss data

temp (°C)	% weight loss	% residual wt. loss	total %
80 (#1)	12.0	6.7	17.7
80 (#2)	8.9	9.1	18.0
120	15.6	3.3	18.9
140	12.5	4.3	16.7
160 (#1)	17.0	5.0	22.0
160 (#2)	6.8	13.7	20.5

 average total weight loss = 19.0%
 theoretical weight loss = 16.7%

Table 3b

1:1 BTDE/MDA weight loss data

temp (°C)	% weight loss	% residual wt. loss	total %
80	5.7	13.9	19.7
105 (#1)	6.9	9.5	16.3
105 (#2)	11.1	9.6	20.7
120	12.2	7.8	20.0
140	5.9	9.5	15.4
160	12.6	3.9	16.5

 average total weight loss = 18.1 %
 theoretical weight loss = 17.1 %

From equation 1,

$$d\alpha/dt = k(1 - \alpha)^m \quad (1)$$

or

$$\log d\alpha/dt = \log k + m \cdot \log(1 - \alpha) \quad (2)$$

we see that plots of $\log d\alpha/dt$ versus $\log(1 - \alpha)$ would yield a slope of m , where m is the reaction order. Figures 3.7 -3.18 are plots of equation 2 for both reactions at each temperature.

Because only the initial part of the imidization reaction is controlled by the initial rate constant (as the medium becomes more viscous the reaction becomes increasingly more dependent upon the diffusion of the reacting species through the medium), this kinetic analysis deals only with that initial part. Hence, m is determined only from the slope of the final flat part of the curve. (The upper right corner of the plot corresponds to the lower alphas.) Tables 3c and 3d list the slopes calculated in such a manner for NE/MDA and BTDE/MDA.

Table 3c
2:1 NE/MDA
reaction orders

<u>temp(°C)</u>	<u>m</u>
80 (#1)	3.9
80 (#2)	2.1
120	3.7
140	3.6
160 (#1)	3.8
160 (#2)	

	avg.= 4.0

Table 3d
1:1 BTDE/MDA
reaction orders

<u>temp(°C)</u>	<u>m</u>
80 (#1)	9.4
105 (#1)	12
105 (#2)	8.8
120	3.4
140	3.6
160	3.1

	avg.= 6.7

The NE/MDA reaction order ranges from 2 to 7, with an average of 4. The BTDE/MDA reaction also yields a variable order ranging from 3-12. However, if we ignore the first three values of m , which are intuitively high, the three highest temperatures indicate an order of 3. Since the two reactions involve similar functional groups (acid/ester with amine to form imide) we would expect identical reaction orders. Thus the imidizations have an order of 3 or greater.

Both reactions occur in a 1:1 molar ratio (considering each amine of the dianiline as a separate species and each acid/ester of the BTDE a separate species). Therefore simple rate equations can be devised. If the reaction is first order:

$$c_t = c_0 e^{-kt} \quad (3)$$

where c_t is the concentration of either reactant at time t and c_0 its initial concentration⁴. Arbitrarily assuming an initial concentration of 1, $c_t = 1 - \alpha$.

For a second order reaction :

$$1 / c_t = kt + 1 / c_0 \quad (4)^4$$

A rate expression for a third order reaction can also be derived. For a third order reaction with two reactants:

$$d(\xi / V) / dt = k c_A c_B^2 \quad (5)$$

where ξ / V is the advancement of the reaction in units of concentration, c_A is the concentration of species A at time t , and c_B is the concentration of species B at time t .⁴

If the reaction is 1:1, then $c_A = c_B$, and:

$$d(\xi/V) = kc^3 \quad (6)$$

where c is the concentration of either reactant at time t .

Defining change in concentration in terms of (ξ/V) :

$$dc/dt = -d(\xi/V)/dt \quad (7)$$

Substituting equation 7 into equation 6 yields:

$$-dc/dt = kc^3 \quad (8).$$

The variables are separated:

$$-dc/c^3 = kdt \quad (9)$$

and equation 9 is integrated from $(c_0, 0)$ to (c_t, t) :

$$\int_c^{c_t} -dc/c^3 = \int_0^t kdt \quad (10).$$

This yields:

$$1/c_t^2 = 2kt + 1/c_0^2 \quad (11)$$

where the variables are defined as in equation 3.

Thus the plot of the data for a certain temperature that yields a linear fit should identify that equation and that order as the correct one.

Figures 3.19 - 3.30 show plots of $1/c_t^2$ versus time for the TGA data. There is an initial linear fit, followed by a nonlinear region. The first, linear part is the third order reaction. The second, nonlinear region of the cure is where the reaction rate becomes increasingly dependent on viscosity. As the medium becomes more viscous (i.e. as T_g approaches cure temperature), the rate of diffusion of the reacting species slows.

From equation 11, the linear fit should give an initial slope of $2k$. Tables 3e and 3f give the rate constants at their respective temperatures for the two reactions.

The Arrhenius expression relates the rate constant to the activation energy and temperature.

$$k = Ae^{-E^*/RT} \quad (12)$$

Table 3e

2:1 NE/MDA

<u>T(°C)</u>	<u>k(mol⁻²*min⁻¹)</u>
80	.0043
80	.0037
120	.065
140	.045
160	.19
160	.12

Table 3f

1:1 BTDE/MDA

<u>T(°C)</u>	<u>k(mol⁻²*min⁻¹)</u>
80	.0085
105	.022
105	.019
120	.034
140	.055
160	.094

where A is the Arrhenius pre-exponential factor, E^* the energy of activation, R the gas constant in J/mol*K, and T the temperature in Kelvin. A plot of $\ln k$ versus $1/T$ yields a slope of $-E^*/R$ and a y-intercept of $\ln A$. Figures 3.31 and 3.32 are the Arrhenius fits of the two sets of data. Table 3g lists the resultant activation energies and pre-exponential factors.

The activation energy for the BTDE imidization is lower than that for the NE. This conflicts with prior studies which reported that nadimide formation occurs at lower temperatures

TABLE 3g

<u>monomers</u>	<u>E* (J/mol)</u>	<u>A (min⁻¹*mol⁻²)</u>
2:1 NE/MDA	55	65600
1:1 BTDE/MDA	39	4200

(as low as 12°C) than BTDE imidization.⁵ However, the apparent inconsistency could be explained by two different rate constants in the 2:1 NE/MDA reaction -- one for nadimide formation from NE and MDA and one for bisnadimide formation from NE and nadimide. The TGA experiments here would only be measuring an average of the two rate constants, and it could still be said that $E_{NI}^* < E_{BTDE}^* < E_{BNI}^*$.

CONCLUSIONS

Thermogravimetric analysis shows the NE/MDA and the BTDE/MDA reactions to be third order or greater. Degree of cure versus time data were applied to a third order rate expression for both systems to yield third order rate constants. Arrhenius fits of the rate constants gave an activation energy of 55 J/mol and a pre-exponential factor of 66000 min⁻¹*mol⁻² for NE/MDA, and 39 J/mol and 4200 min⁻¹*mol⁻² for the BTDE/MDA. The experiments did not show the overall NE/MDA reaction to be faster than the BTDE/MDA reaction, as previously suggested by previous studies. However, this particular conclusion does not rule out the possibility that nadimide formation is faster than the BTDE/MDA reaction.

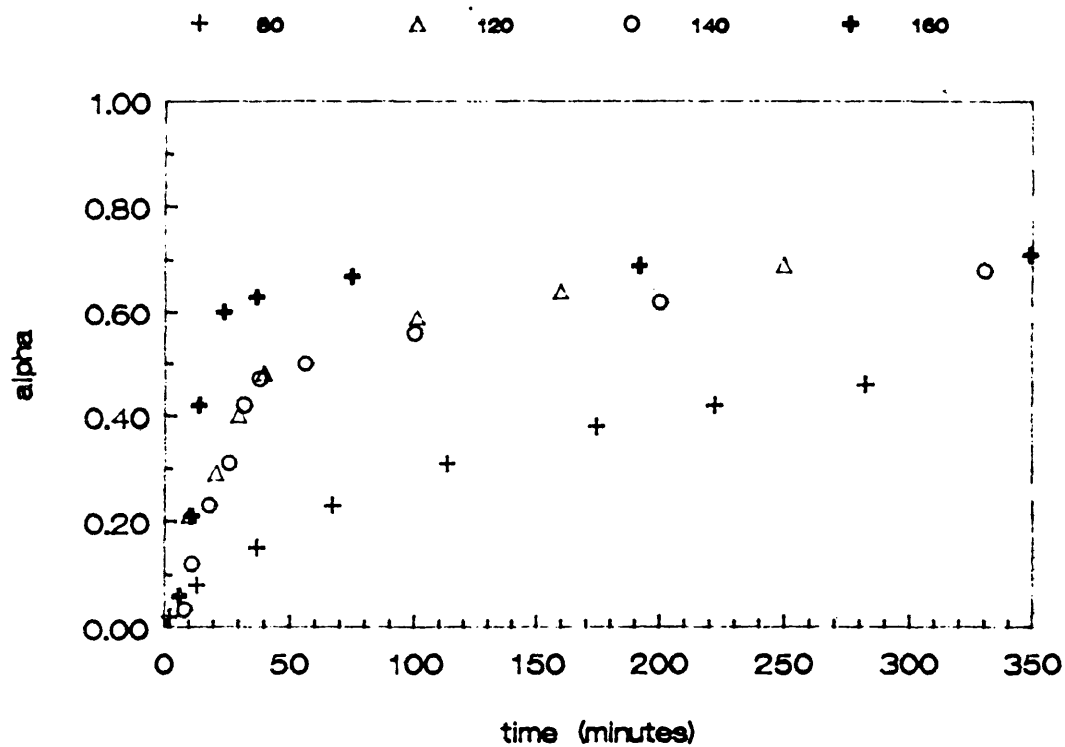


Figure 3.2: 2:1 NE/MDA: alpha vs. time.

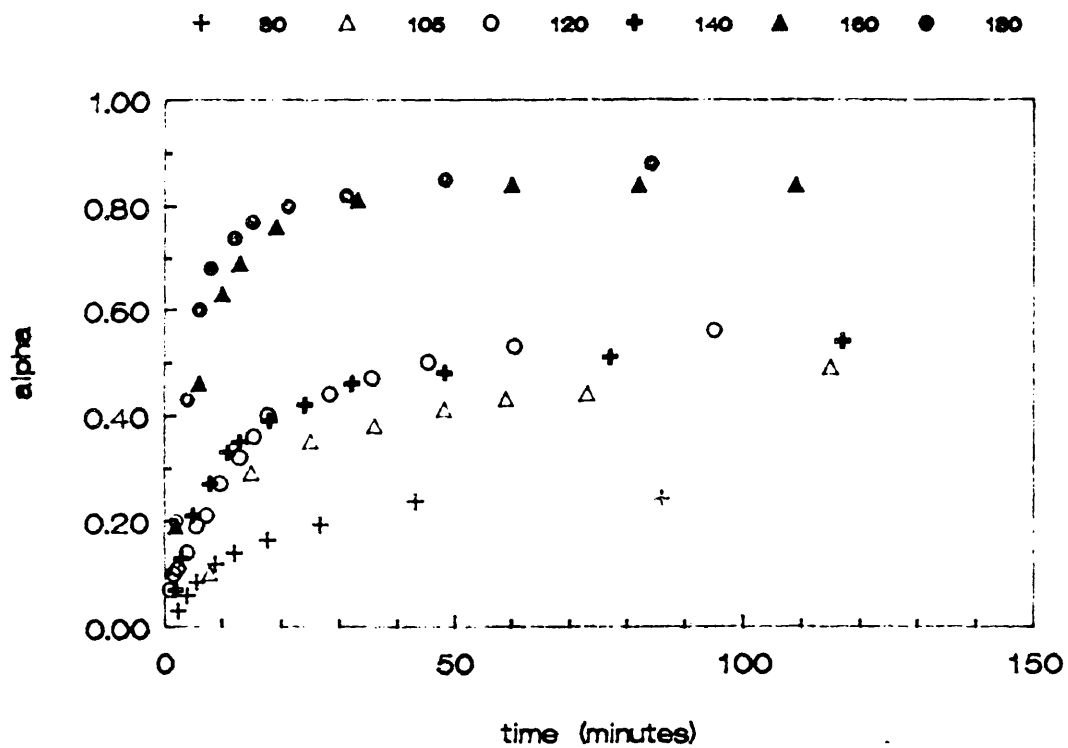


Figure 3.3: 1:1 BTDE/MDA: alpha vs. time.

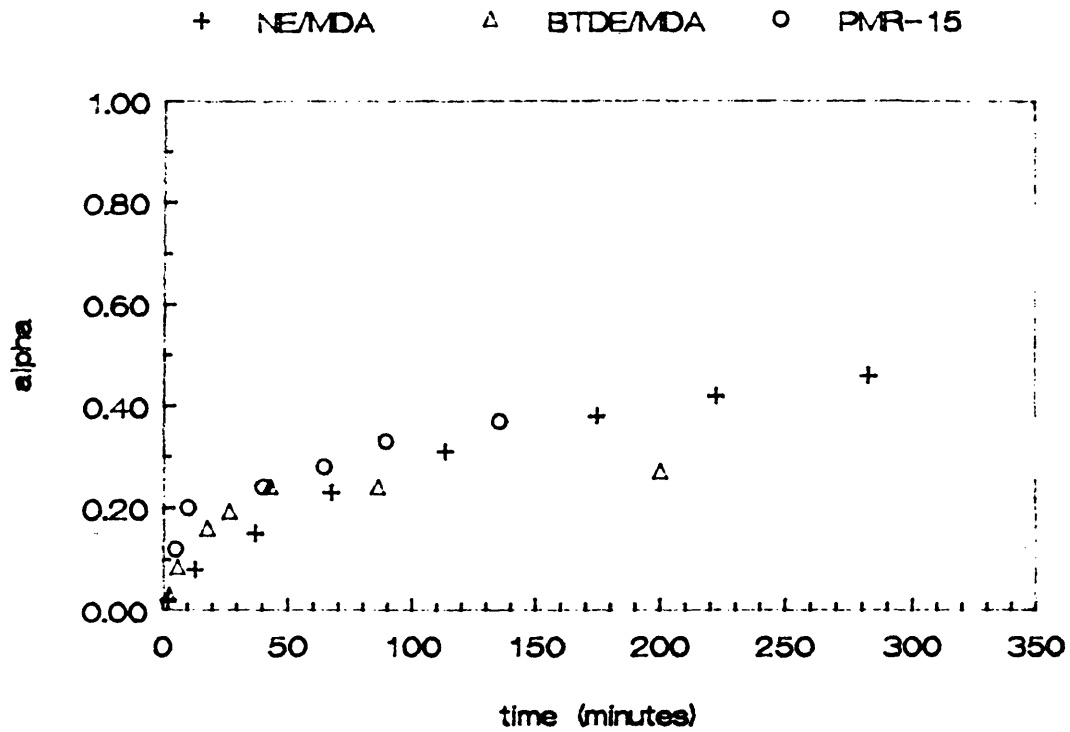


Figure 3.4: Alpha vs. time for NE/MDA, BTDE/MDA and PMR-15 at 80°C.

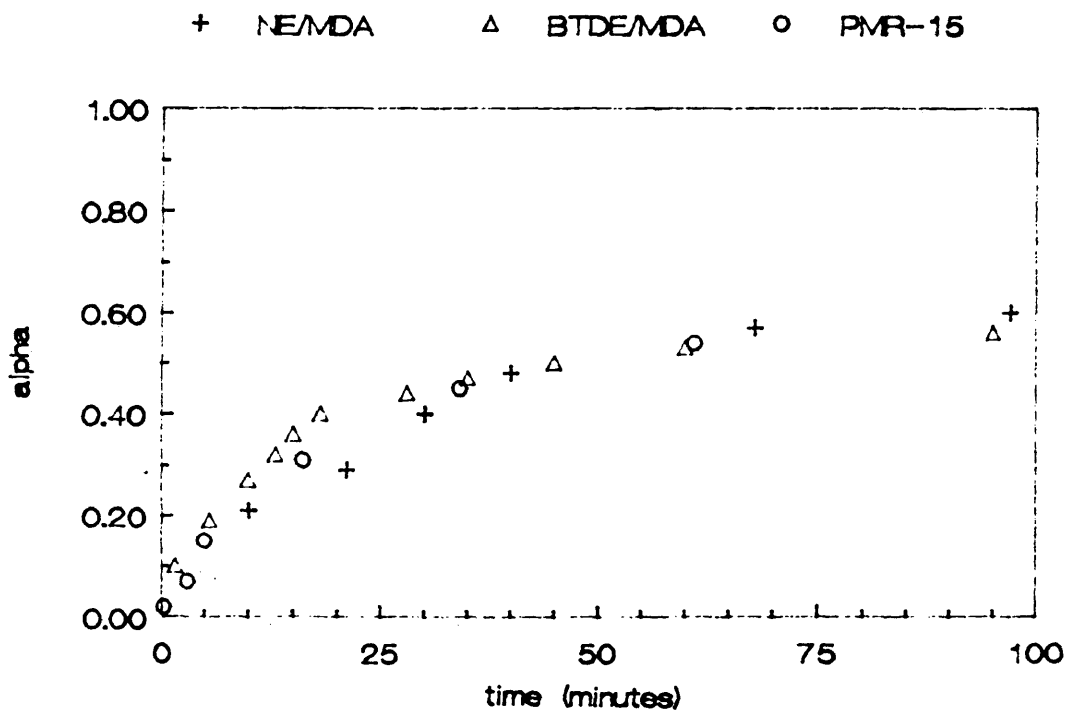


Figure 3.5: Alpha vs. time for NE/MDA, BTDE/MDA, and PMR-15 at 120°C.

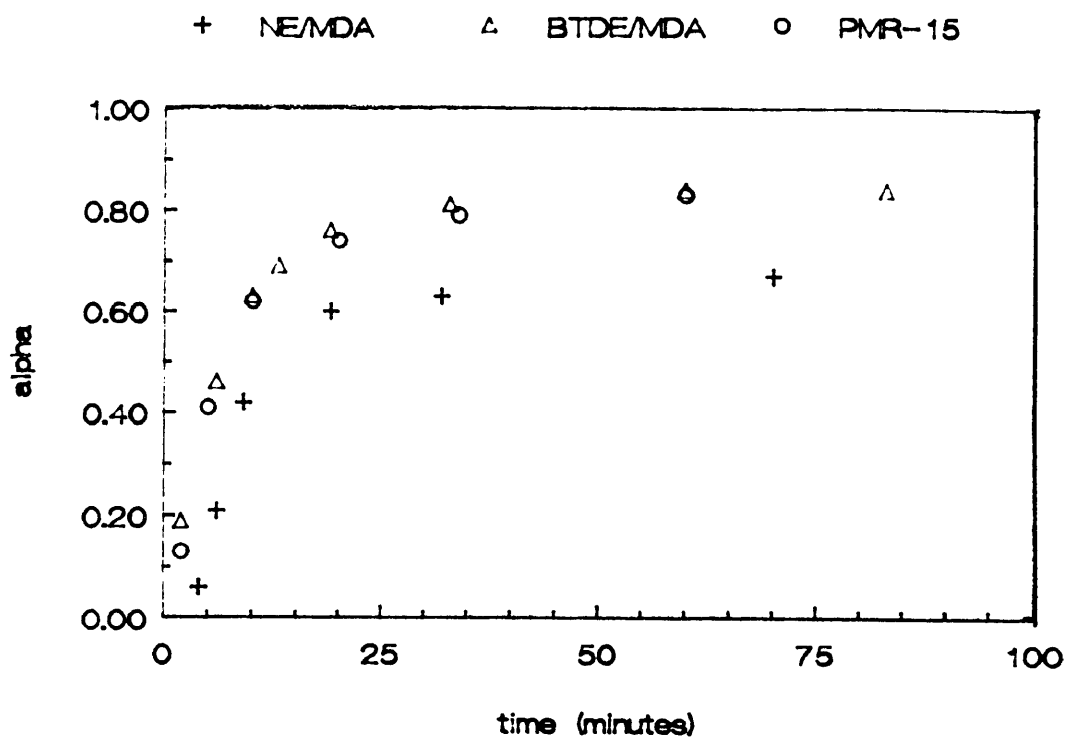


Figure 3.6: Alpha vs. time for NE/MDA, BTDE/MDA, and PMR-15 at 160°C.

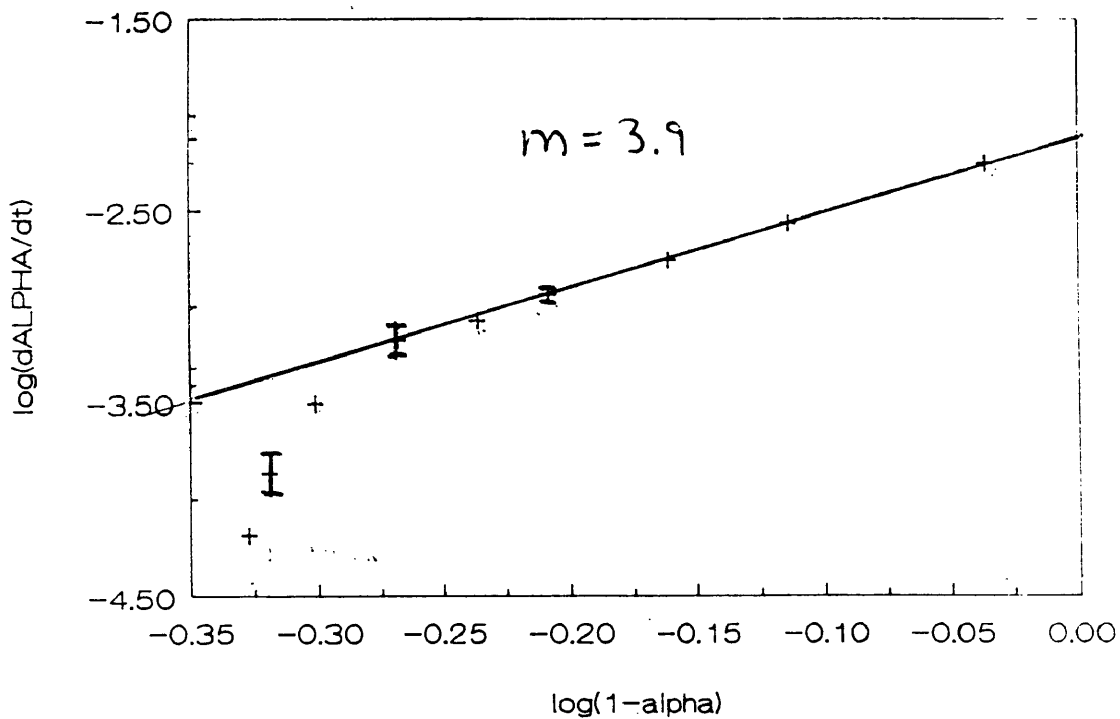


Figure 3.7: NE/MDA reaction order determination at 80°C (#1).

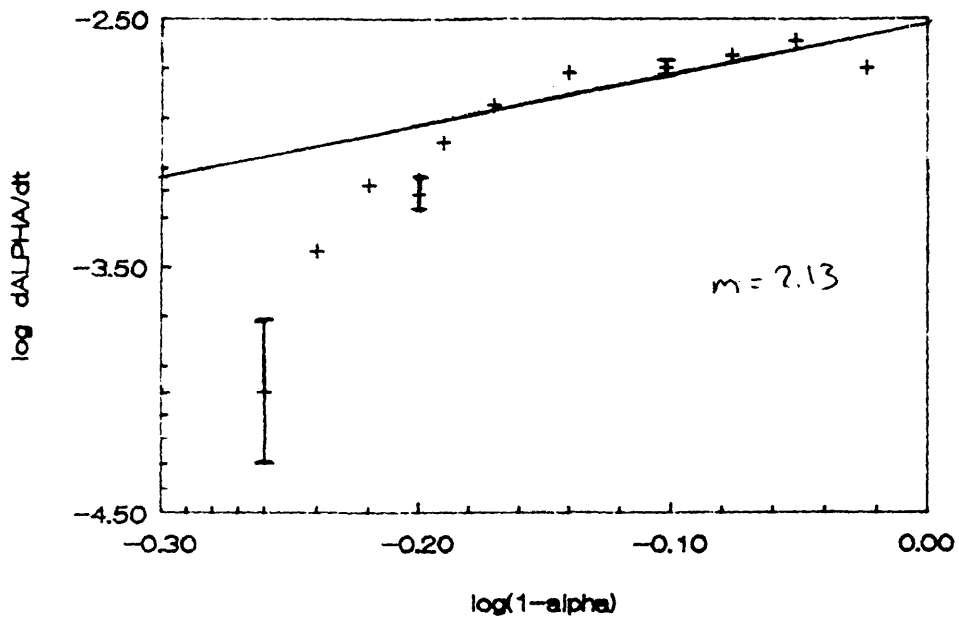


Figure 3.8: NE/MDA reaction order determination at 80°C (#2).

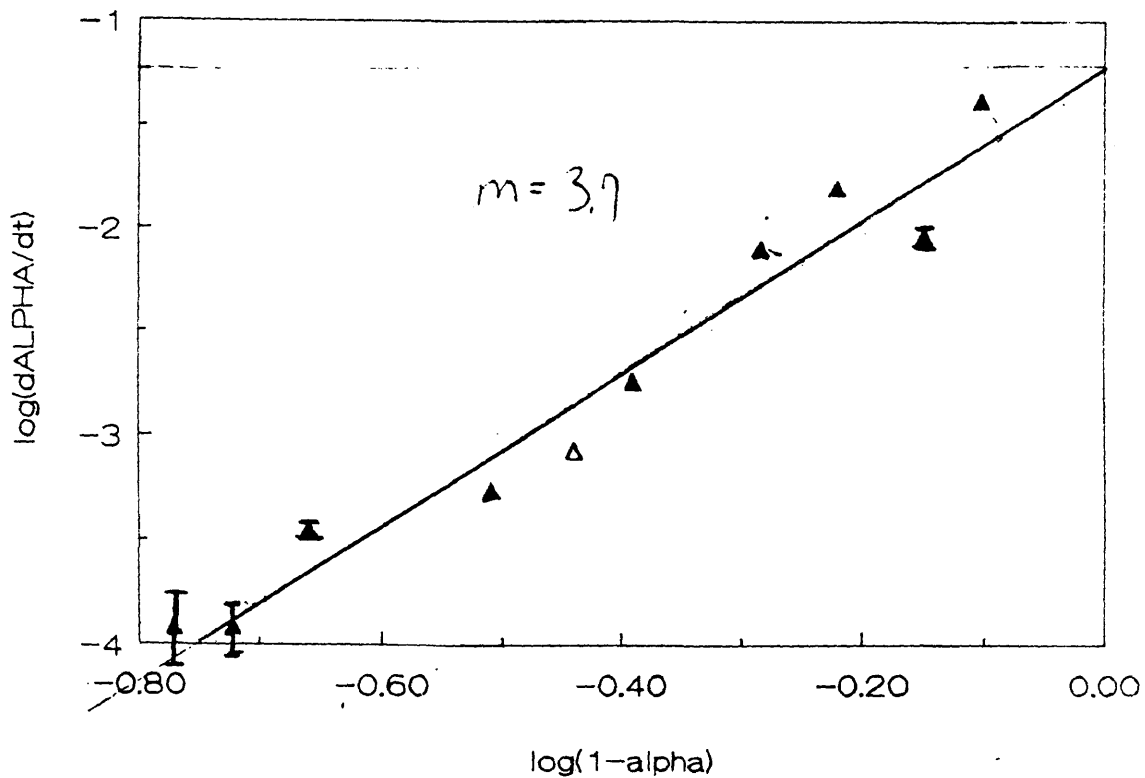


Figure 3.9: NE/MDA reaction order determination at 120°C.

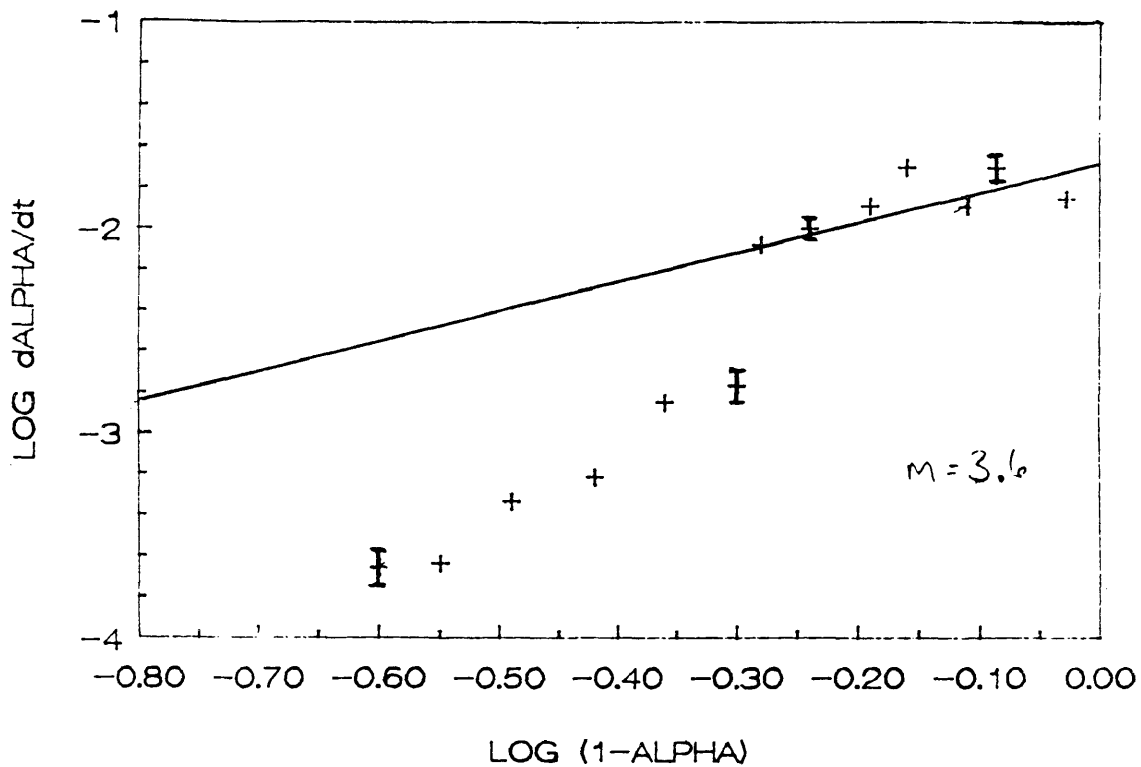


Figure 3.10: NE/MDA reaction order determination at 140°C .

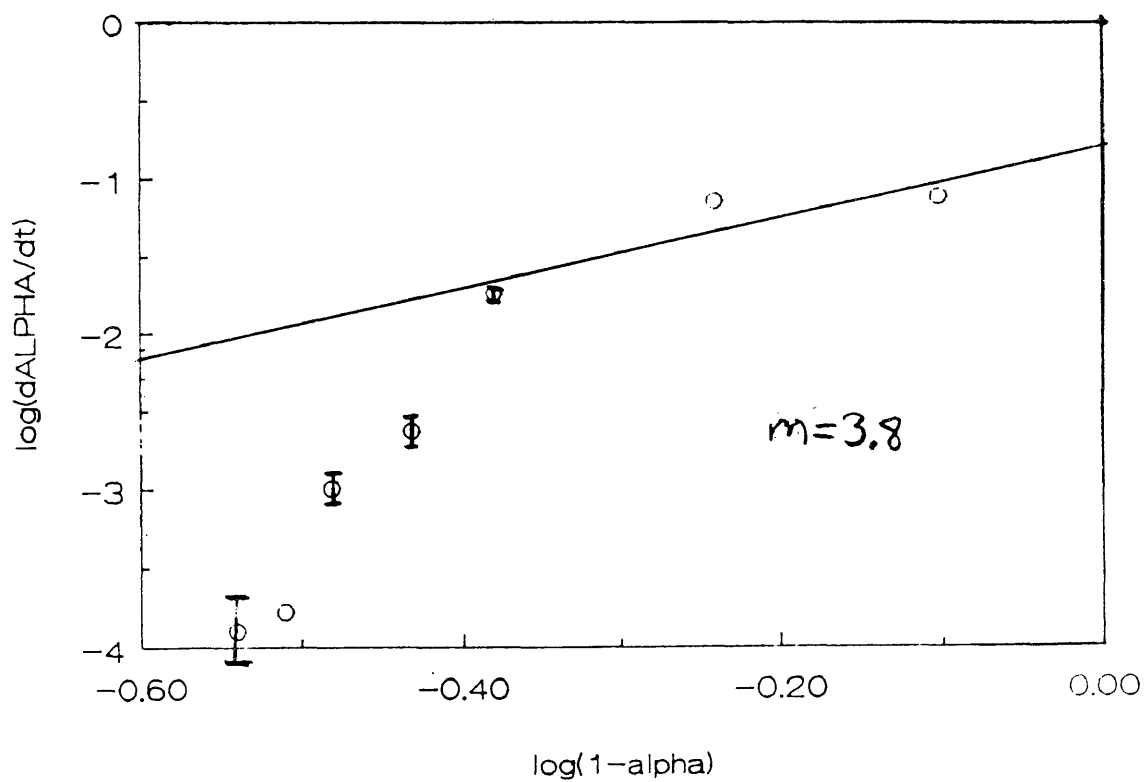


Figure 3.11: NE/MDA reaction order determination at 160°C (#1).

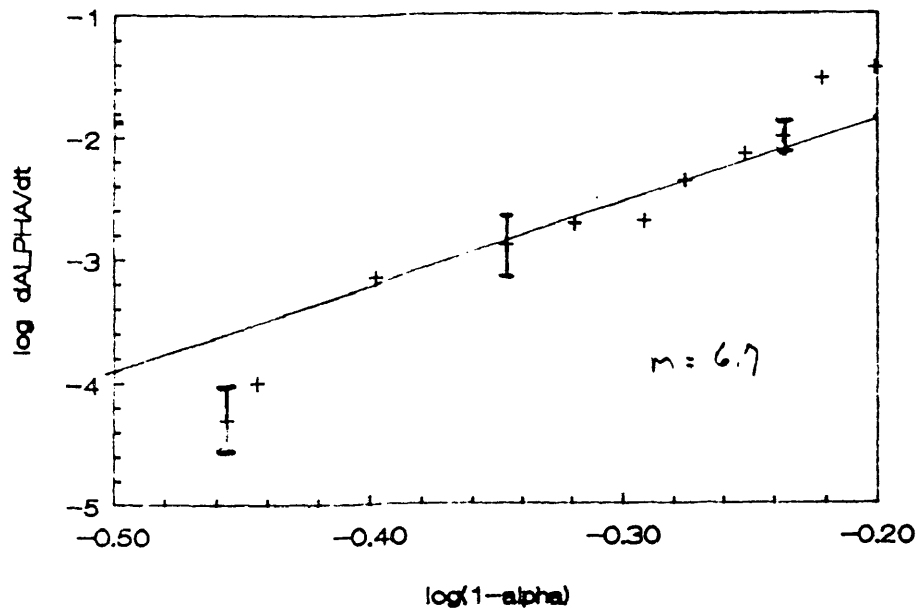


Figure 3.12: NE/MDA reaction order determination at 160°C (#2).

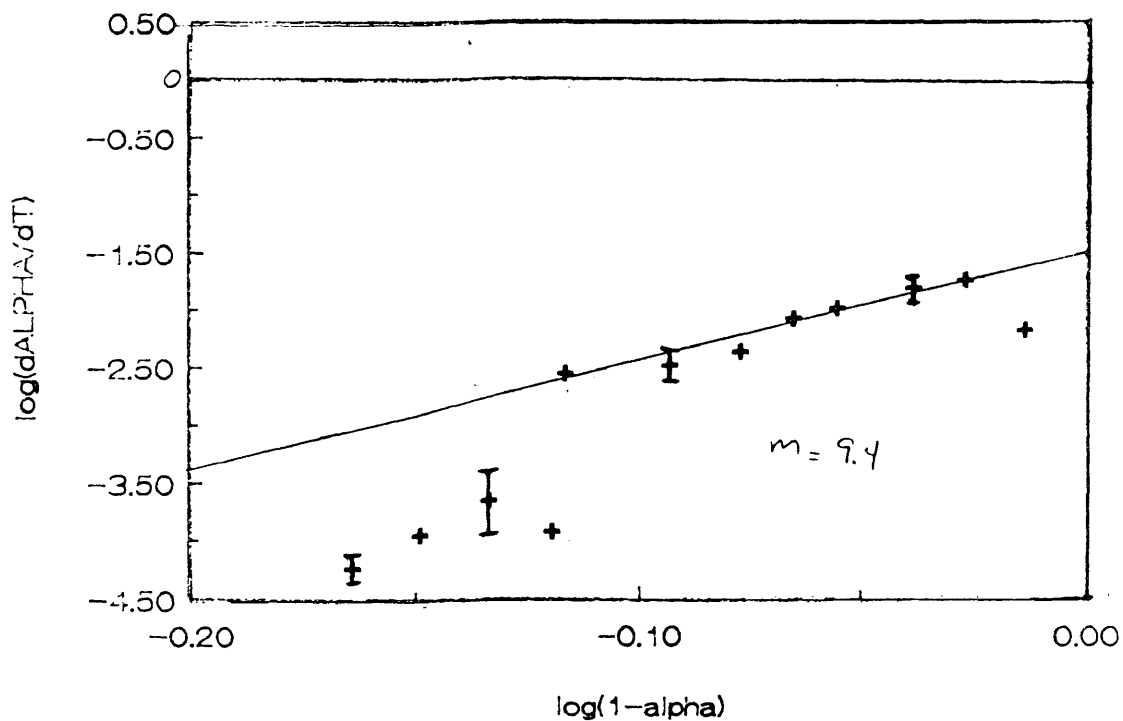


Figure 3.13: BTDE/MDA reaction order determination at 80°C.

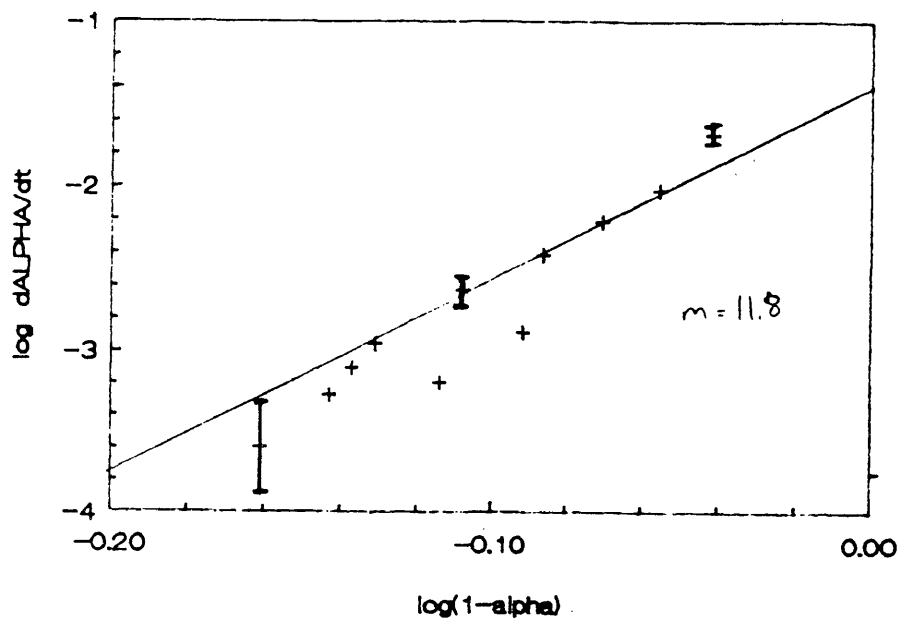


Figure 3.14: BTDE/MDA reaction order determination at 105°C (#1).

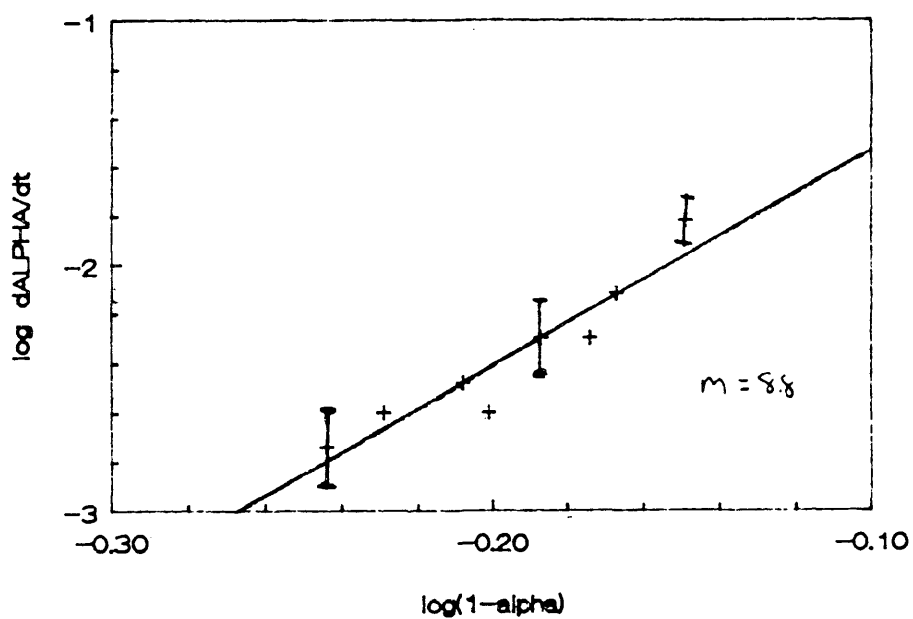


Figure 3.15: BTDE/MDA reaction order determination at 105°C (#2).

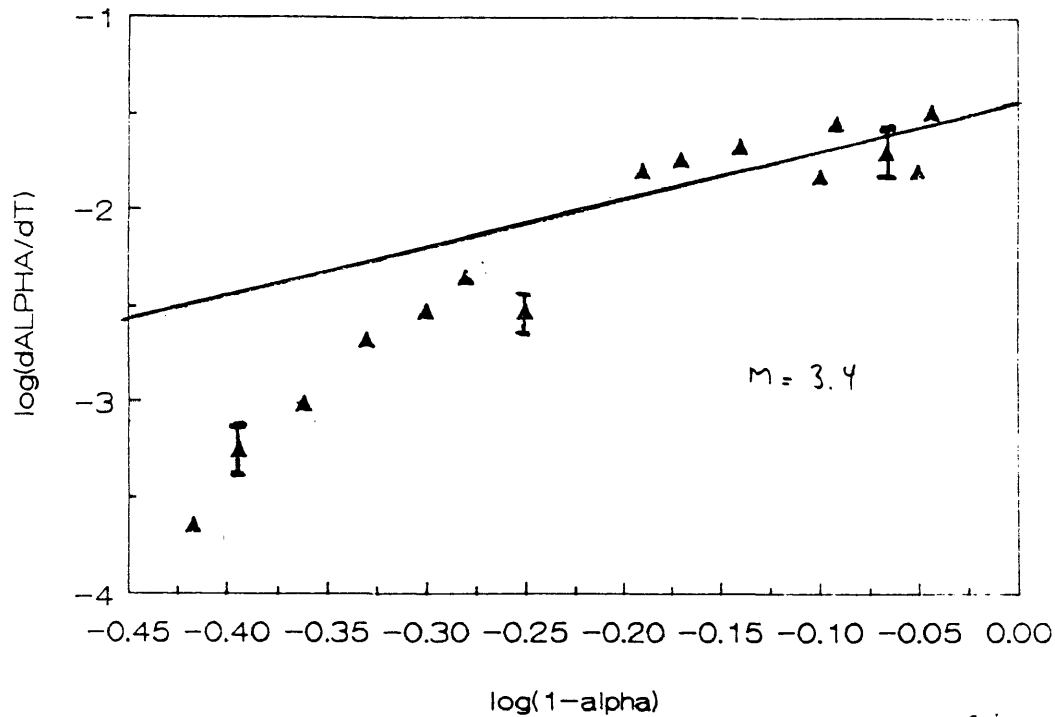


Figure 3.16: BTDE/MDA reaction order determination at 120°C .

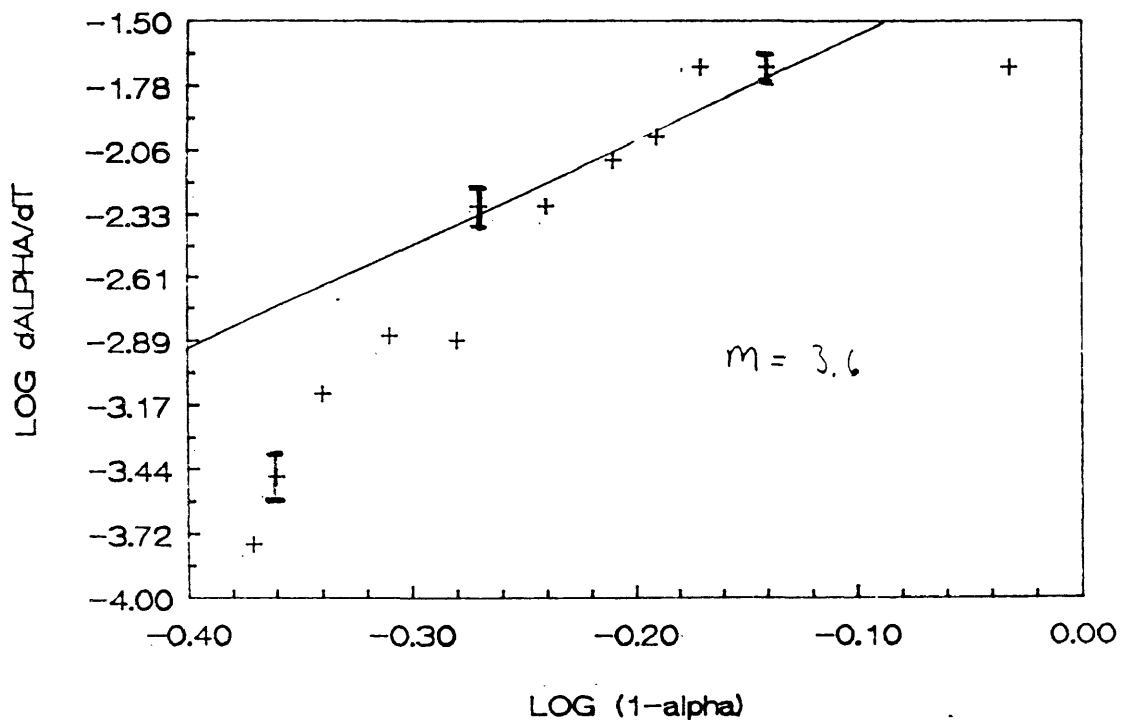


Figure 3.17: BTDE/MDA reaction order determination at 140°C .

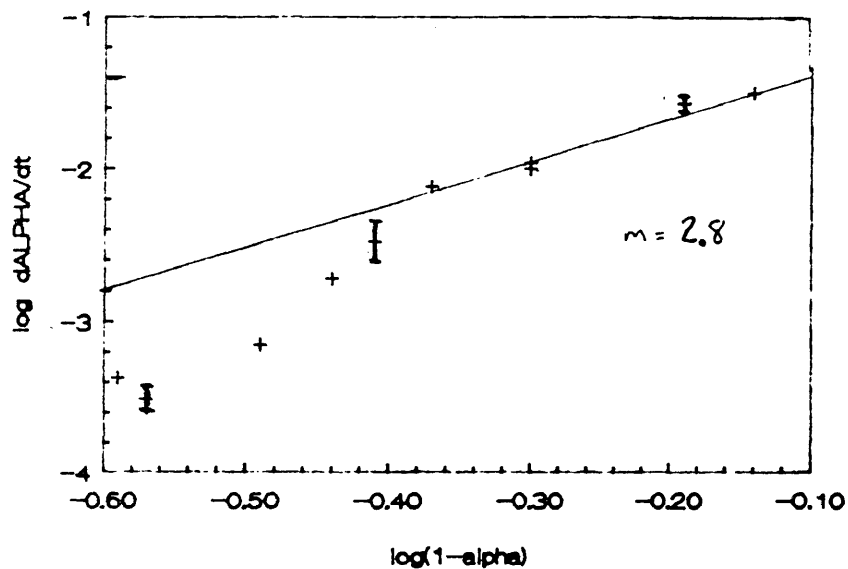


Figure 3.18: BTDE/MDA reaction order determination at 160°C.

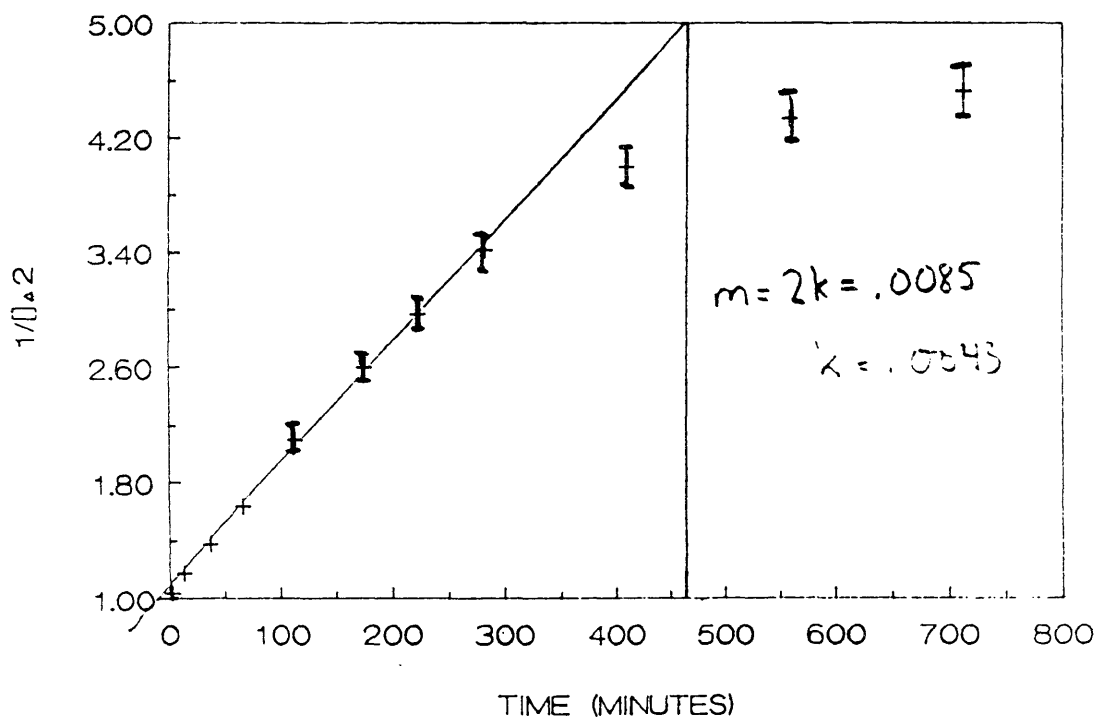


Figure 3.19: NE/MDA at 80°C (#1): 3rd order rate constant.

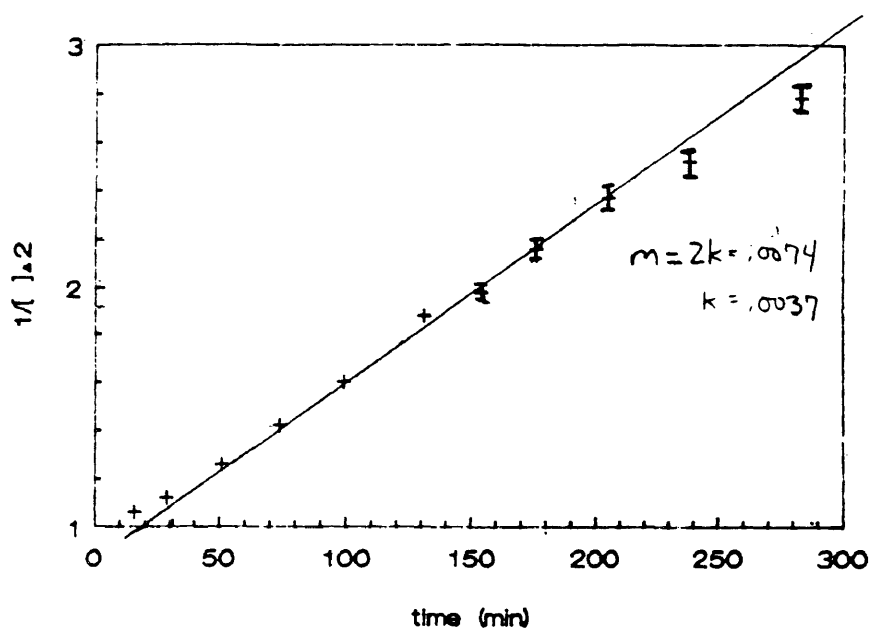


Figure 3.20: NE/MDA at 80°C (#2): 3rd order rate constant.

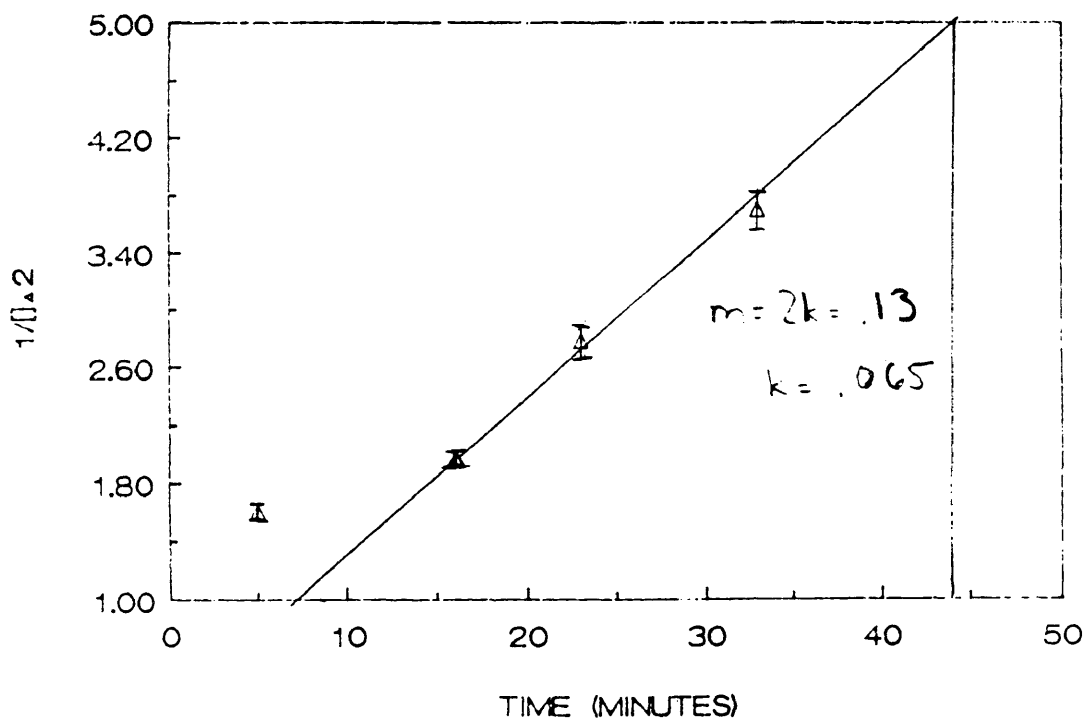


Figure 3.21: NE/MDA at 120°C: 3rd order rate constant.

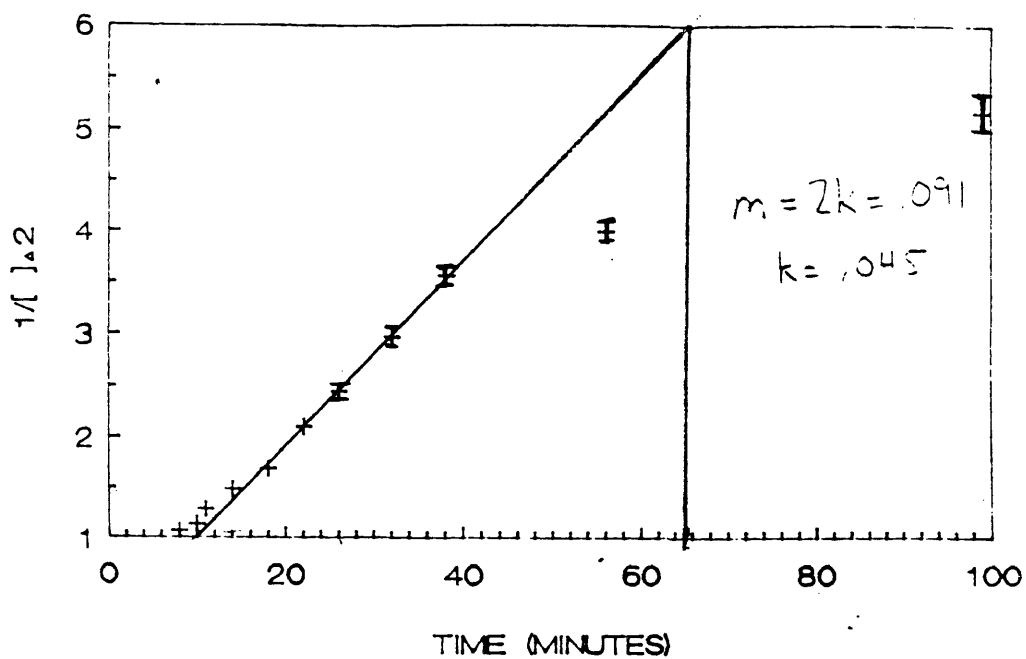


Figure 3.22: NE/MDA at 140°C: 3rd order rate constant.

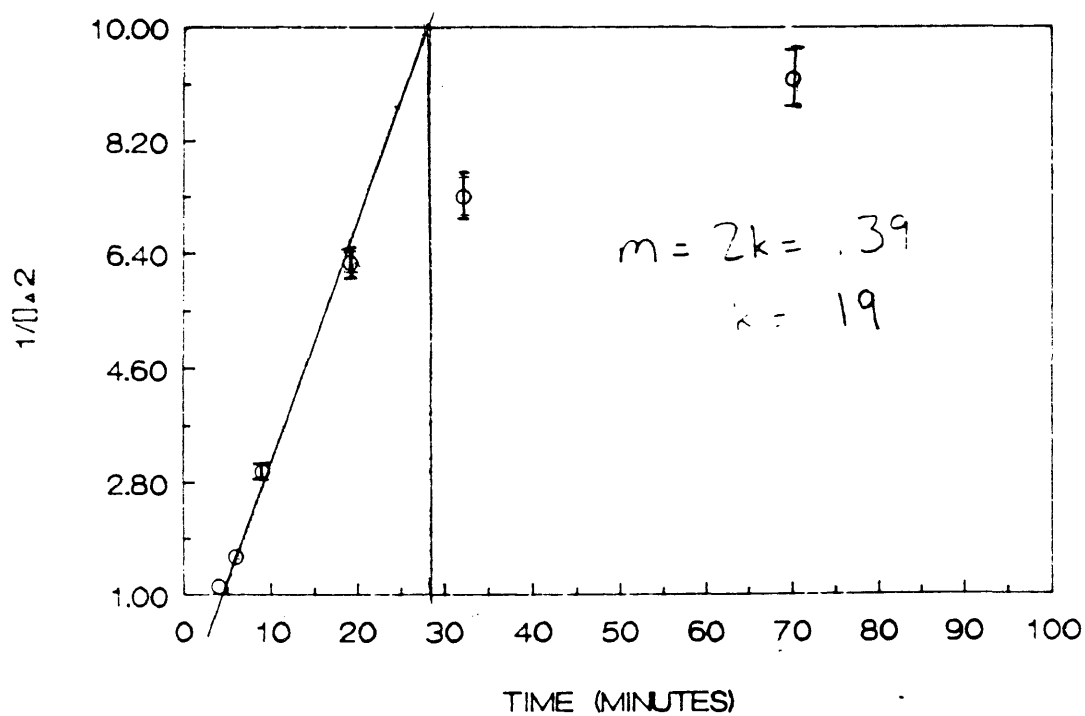


Figure 3.23: NE/MDA at 160°C (#1): 3rd order rate constant.

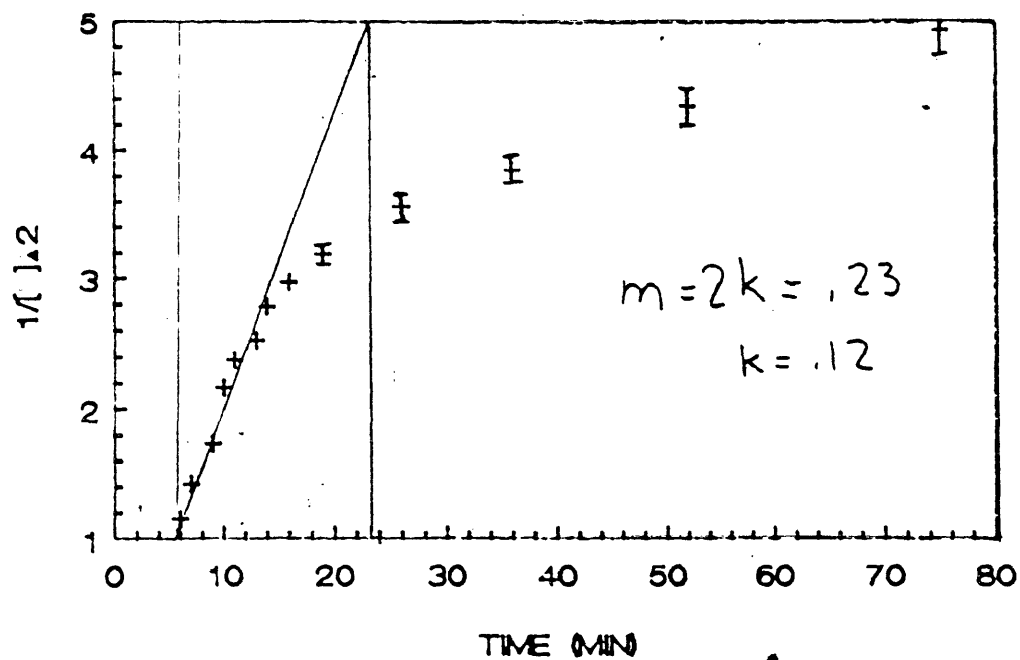


Figure 3.24: NE/MDA at 160°C(#2): 3rd order rate constant.

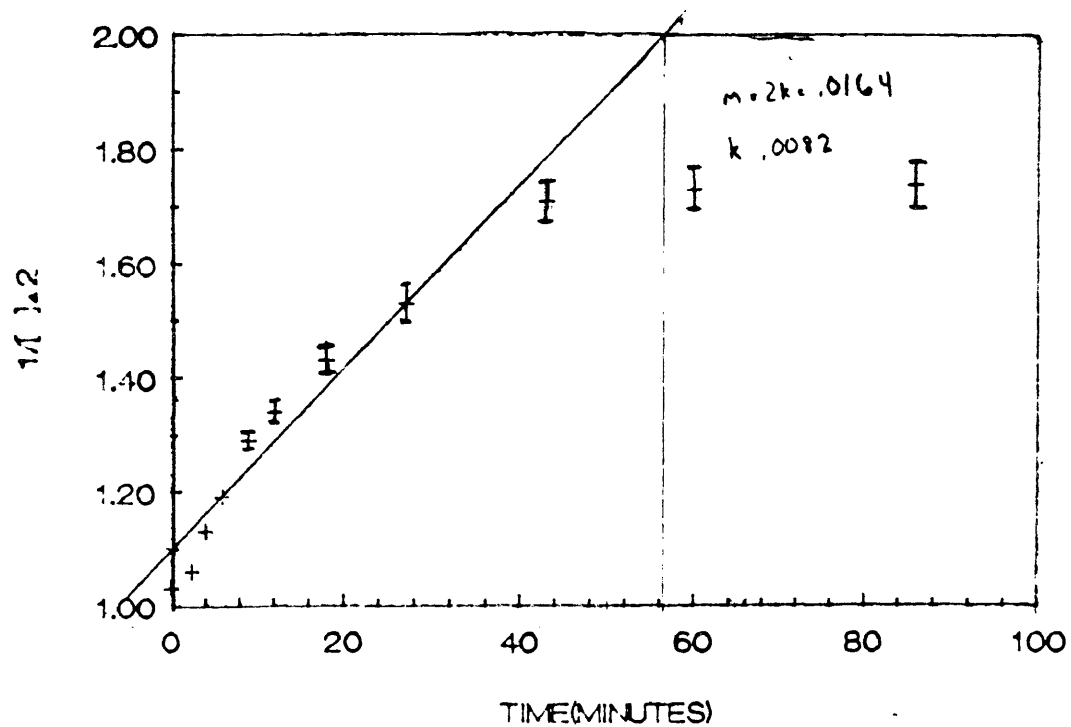


Figure 3.25: BTDE/MDA at 80°C: 3rd order rate constant.

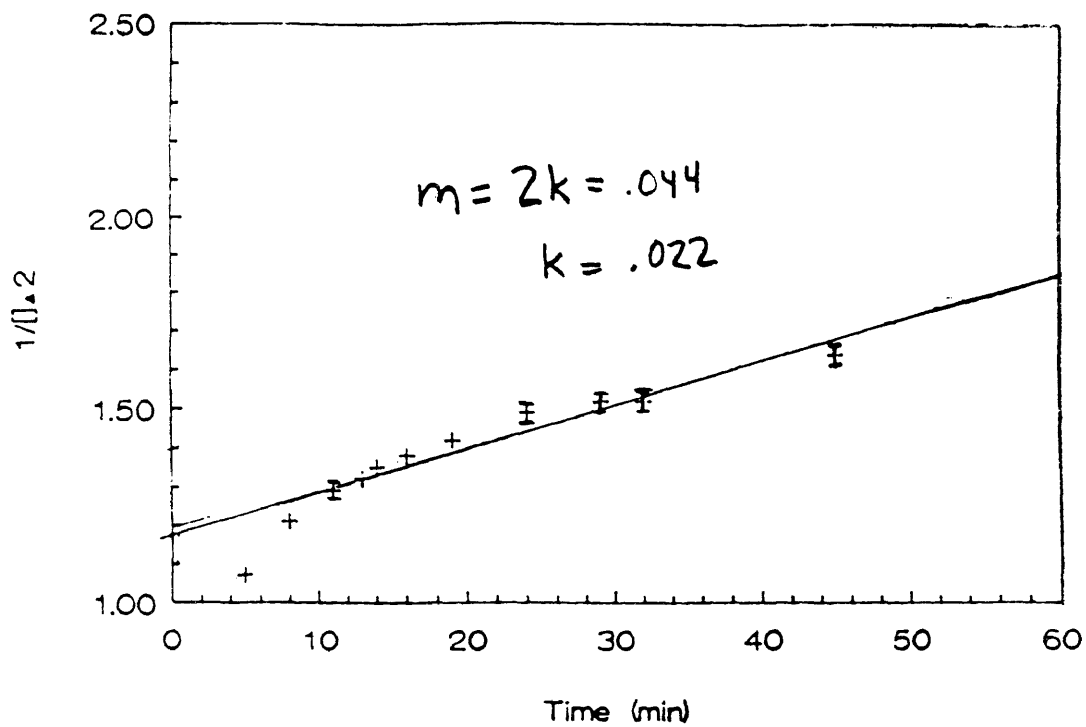


Figure 3.26: BTDE/MDA at 105°C (#1): 3rd order rate constant.

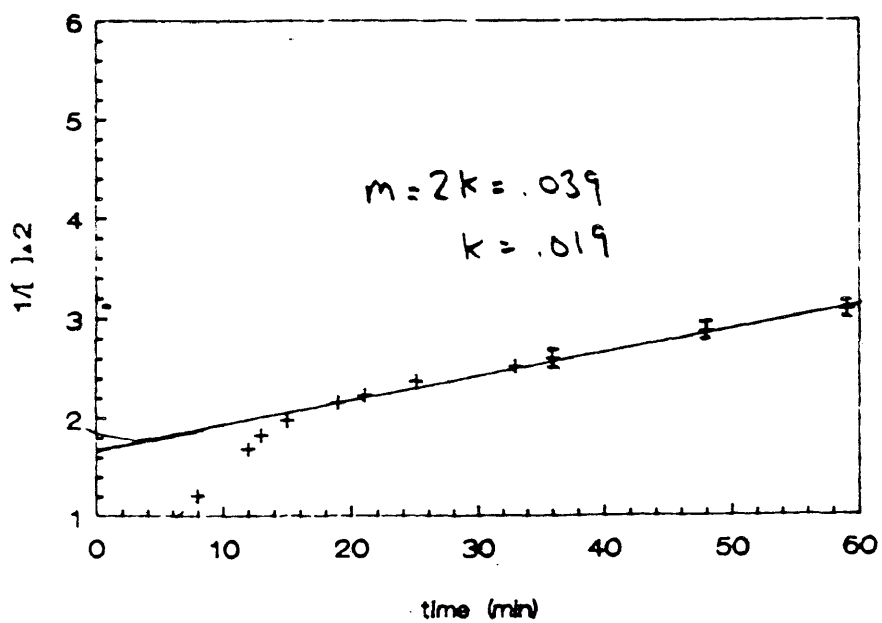


Figure 3.27: BTDE/MDA at 105°C (#2): 3rd order rate constant.

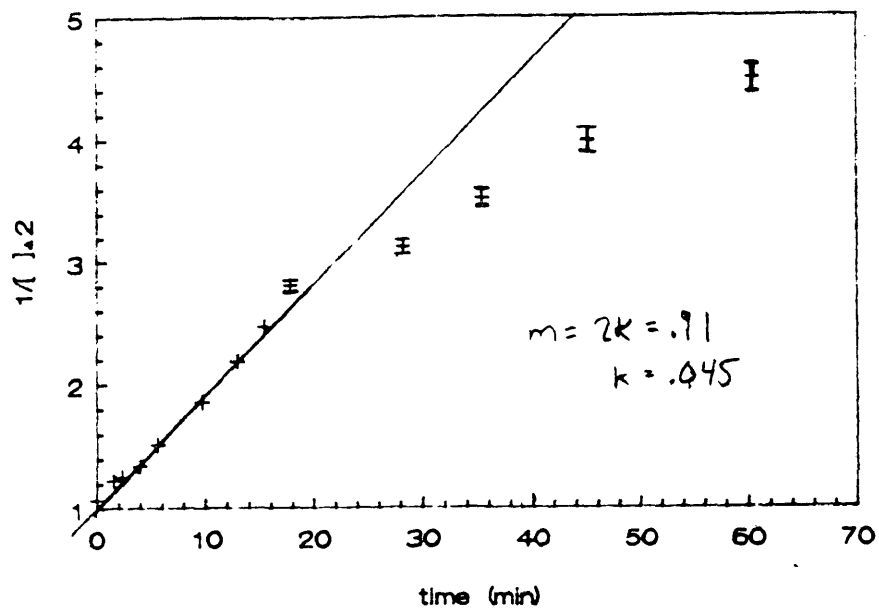


Figure 3.28: BTDE/MDA at 120°C: 3rd order rate constant.

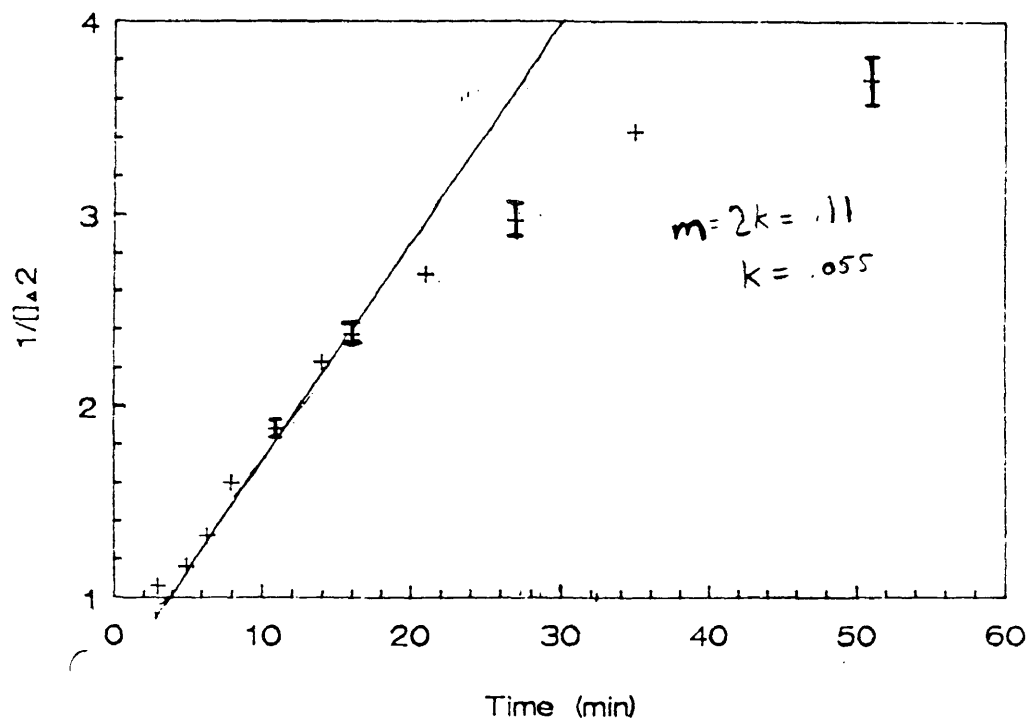


Figure 3.29: BTDE/MDA at 140°C: 3rd order rate constant.

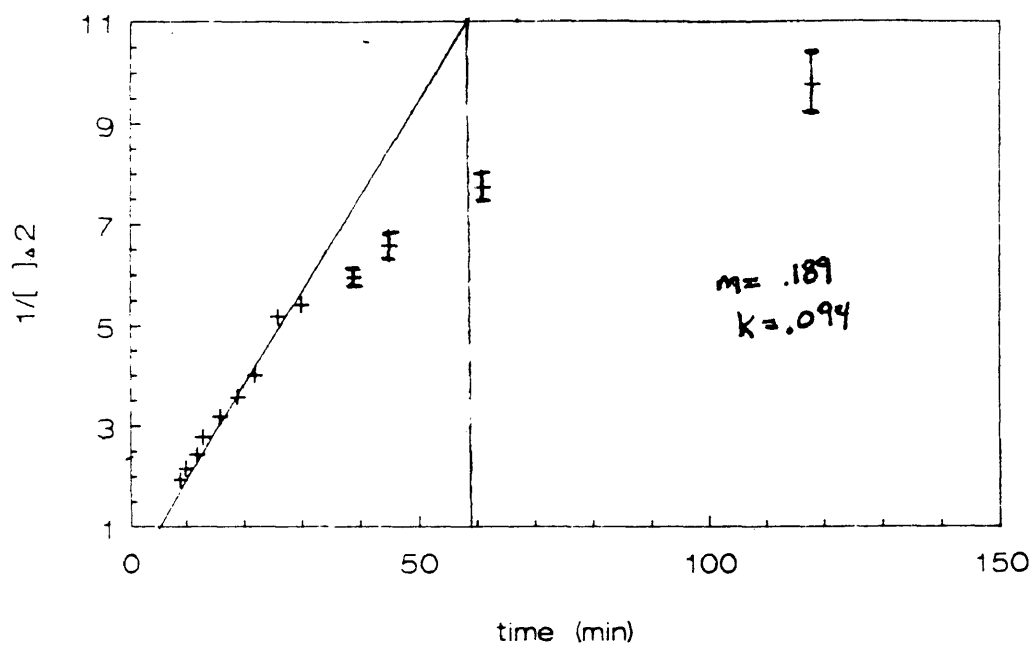


Figure 3.30: BTDE/MDA at 160°C: 3rd order rate constant.

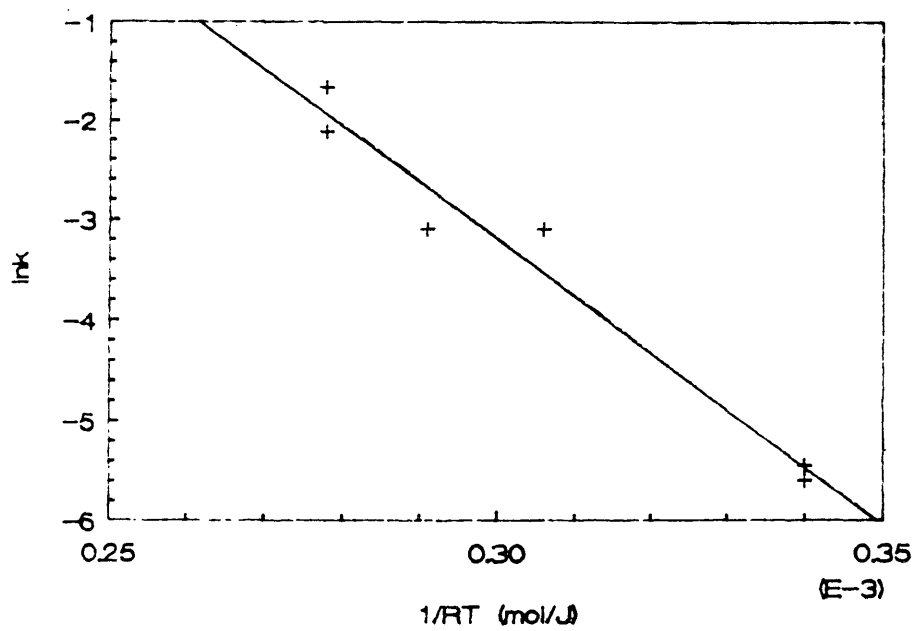


Figure 3.31: 2:1 NE/MDA: $\ln k$ vs. $1/RT$.

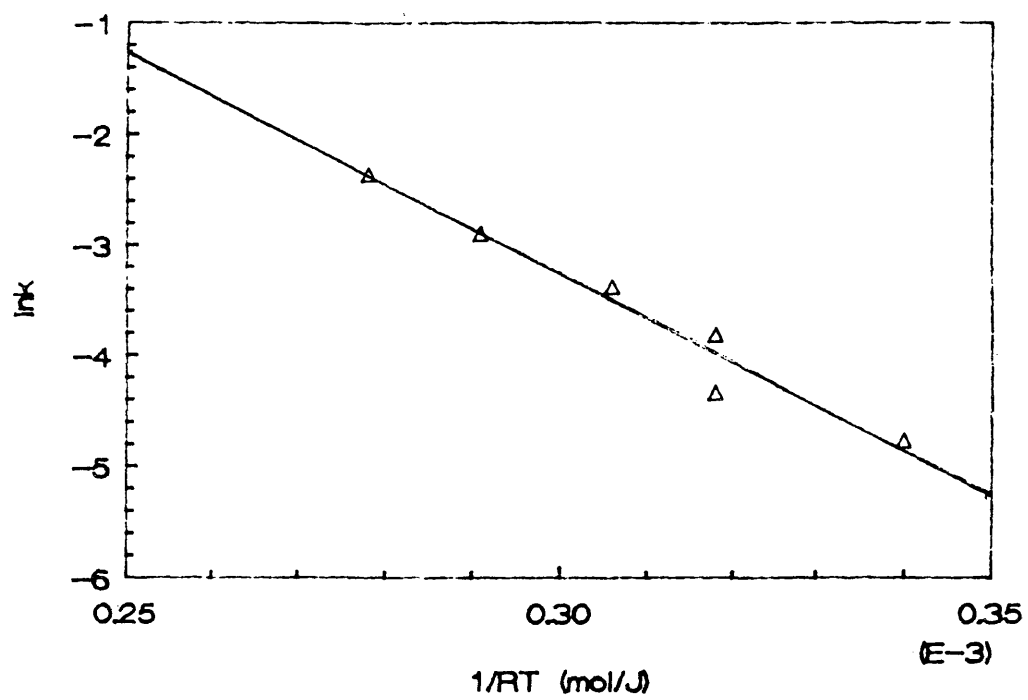


Figure 3.32: 1:1 BTDE/MDA: $\ln k$ vs. $1/RT$.

NOTES FOR CHAPTER III

1. R. Clark, Master's Thesis. College of William and Mary, 1989.
2. H.M. Walton, J. Org. Chem., 22, 308 (1957).
3. M. Whitham, Master's Thesis. College of William and Mary, 1986.
4. G.W. Castellan, Physical Chemistry, Reading, MA: Addison-Wesley, 1983, 3rd edition.
5. S.E. Delos, R.K. Schellenberg, J.E. Smedley, and D.E. Kranbuehl, J. Appl. Polymer Sci., 27, 4295 (1982).

CHAPTER IV

A COMPUTERIZED KINETIC MODEL OF
THE PMR-15 IMIDIZATION REACTION

The final stage of this study of PMR-15 uses the information gained from the kinetic studies of the imidization reaction to build a computer simulation of chain growth at any given temperature. The program described below monitors the formation of all possible chains (up to a given length) from a stoichiometric mixture of the three PMR-15 monomers at a given temperature using the two rate constants for that temperature.

First, a system of nomenclature was devised to categorize the species present in the reacting mixture. In this system BTDE is designated "B", MDA is designated "M", and NE is designated "N". Besides monomers, there are 6 basic types of species (chains) present in the reacting PMR-15 system.

1.) Chains capped on each end by a BTDE unit. These are hereafter designated as BB(N), where N equals the number of MDA units in the chain. For example, the chain B-M-B-M-B is BB(2). BB(0) is simply the BTDE monomer.

2.) Chains capped on one end by BTDE and the other end by MDA. These designated BM(N), where N equals the number of BTDE units between the endgroups. Thus BM(0) is B-M, BM(2) is

B-M-B-M-B-M, etc.

3.) Chains capped on both ends by MDA. These are designated MM(N), and N equals the number of BTDE units in the chain.

4.) Chains capped on one end by NE and the other by BTDE. The chains are designated NEMB(N), and N is the number of BTDE units between the end groups (as in category 2 above).

5.) Chains capped on one end by NE and the other by MDA. The chains are designated NEMM(N) and N is the number of BTDE units in the chain.

6.) Chains capped on both ends by NE. They are called NN(N), and N is the number of BTDE units in the chain. Since we assume no chain degradation, these chains are unreactive and thus final products.

Some basic assumptions are made to simplify the model. As in the TGA studies in Chapter III, there are assumed to be only two rate constants: one for amine reacting with BTDE acid/ester and one for amine reacting with nadic acid/ester. Hence no distinction is made between the reaction rates of chains of different length.

Third order kinetics are assumed (see Chapter III). March and others have reported that the reaction between primary or secondary amine and ester is third order and involves two molecules of amine and one molecule of ester.^{1,2} This is consistent with an earlier study of PMR-15 by Dr. Kranbuehl which gave the reaction order as 3 or greater and gave the

rate equation as:

$$d[\text{imide}] = k[\text{amine}]^2[\text{acid/ester}]dt \quad (13).^3$$

Therefore the same rate equation was used for this simulation.

As stated in Chapter III, TGA studies indicate that rate constants become increasingly dependent upon decreasing functional group mobility as the viscosity of the reaction medium increases. The model does not take into account this phenomenon.

A brief description of the computer program (file name NEWPMR3.BAS), written in the Microsoft Quickbasic language, follows. (A printout of the program is included at the end of this chapter.)

First a temperature is assigned. From this temperature is calculated the rate constants for the two reactions using the Arrhenius expression given in Chapter III (equation 12). K1 is the rate constant for the BTDE/MDA reaction, and K2 is the rate constant for the NE/MDA reaction.

The initial dry concentrations of the three reactants -- NE, BB(0), and MM(0) -- are given for one mole of reactants. The change in concentrations of all possible species are calculated by the third order rate equation:

$$d[\text{species}] = K[\text{amine}]^2[\text{acid/ester}]dt \quad (13)$$

where $K = K1$ or $K2$ in $\text{mol}^{-2} \cdot \text{min}^{-1}$ and dt is the chosen time interval. A subprogram was written for the formation of each

of the six types of chains. Each subprogram calculates the concentration change for $N = 0$ to 5. (Concentrations of longer chains are assumed to be insignificant.) Since with increasing N there are an increasing number of possible chain combinations to form a chain of that N , the number of possibilities of chain combination are accounted for in subloops of each subprogram. For example, for a chain of $BB(N)$ there are N different possibilities of chain combination to form that chain.

After going through the six subroutines for the specified time interval, printouts are obtained for the concentration of each species at that point in the reaction.

Alpha (degree of conversion) is calculated for each time by dividing the total number of imide linkages present by the number possible. Since there are .4303 MDA molecules present in a mole of unreacted PMR-15 and each MDA possesses two amines, the total possible here is .8606.

A useful and simple method of characterizing the chains in the reacting mixture is by the number of imides present in each chain. The number of imides is given by the number of monomer units in the chain minus one. Figures 4.1 - 4.4 show the imidization distribution over time for the PMR-15 reaction at 80°C, 120°C, 160°C, and 200°C. It is interesting to note that, in this model, we do not see a significant buildup of the concentration of the actual PMR-15 prepolymer molecule (NN(2), #imides = 6) even at 200°C (mole fraction = .003 at

300 minutes). The most populous species here are those with #imides = 2 (NMN, BMB, MBM, and NMB). The longer chains are present in a broad distribution of small concentrations. Chains of 7 imides and greater are not plotted in Figures 4.1 - 4.4 because their concentrations are very small (mole fraction = .005 or less).

To better compare the concentration buildup of the longer chains, the data from Figures 4.1 - 4.4 were plotted using a semi-log scale. The results are shown in Figures 4.5 - 4.8. These figures are better for comparing the expected concentration buildups of longer chains at the higher temperatures.

To see the interplay of the two reactions' rate constants in the overall reaction, the simulation was next run in three hypothetical cases:

- 1.) $k(\text{NE/MDA})$ is twice as large as $k(\text{BTDE/MDA})$;
- 2.) $k(\text{NE/MDA})$ is equal to $k(\text{BTDE/MDA})$;
- 3.) $k(\text{NE/MDA})$ is half as large as $k(\text{BTDE/MDA})$.

Figures 4.9 - 4.11 show the chain distributions versus alpha for the three simulations. (These figures show concentrations of chains with #imides = 0, 1, 2, 3, 4, 5, 6, and 8. Other chains' concentrations are smaller and not plotted.) As above, these data were also plotted with a semi-log scale (Figures 4.12 - 4.14). The concentrations of each species for each case at alpha = .98 is given in Table 4a.

The first observation to be made here is that, as

predicted, a large amount of species of two imides remains in the first case. As $k(\text{BTDE}/\text{MDA})$ increases relative to $k(\text{NE}/\text{MDA})$ (i.e. from Case 1 to Case 2 to Case 3), there are less of the two imide species present. This is explained by the buildup of bisnadimide ($\text{NN}(0)$, #imides = 2) when the NE/MDA reaction is the faster one.

Similarly, chains with an even number of imides show a significant buildup at the late stages of the reaction in all three cases. This is due to the buildup of the non-reactive, doubly endcapped species (all with #imides even); in all three cases, species with #imides odd disappear as alpha approaches one.

In Table 4a, we see that, as $k(\text{BTDE}/\text{MDA})$ increases relative to $k(\text{NE}/\text{MDA})$, the concentrations of the longer chains (those with #imide = 8, 10, 12) are greater. However, there are more of the smaller chains (those with #imide = 2 and 4) when the NE/MDA reaction is the faster one. This is as expected, since less of the smaller chains would be end-capped in Case 3 and thus free to react further to form the larger chains.

Finally, this simulation shows that the prepolymer of molecular weight 1500 shown in the general PMR-15 mechanism (Figure 1.2) is only the average; there is really a very broad distribution of molecular weights in a mixture of imidized PMR-15.

An average imidization analogous to number average

molecular weight is given by:

$$\text{avg. imidization} = \frac{\sum (N_i * i)}{N_{\text{tot}}} \quad (14)$$

where i is the number of imides in given chain, N_i is the number of chains with i imides, and N_{tot} is the total number of chains.

Figure 4.15 shows the average imidization versus alpha for PMR-15. This model predicts that the expected average

Table 4a

Chain concentrations for PMR-15
at alpha = .98

$x = k(\text{NE}/\text{MDA}) / k(\text{BTDE}/\text{MDA})$

#imides	x = 2	x = 1	x = .5
0	.010	.034	.050
1	.002	.002	.001
2	.083	.062	.038
3	.002	.002	.001
4	.044	.042	.035
5	.002	.002	.002
6	.025	.026	.026
7	.002	.002	.001
8	.014	.016	.018
9	.002	.002	.001
10	.009	.010	.012
11	.001	.001	.001
12	.005	.005	.008

avg. imidization	3.78	3.87	3.98

imidization of 6 is reached only very late in the reaction. Table 4a lists the average imidizations at alpha = .98. The

data shows that average imidization increases as $k(\text{BTDE/MDA})$ increases relative to $k(\text{NE/MDA})$.

CONCLUSIONS

Though the model described above is by no means meant to be a quantitative analysis of species distribution in the PMR-15 system, it is useful in demonstrating that there is a broad distribution of species in the reacted mixture. In addition it can be used to see the effect of the interplay between the two reactions: one essentially a propagation reaction and the other a termination reaction. Varying the temperature (i.e. varying the ratio of $k(\text{NE/MDA})$ to $k(\text{BTDE/MDA})$) not only affects the rate of chain growth, but also the lengths and types of chains formed. Finally it shows that the final expected average molecular weight of PMR-15 prepolymer (m.w. = 1500, #imides = 6) is reached only as α approaches unity.

```

DECLARE SUB NNSUB ( )
DECLARE SUB NMBSUB ( )
DECLARE SUB NMMSUB ( )
DECLARE SUB BBSUB ( )
DECLARE SUB MMSUB ( )
DECLARE SUB BMSUB ( )

COMMON SHARED /VARIABLES/ T, BM(), MM(), BB(), NE, NEMM(), NEMB(), NN(), SUMdBm1
(), SUMdBm2(), SUMdMM(), SUMdBB(), dBm1(), dBm2(), dBb(), dMM(), K1, K2, DT
DIM BB(0 TO 11), MM(0 TO 11), BM(0 TO 11), NEMM(0 TO 11), NEMB(0 TO 11), NN(0 TO
11), SUMdSM1(0 TO 11), SUMdBm2(0 TO 11), SUMdMM(0 TO 11), SUMdRB2(0 TO 11), SUMd
NEMM2(0 TO 11), SUMdNEMM3(0 TO 11), SUMdNEMB2(0 TO 11), SUMdNEMB3(0 TO 11), SUMd
NN2(0 TO 11)
DIM dBm1(0 TO 11), dBm2(0 TO 11), dBb(0 TO 11), dMM(0 TO 11), dNEMM1(0 TO 11), d
NEMM2(0 TO 11), dNEMM3(0 TO 11), dNEMB2(0 TO 11), dNEMB3(0 TO 11), dNN1(0 TO 11)
, dNN2(0 TO 11)
DIM IMIDE(12)

TEMP = 80
LPRINT "PMR-15 KINETICS"
LPRINT "TEMPERATURE="; TEMP; "C"
BB(0) = .2909
MM(0) = .4303
NE = .2788
K1a = 6260 * EXP(-40000 / (8.314 * (TEMP + 273)))
K2a = 1100000 * EXP(-57000 / (8.314 * (TEMP + 273)))
DT = 5
K1 = K1a * DT / 60
K2 = K2a * DT / 60
LPRINT "K(BTDE/MDA)="; K1a
LPRINT "K(NE/MDA)="; K2a
LPRINT "DT="; DT
LPRINT ""

FOR T = 1 TO 100
FOR Z = 1 TO 120
CALL BMSUB
CALL MMSUB
CALL BBSUB
CALL NMMSUB
CALL NMBSUB
CALL NNSUB
NEXT Z

T1 = T * 2
LPRINT "T="; T1; "MINUTES"
LPRINT "NE "; NE

SUMchain = NE
SUMTOTimide = 0
FOR N = 0 TO 6
dSUMchain = MM(N) + BB(N) + BM(N) + NEMM(N) + NEMB(N) + NN(N)
SUMchain = SUMchain + dSUMchain
TOTimideMM(N) = 2 * N * MM(N)
TOTimideBB(N) = 2 * N * BB(N)
TOTimideBM(N) = (2 * N + 1) * BM(N)
TOTimideNEMM(N) = (2 * N + 1) * NEMM(N)
TOTimideNEMB(N) = (2 * N + 2) * NEMB(N)
TOTimideNN(N) = (2 * N + 2) * NN(N)
dSUMTOTimide = TOTimideMM(N) + TOTimideBB(N) + TOTimideBM(N) + TOTimideNEMM(N) +
TOTimideNEMB(N) + TOTimideNN(N)
SUMTOTimide = SUMTOTimide + dSUMTOTimide
NEXT N
NavgIMIDE = SUMTOTimide / SUMchain

```



```

FOR N = 0 TO 6
  imideMM = 2 * N
  imideBB = 2 * N
  imideBM = 2 * N + 1
  imideNEMM = 2 * N + 1
  imideNEMB = 2 * N + 2
  imideNN = 2 * N + 2
  LPRINT "MM("; N; ")", MM(N)
  LPRINT "  imides per chain =", imideMM
  LPRINT "BB("; N; ")", BB(N)
  LPRINT "  imides per chain =", imideBB
  LPRINT "BM("; N; ")", BM(N)
  LPRINT "  imides per chain =", imideBM
  LPRINT "NEMM("; N; ")", NEMM(N)
  LPRINT "  imides per chain =", imideNEMM
  LPRINT "NEMB("; N; ")", NEMB(N)
  LPRINT "  imides per chain =", imideNEMB
  LPRINT "NN("; N; ")", NN(N)
  LPRINT "  imides per chain =", imideNN
NEXT N

IMIDE(0) = NE + MM(0) + BB(0)
IMIDE(1) = BM(0) + NEMM(0)
IMIDE(2) = NEMB(0) + NN(0) + MM(1) + BB(1)
IMIDE(3) = BM(1) + NEMM(1)
IMIDE(4) = NEMB(1) + NN(1) + MM(2) + BB(2)
IMIDE(5) = BM(2) + NEMM(2)
IMIDE(6) = NEMB(2) + NN(2) + MM(3) + BB(3)
IMIDE(7) = BM(3) + NEMM(3)
IMIDE(8) = NEMB(3) + NN(3) + MM(4) + BB(4)
IMIDE(9) = BM(4) + NEMM(4)
IMIDE(10) = NEMB(4) + NN(4) + MM(5) + BB(5)
IMIDE(11) = BM(5) + NEMM(5)
IMIDE(12) = NEMB(5) + NN(5)

FOR P = 0 TO 12
  LPRINT "IMIDE("; P; ")="; IMIDE(P)
NEXT P

ALPHA = 0
FOR N = 0 TO 5
  DALPHA = ((2 * N + 1) * BM(N) + (2 * N) * MM(N) + (2 * N) * BB(N) + (2 * N + 1)
  * NEMM(N) + (2 * N + 2) * NEMB(N) + (2 * N + 2) * NN(N)) / .8606
  ALPHA = ALPHA + DALPHA
NEXT N
LPRINT "ALPHA = "; ALPHA
LPRINT "NavgIMIDE="; NavgIMIDE
LPRINT "-----"
NEXT T

```

```

SUB RESUB
FOR N = 0 TO 5
SUMdBB(N + 1) = 0
FOR i = 0 TO N
dBB(N + 1) = K1 * (BM(i) ^ 2) * 2 * BB(N - i) * DT
SUMdBB(N + 1) = SUMdBB(N + 1) + dBB(N + 1)
BM(i) = BM(i) - dBB(N + 1)
BB(N - i) = BB(N - i) - dBB(N + 1)
NEXT i
BB(N + 1) = BB(N + 1) + SUMdBB(N + 1)
NEXT N
END SUB

```

```

SUB BMSUB
FOR N = 0 TO 5
SUMdBM1(N + 1) = 0
SUMdBM2(N) = 0
FOR i = 0 TO N
dBM1(N + 1) = K1 * (BM(i) ^ 2) * BM(N - i) * DT
SUMdBM1(N + 1) = SUMdBM1(N + 1) + dBM1(N + 1)
BM(i) = BM(i) - dBM1(N + 1)
BM(N - i) = BM(N - i) - dBM1(N + 1)
dBM2(N) = K1 * 4 * (MM(i) ^ 2) * 2 * BB(N - i) * DT
SUMdBM2(N) = SUMdBM2(N) + dBM2(N)
MM(i) = MM(i) - dBM2(N)
BB(N - i) = BB(N - i) - dBM2(N)
NEXT i
BM(N) = BM(N) + SUMdBM2(N)
BM(N + 1) = BM(N + 1) + SUMdBM1(N + 1)
NEXT N
END SUB

```

```

SUB MMSUB
FOR N = 0 TO 5
SUMdMM(N + 1) = 0
FOR i = 0 TO N
dMM(N + 1) = K1 * 4 * (MM(i) ^ 2) * BM(N - i) * DT
SUMdMM(N + 1) = SUMdMM(N + 1) + dMM(N + 1)
MM(i) = MM(i) - dMM(N + 1)
BM(N - i) = BM(N - i) - dMM(N + 1)
NEXT i
MM(N + 1) = MM(N + 1) + SUMdMM(N + 1)
NEXT N
END SUB

```

```

SUB NMBSUB
FOR N = 0 TO 5
SUMdNEMB2(N + 1) = 0
SUMdNEMB3(N) = 0
dNEMB1(N) = K2 * (BM(N) ^ 2) * NE * DT
BM(N) = BM(N) - dNEMB1(N)
NE = NE - NEMB1(N)
FOR i = 0 TO N
dNEMB2(N + 1) = K1 * (BM(i) ^ 2) * NEMB(N - i) * DT
BM(i) = BM(i) - dNEMB2(N + 1)
NEMB(N - i) = NEMB(N - i) - dNEMB2(N + 1)
SUMdNEMB2(N + 1) = SUMdNEMB2(N + 1) + dNEMB2(N + 1)
dNEMB3(N) = K1 * (NEMM(i) ^ 2) * 2 * BB(N - i) * DT
NEMM(i) = NEMM(i) - dNEMB3(N)
BB(N - i) = BB(N - i) - dNEMB3(N)
SUMdNEMB3(N) = SUMdNEMB3(N) + dNEMB3(N)
NEXT i
NEMB(N) = NEMB(N) + dNEMB1(N) + SUMdNEMB3(N)
NEMB(N + 1) = NEMB(N + 1) + SUMdNEMB2(N + 1)
NEXT N
END SUB

```

```

SUB NMMSUB
FOR N = 0 TO 5
SUMdNEMM2(N + 1) = 0
SUMdNEMM3(N + 1) = 0
dNEMM1(N) = K2 * 4 * (MM(N) ^ 2) * NE * DT
MM(N) = MM(N) - dNEMM1(N)
NE = NE - dNEMM1(N)
FOR i = 0 TO N
dNEMM2(N + 1) = K1 * (NEMM(i) ^ 2) * BM(N - i) * DT
NEMM(i) = NEMM(i) - dNEMM2(N + 1)
BM(N - i) = BM(N - i) - dNEMM2(N + 1)
SUMdNEMM2(N + 1) = SUMdNEMM2(N + 1) + dNEMM2(N + 1)
dNEMM3(N + 1) = K1 * (4 * MM(i) ^ 2) * NEMB(N - i) * DT
MM(i) = MM(i) - dNEMM3(N + 1)
NEMB(N - i) = NEMB(N - i) - dNEMM3(N + 1)
SUMdNEMM3(N + 1) = SUMdNEMM3(N + 1) + dNEMM3(N + 1)
NEXT i
NEMM(N) = NEMM(N) + dNEMM1(N)
NEMM(N + 1) = NEMM(N + 1) + SUMdNEMM2(N + 1) + SUMdNEMM3(N + 1)
NEXT N
END SUB

```

```

SUB NNSUB
FOR N = 0 TO 5
SUMdNN2(N + 1) = 0
dNN1(N) = K2 * (NEMM(N) ^ 2) * NE * DT
NEMM(N) = NEMM(N) - dNN1(N)
NE = NE - dNN1(N)
FOR i = 0 TO N
dNN2(N + 1) = K1 * (NEMM(i) ^ 2) * NEMB(N - i) * DT
NEMM(i) = NEMM(i) - dNN2(N + 1)
NEMB(N - i) = NEMB(N - i) - dNN2(N + 1)
SUMdNN2(N + 1) = SUMdNN2(N + 1) + dNN2(N + 1)
NEXT i
NN(N) = NN(N) + dNN1(N)
NN(N + 1) = NN(N + 1) + SUMdNN2(N + 1)
NEXT N
END SUB

```

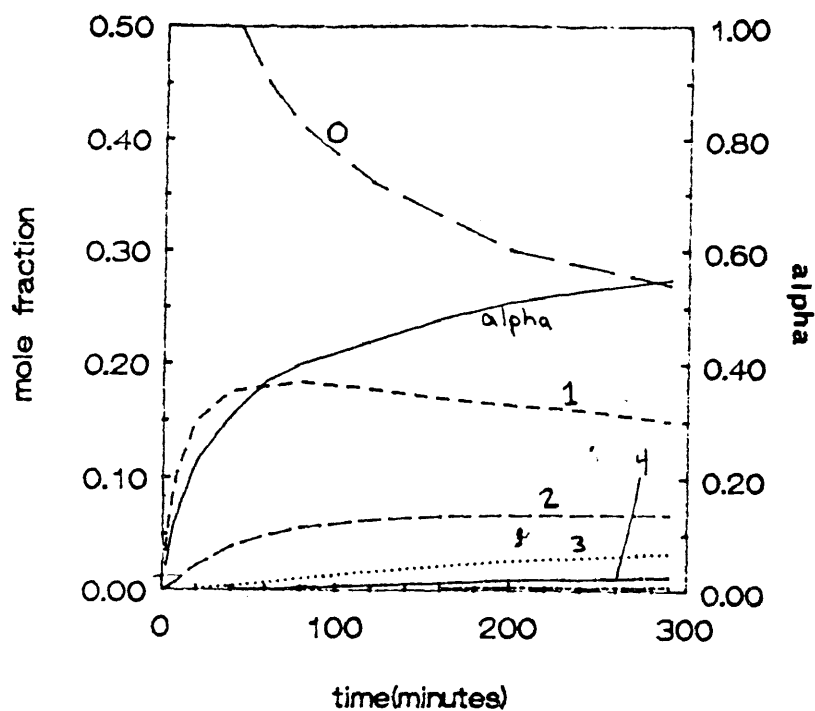


Figure 4.1: PMR-15 imidization simulation at 80°C: chain distribution vs. time.

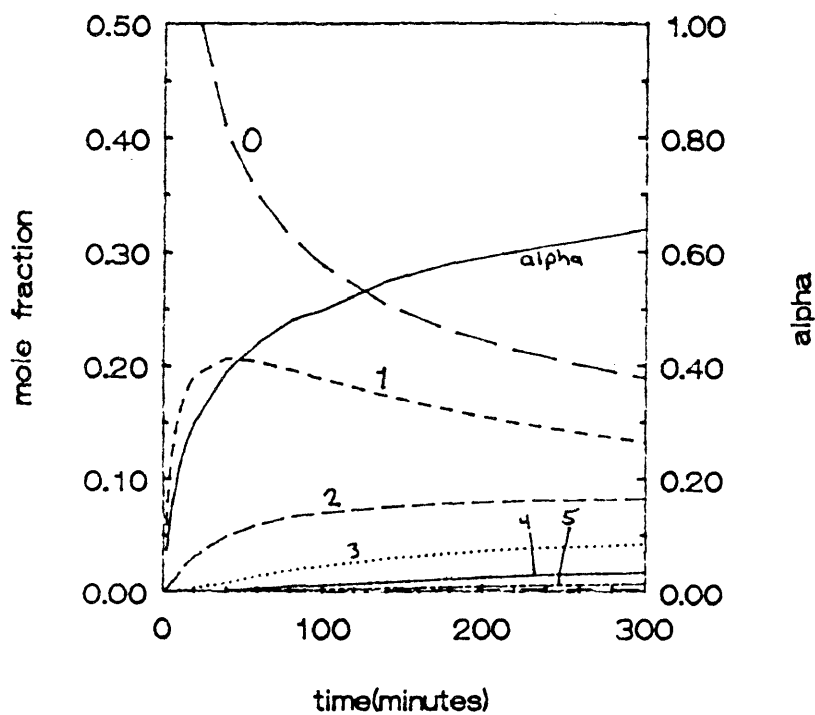


Figure 4.2: PMR-15 imidization simulation at 120°C: chain distribution vs. time.

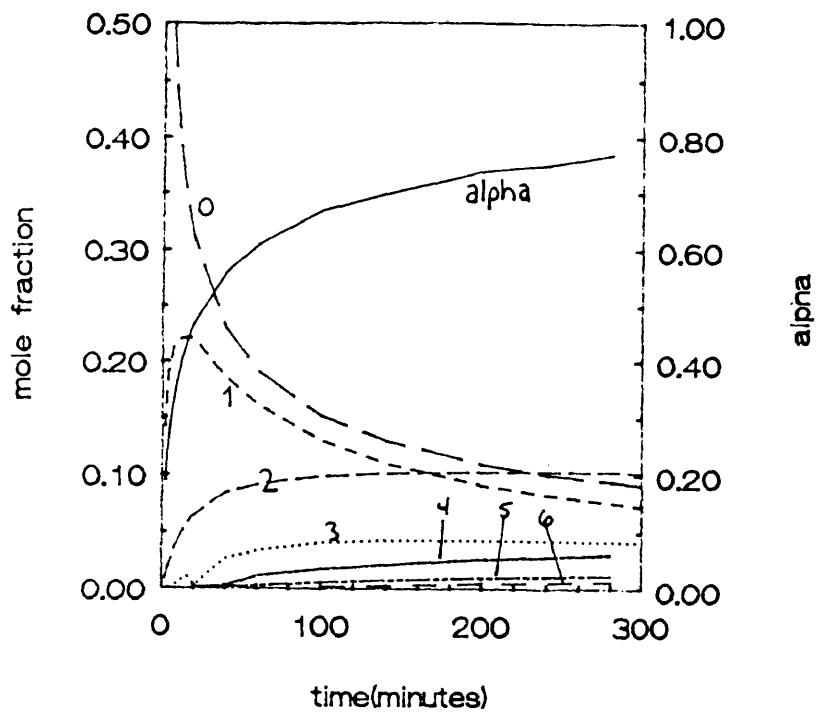


Figure 4.3: PMR-15 imidization simulation at 160°C: chain distribution vs. time.

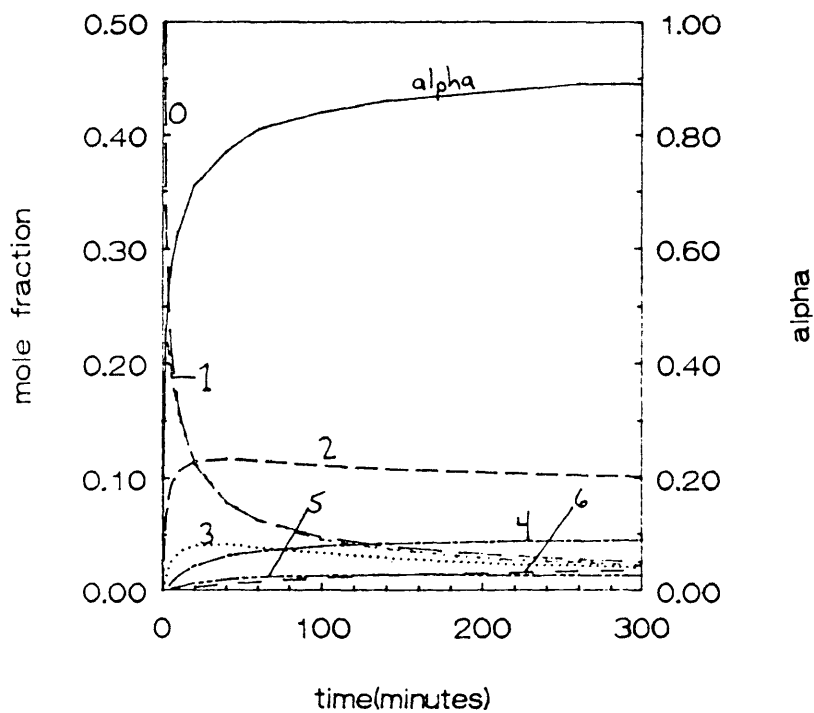


Figure 4.4: PMR-15 imidization simulation at 200°C: chain distribution vs. time.

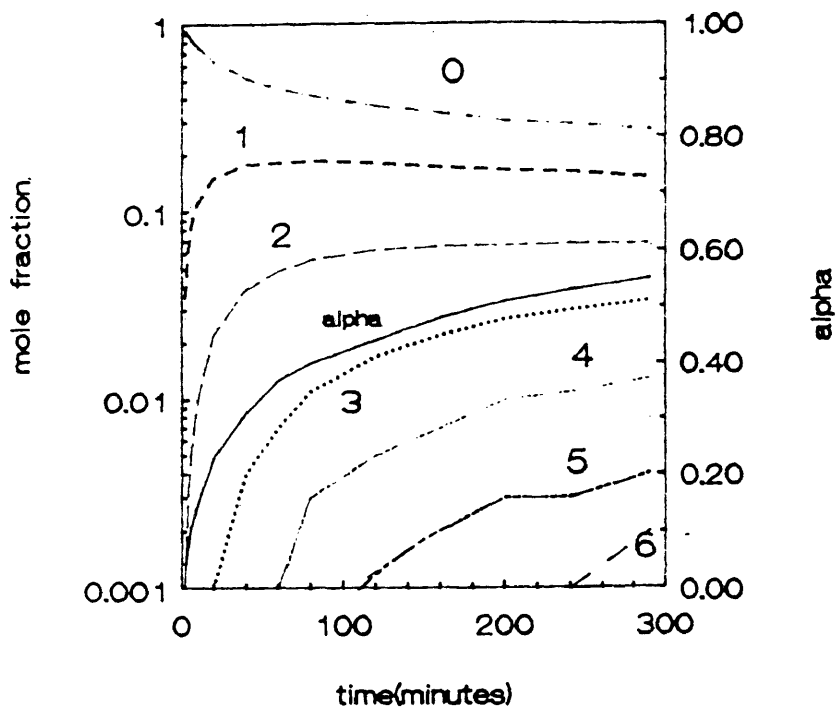


Figure 4.5: PMR-15 imidization simulation at 80°C: chain concentration vs. time.

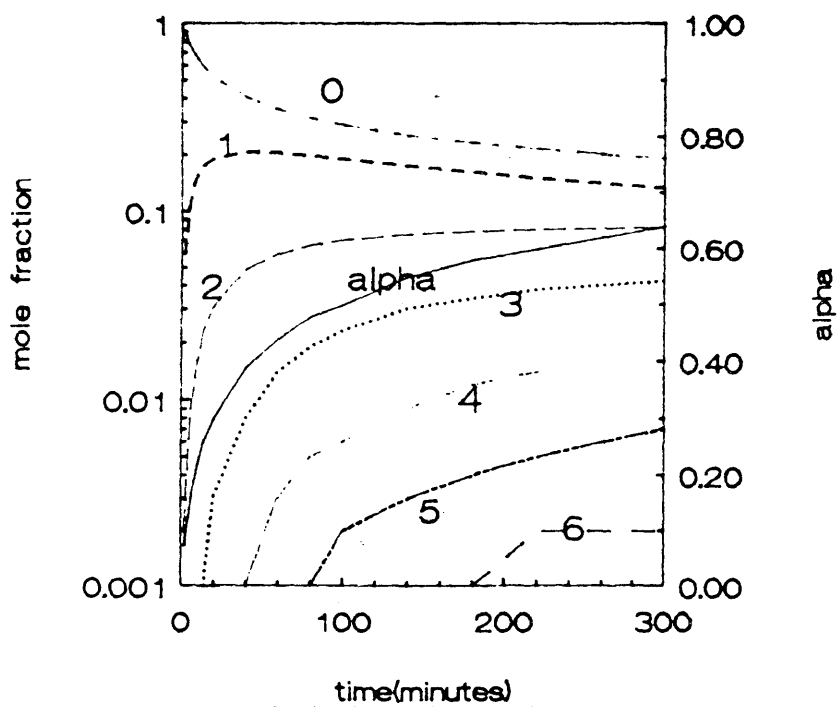


Figure 4.6: PMR-15 imidization simulation at 120°C: chain concentration vs. time.

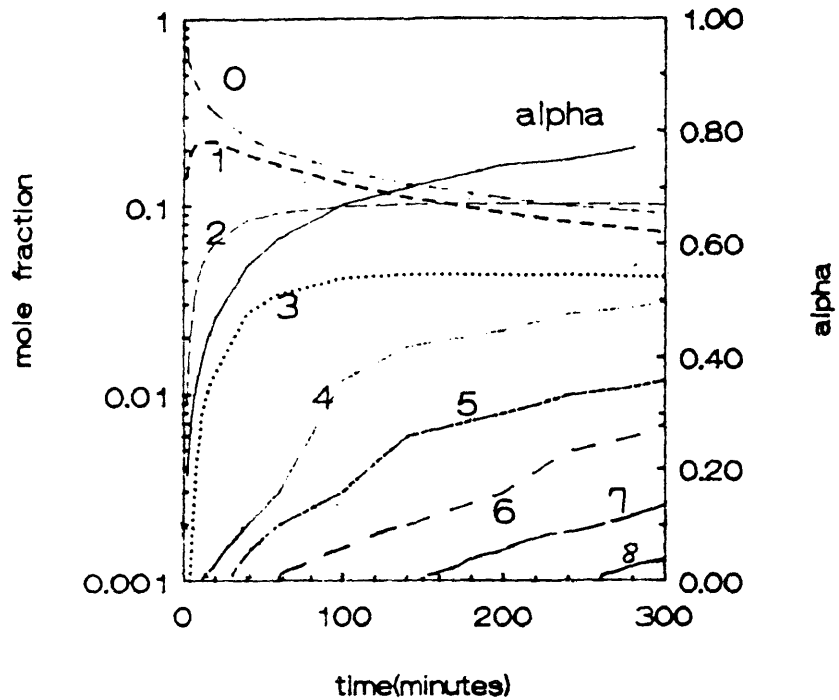


Figure 4.7: PMR-15 imidization simulation at 160°C:
chain concentration vs. time.

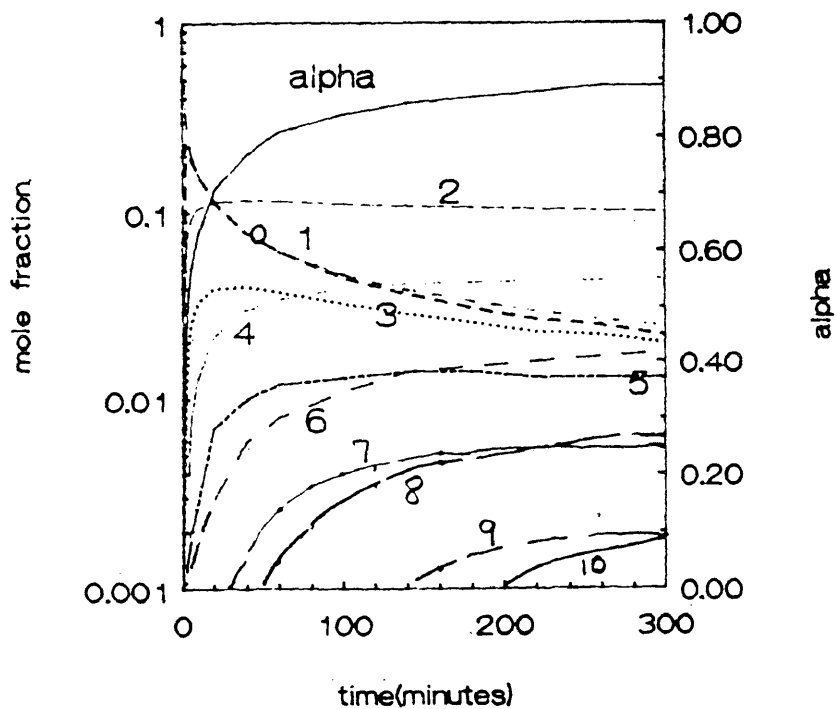


Figure 4.8: PMR-15 imidization simulation vs. time:
chain concentration vs. time.

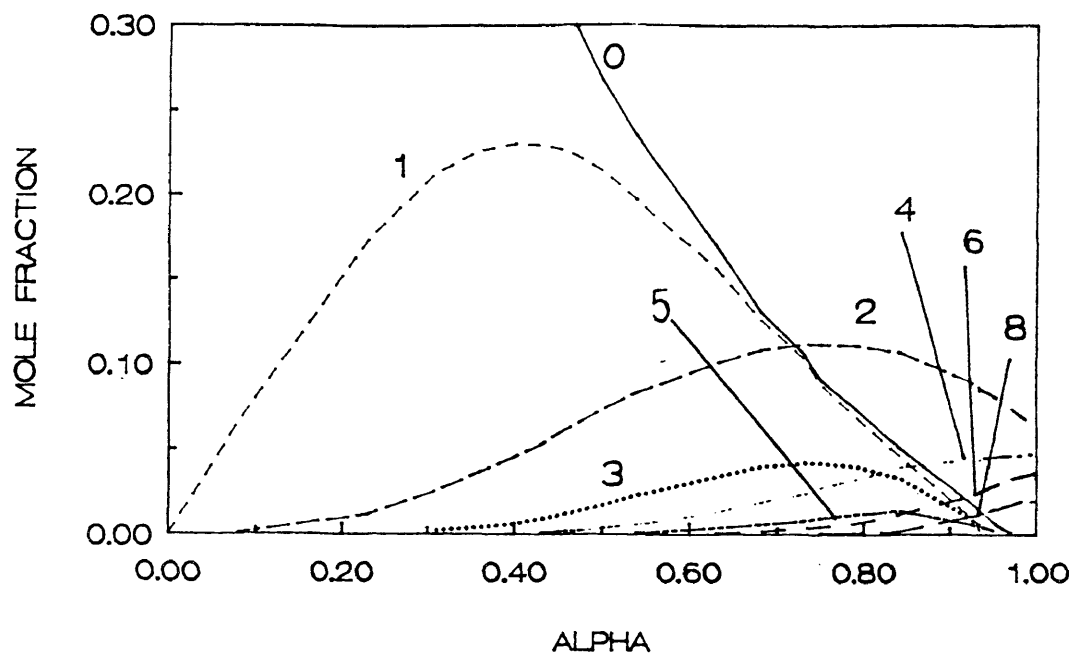


Figure 4.9: PMR-15 chain distribution vs. alpha:
 $k(\text{NE}/\text{MDA}) = 2 * k(\text{BTDE}/\text{MDA})$.

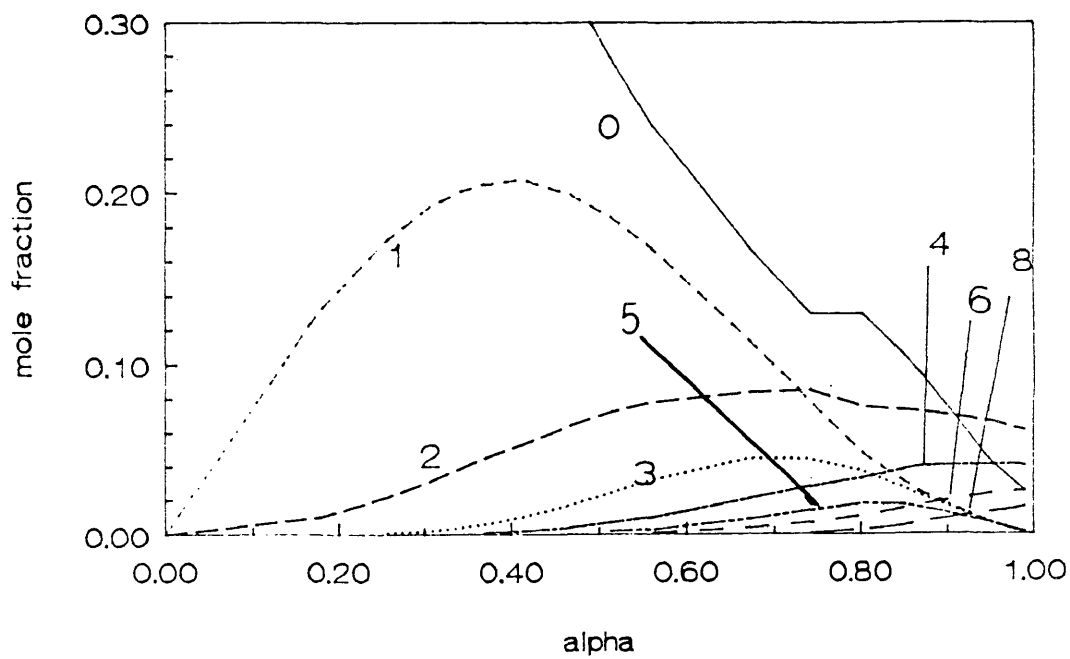


Figure 4.10: PMR-15 chain distribution vs. alpha:
 $k(\text{NE}/\text{MDA}) = k(\text{BTDE}/\text{MDA})$.

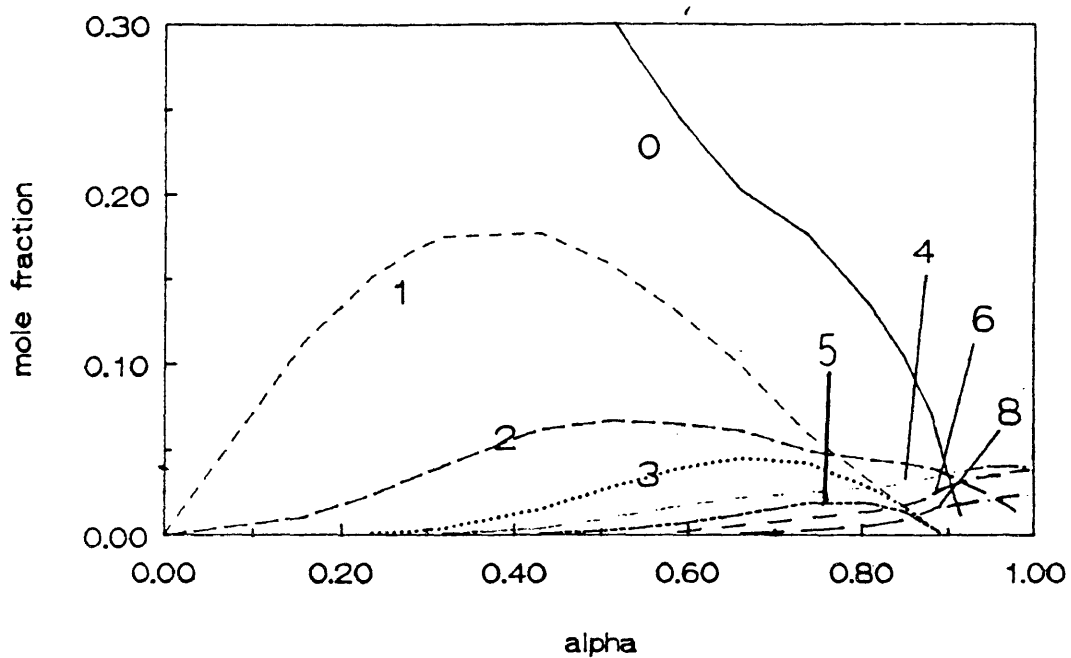


Figure 4.11: PMR-15 chain distribution vs. alpha:
 $2 * k(\text{NE}/\text{MDA}) = k(\text{BTDE}/\text{MDA})$.

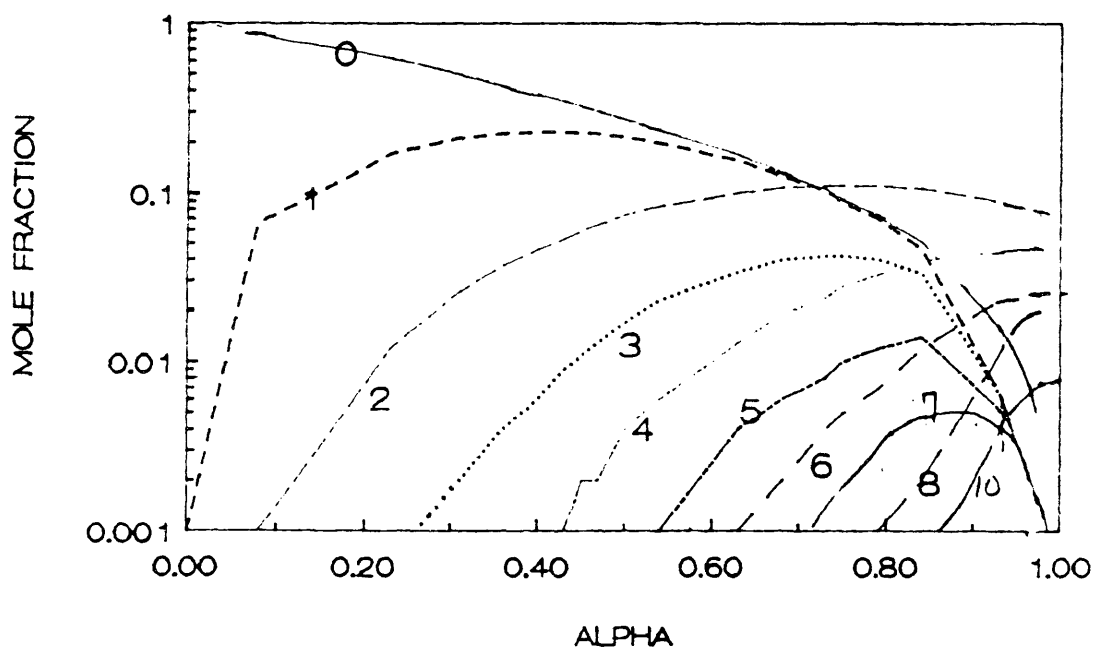


Figure 4.12: PMR-15 chain concentration vs. alpha:
 $k(\text{NE}/\text{MDA}) = 2 * k(\text{BTDE}/\text{MDA})$

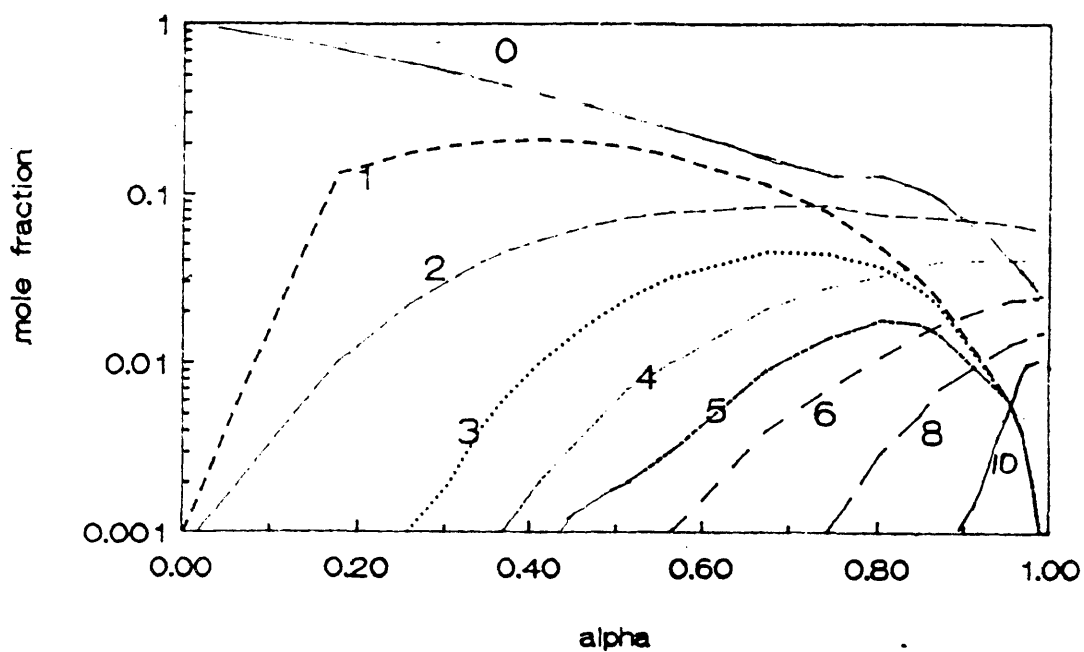


Figure 4.13: PMR-15 chain concentration vs. alpha:
 $k(\text{NE}/\text{MDA}) = k(\text{BTDE}/\text{MDA})$

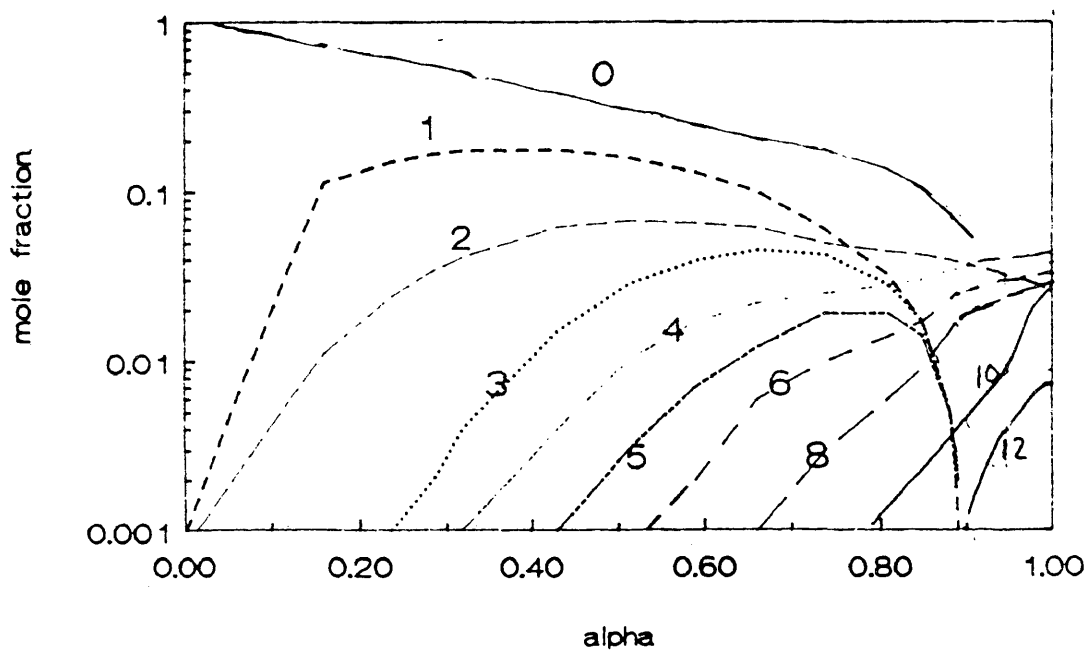


Figure 4.14: PMR-15 chain concentration vs. alpha:
 $2 * k(\text{NE}/\text{MDA}) = k(\text{BTDE}/\text{MDA})$

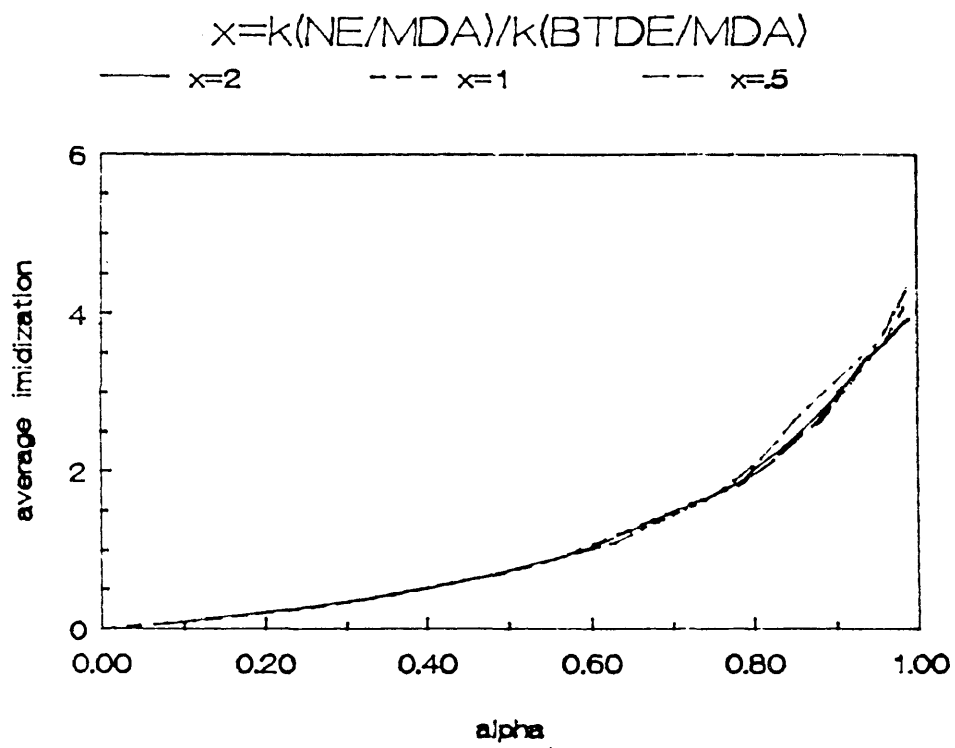


Figure 4.15: PMR-15 average imidization vs. alpha for the three cases.

NOTES FOR CHAPTER IV

1. J. March, Advanced Organic Chemistry, NY, John Wiley and Sons, 1985, 3rd edition.
2. T. C. Bruce and S. M. Felton, J. Am. Chem. Soc., 91, 2799 (1969).
3. R. Clark, Master's Thesis. College of William and Mary, 1989.

PART 2

RHEOLOGICAL STUDY OF THE RELATIONSHIP
BETWEEN THE GLASS TRANSITION
TEMPERATURE AND DEGREE OF CURE IN
TWO EPOXY RESIN SYSTEMS

INTRODUCTION

An important parameter used in the characterization of polymer systems is the glass transition temperature, T_g , the sharp change that occurs in a polymer from the rubbery to the glassy state. T_g can be measured by a variety of methods and the value obtained will to some extent vary according to the technique used and the experimenter's interpretation of the data. We needed a consistent technique to measure the T_g of epoxy resins and rheology proved a relatively simple one.

The resin systems described in this particular study are both bisphenol-A type epoxies - Dow 138/H41 Tactix and Shell 1282/9470 Epon resins. Viscosity measurements were taken with a Rheometrics RDA-700 Dynamic Analyzer used in the parallel plate mode. Dynamic dielectric measurements were made with the DekDyne Type 3 microsensor and a Hewlett-Packard 4192A LF Impedance Analyzer controlled by a HP-9826 computer.

PROCEDURE

1.) A chart of cure time versus alpha was devised for both resins at chosen cure temperatures. Alpha versus time data

for this experiment was drawn from Differential Scanning Calorimetry (DSC) data taken previously by Dr. Kranbuehl.¹ Alpha data for several temperatures was available, and specific cure temperatures to best compromise between shorter run time and accuracy of the cure.

2.) The RDA-700 was used in the parallel plate mode with 12.5 mm radius disposable discs. The rheometer oven chamber was preheated to the cure temperature and equilibrated. After equilibration the oven was opened and the sample applied. The gap between the discs was closed and the oven closed and quickly reheated.

3.) When the time was reached for the desired alpha, the oven was turned off, opened, and allowed to come to room temperature (or a higher temperature if the expected T_g was well above room temperature).

4.) The gap was reset to allow for expansion or shrinkage and it was recorded in the rheometer run program. The sample was ramped at 2°C/minute. Measurements in this case were taken at 1% strain at 20 rads/sec. Figures 5.1 - 5.6 show viscosity versus time data plotted for the Dow Tactix resin and figures 5.7 - 5.14 show those data plotted for the Shell Epon.

Since the particular instrument in Dr. Kranbuehl's laboratory is cooled only by pressurized air, measurements were limited to those glass transitions above room temperature. To measure T_g at alpha = 0, Dynamic Dielectric Analysis (DDA) was performed on freshly mixed resin. The

microsensor was placed in the resin in a test tube and the test tube chilled rapidly in a Dewar flask of liquid nitrogen. The tube was then allowed to come slowly to room temperature while the sensor monitored capacitance and conductance of the resin at frequencies of 500 Hz, 5 kHz, and 50 kHz.

RESULTS AND DISCUSSION

With the viscosity data, we chose T_g to be the point at which a notable drop in viscosity occurs. In Figures 5.1 - 5.14, the first point of viscosity change for each alpha is noted along with its extrapolation to temperature.

The capacitance (C_d) of a material is related to the ionic mobility (e') through the expression

$$e' = C_d/C \quad (1)$$

where C is the capacitance of air.² Figure 5.15 and 5.16 are plots of the ionic mobility and temperature versus time for the Dow resin at frequencies of 500 Hz and 5 kHz and for the Shell resin at 500Hz, 5 kHz and 50 kHz. The initial flat part of the curve is e' at room temperature. The sharp drop to a minimum occurs due to the cooling in liquid nitrogen. With sample warming, e' remains at the flat minimum until T_g is reached, where the sample viscosity begins to decrease thereby increasing ionic and dipolar mobility. T_g was taken to be the temperature where e' first began to increase.

Tables 5a and 5b list the alpha versus T_g results from

the rheological and dielectric measurements.

Table 5a

DOW 138/H41 -Measured T_g's

<u>alpha</u>	<u>T_g(°C)</u>
0	-29
.5	38
.6	43
.7	63
.8	88
.9	118
1.0	138

Table 5b

SHELL 1282/9470 - Measured T_g's

<u>alpha</u>	<u>T_g(°C)</u>
0	-32
.3	32
.4	43
.5	62
.6	78
.7	93
.8	93
.9	112
1.0	153

DiBenedetto's equation, as reported by L.E. Nielsen³, relates the glass transition temperature to the degree of crosslinking in a polymer:

$$\frac{T_g - T_g^{\circ}}{T_g^{\circ}} = \frac{[E_x/E_M - F_x/F_M] X_c}{1 - (1 - F_x/F_M) X_c} \quad (2)$$

where X_c is the mole fraction of crosslinked monomer units in the polymer, E_x/E_M is the ratio of lattice energies for crosslinked and un-crosslinked polymers, and F_x/F_M the ratio of segmental mobilities for the same two polymers.^{3,4,5} T_g is the glass transition temperature in Kelvin at a specific X_c . T_g° is the glass transition temperature of the polymer of same chemical composition as the crosslinked polymer except that there are no crosslinks.^{3,4,5}

X_c may be defined as the ratio of crosslinked polymers to total possible crosslinks in the system. Alpha is the degree of cure in a reaction. Assuming crosslinking to be the

only reaction taking place in the curing of these two epoxy systems, X_c is equal to alpha. We know the glass transition temperatures for each alpha; T_g^0 is simply the T_g at alpha = 0. At alpha = 1, $T_g = T_g^\infty$ and DiBenedetto's equation reduces to

$$\frac{E_x/E_M}{F_x/F_M} = \frac{T_g^\infty}{T_g^0} \quad (3).^4$$

The unknown parameters E_x/E_M and F_x/F_M were found using a nonlinear least square fitting program by SYSTAT. The resultant values for the two parameters are given in Tables 5c.

TABLE 5c

Empirically Determined DiBenedetto Parameters

<u>Resin System</u>	<u>E_x/E_M</u>	<u>F_x/F_M</u>
Dow 138/H41	.946	.558
Shell 1282/9470	2.026	1.191

These average values are used to fit the T_g versus alpha data for the two epoxies to equation 2 (Figures 5.17 and 5.18).

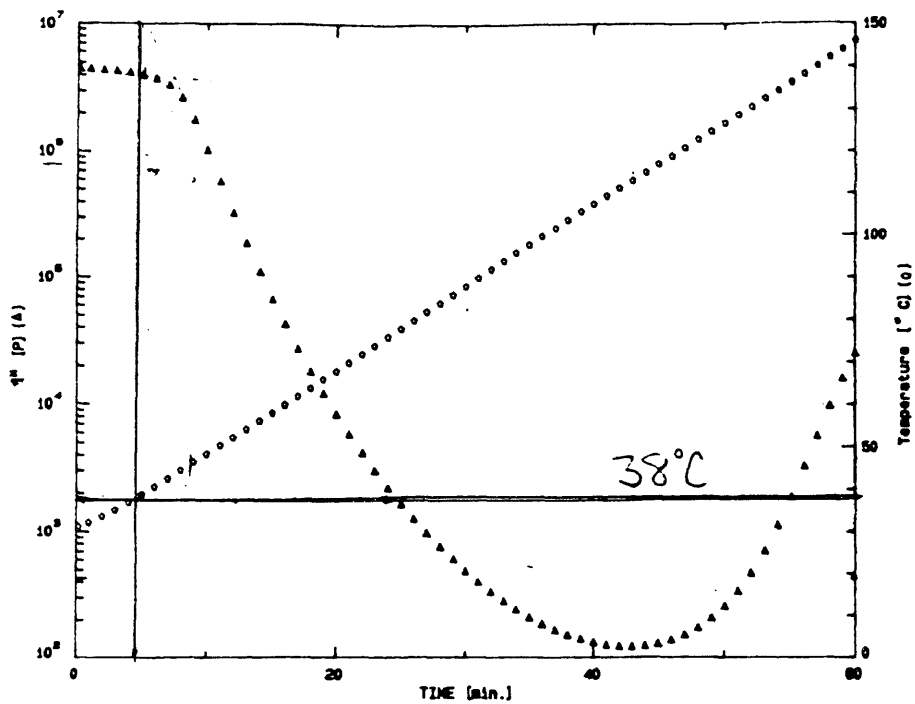


Figure 5.1: Dow at $\alpha = .5$ / viscosity vs. time.

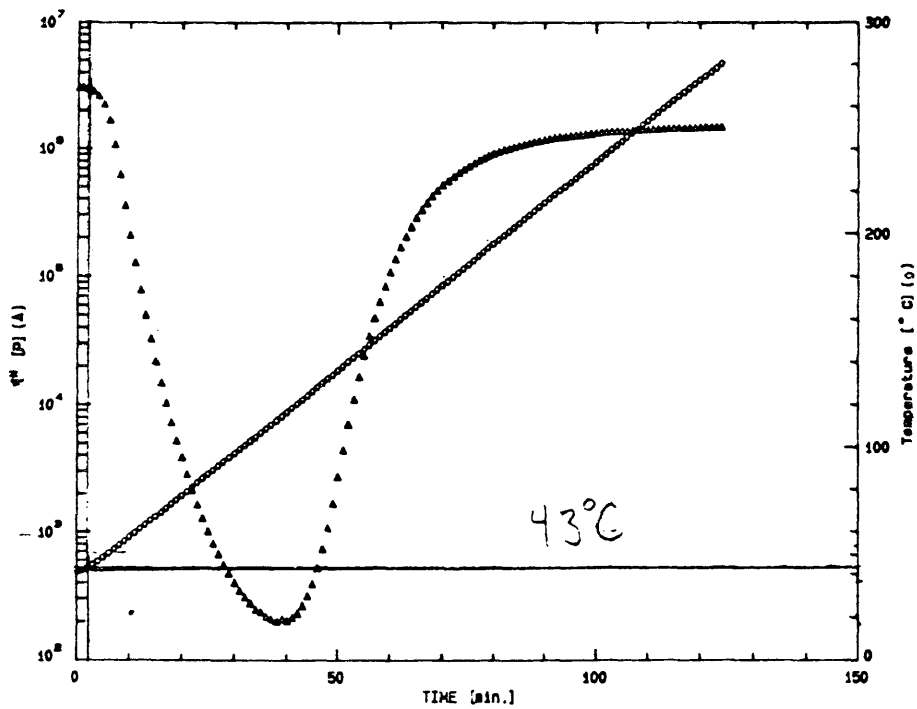


Figure 5.2: Dow at $\alpha = .6$ / viscosity vs. time.

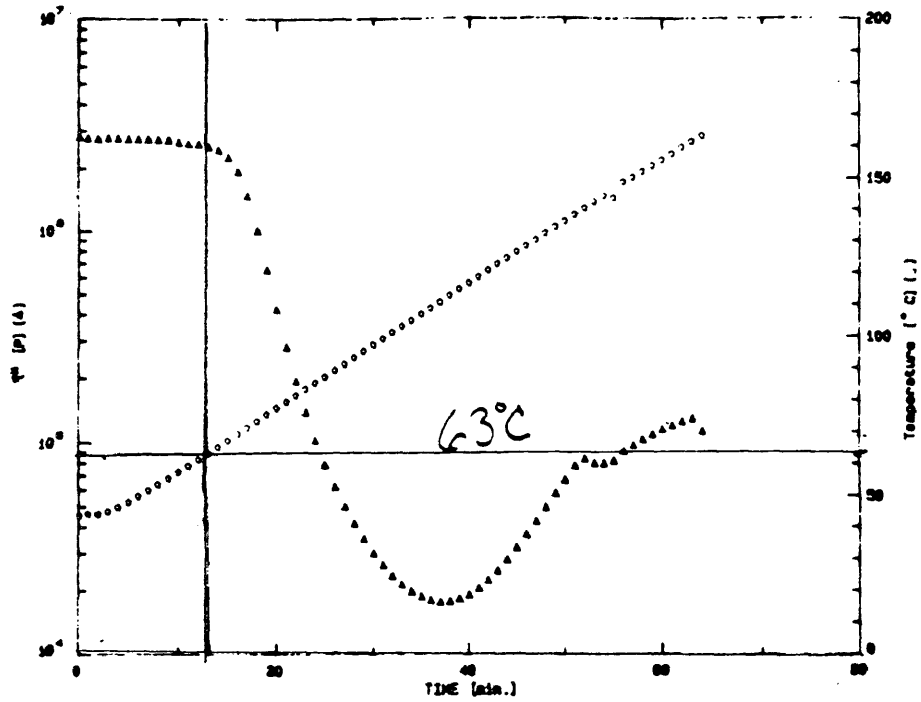


Figure 5.3: Dow at $\alpha = .7$ / viscosity vs. time.

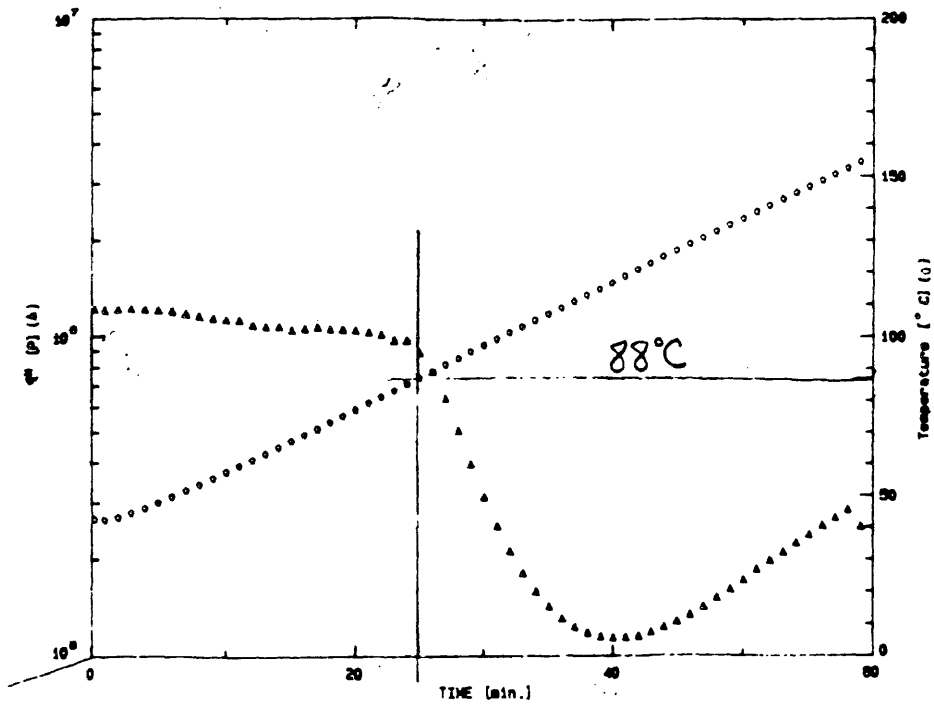


Figure 5.4: Dow at $\alpha = .8$ / viscosity vs. time.

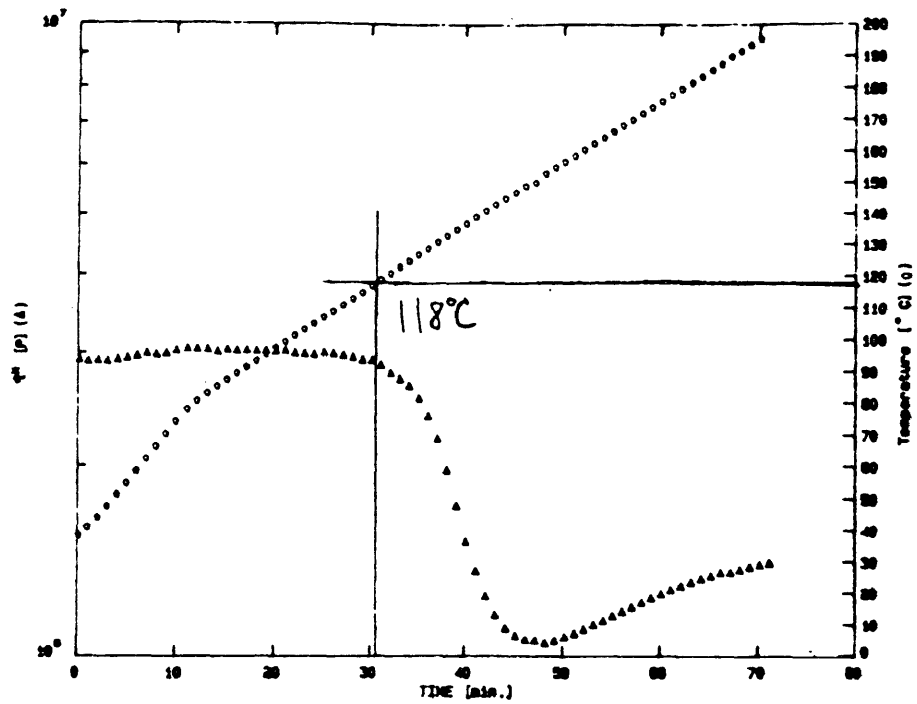


Figure 5.5: Dow at $\alpha = .9$ / viscosity vs. time.

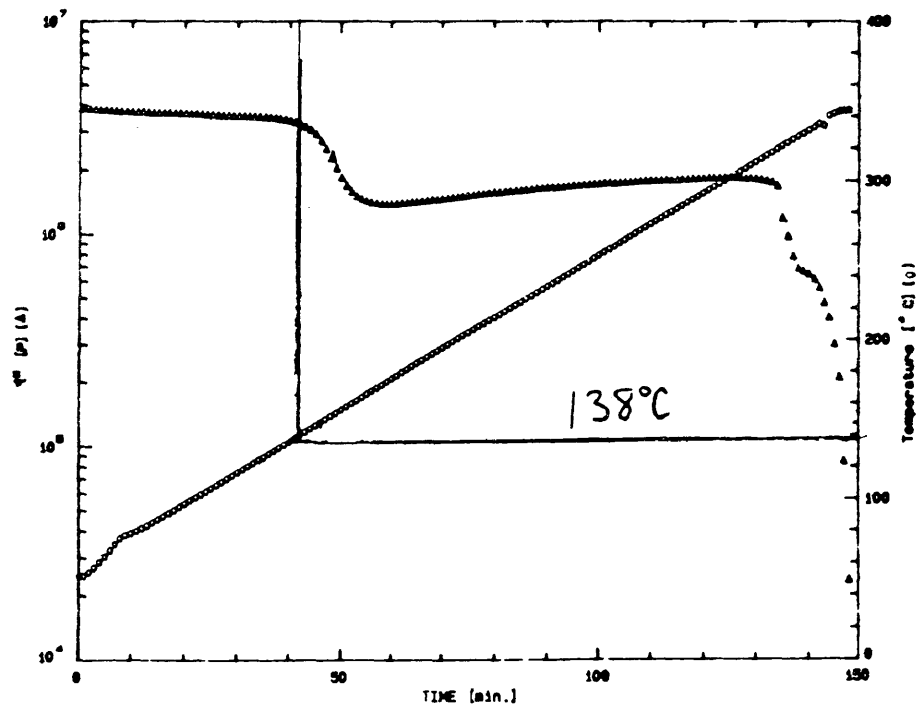


Figure 5.6: Dow at $\alpha = 1$ / viscosity vs. time.

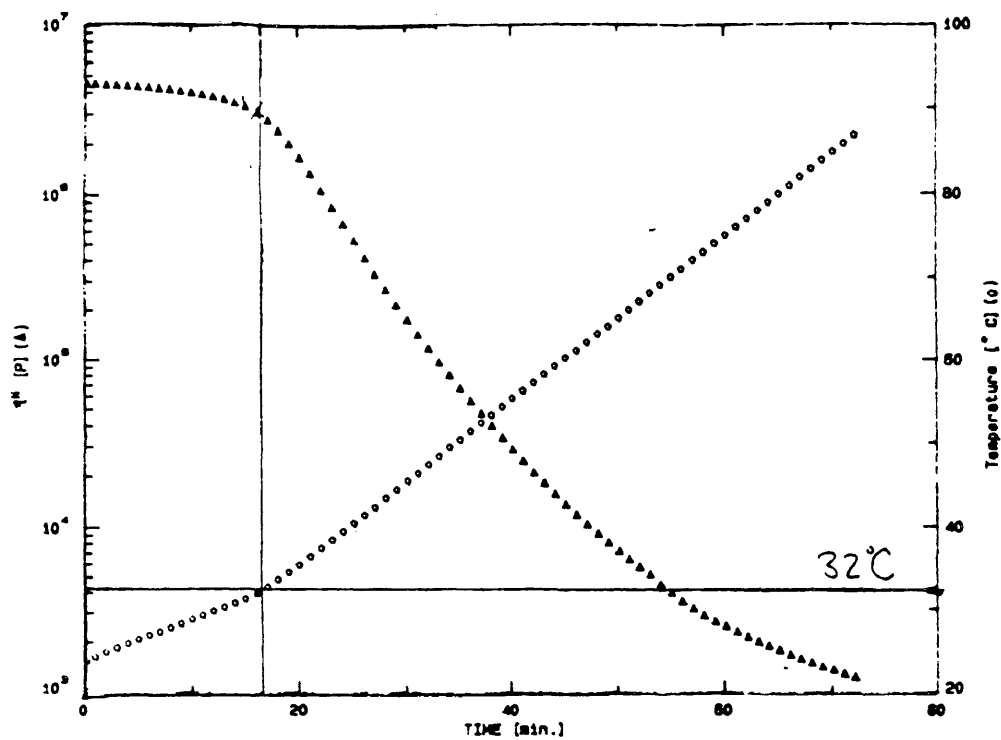


Figure 5.7: Shell at $\alpha = .3$ / viscosity vs. time.

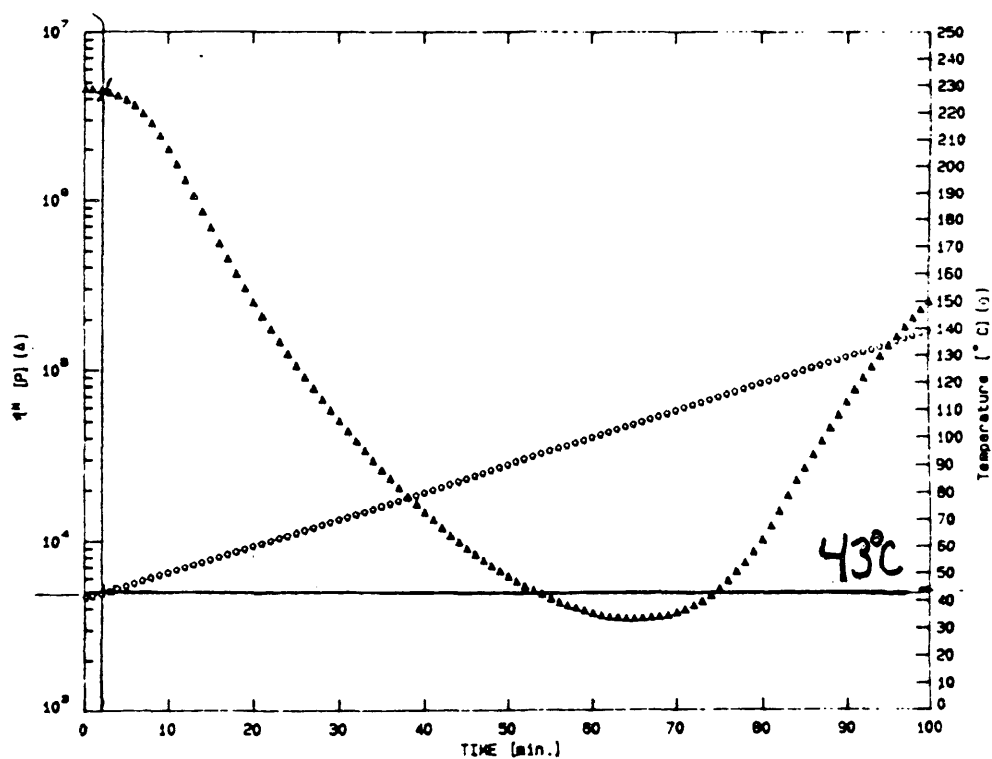


Figure 5.8: Shell at $\alpha = .4$ / viscosity vs. time.

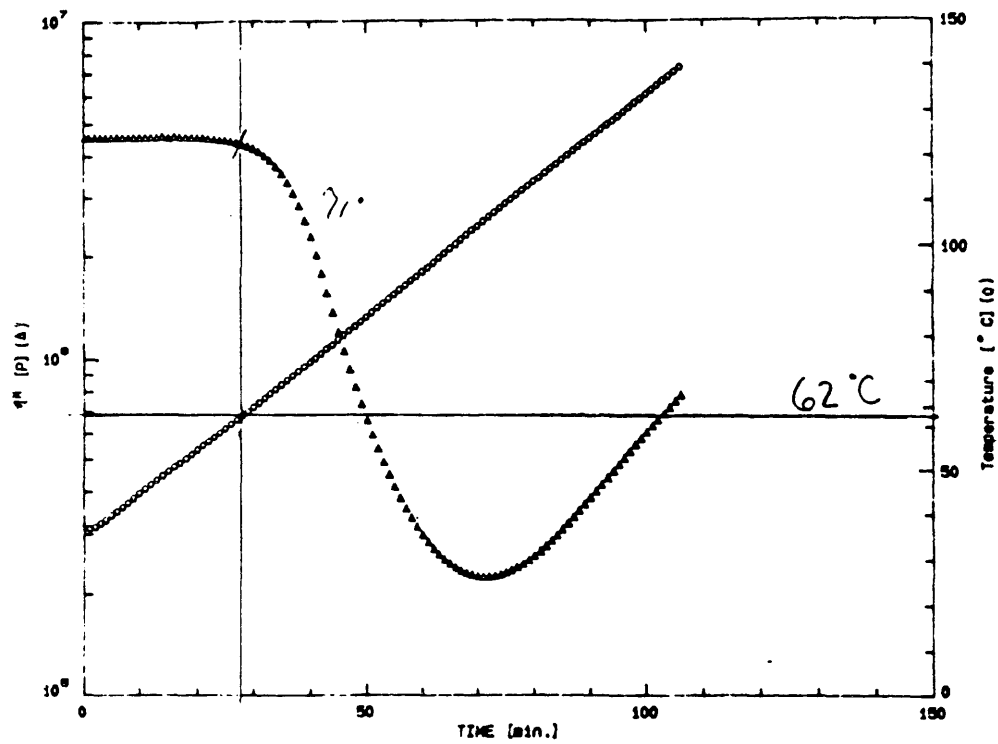


Figure 5.9: Shell at $\alpha = .5$ / viscosity vs. time.

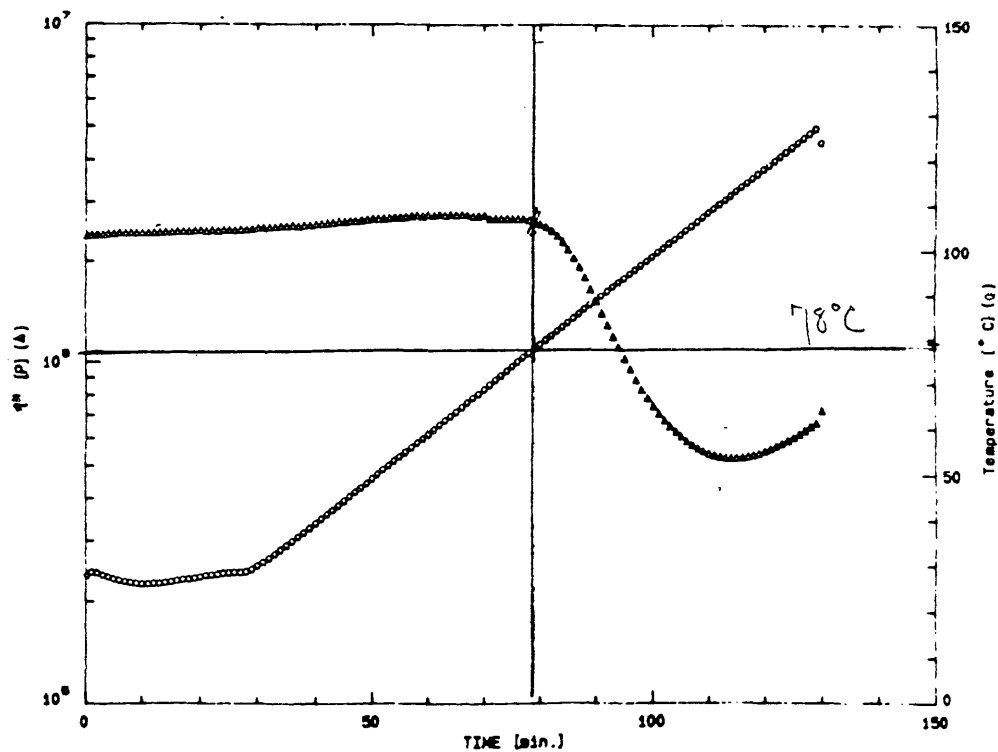


Figure 5.10: Shell at $\alpha = .6$ / viscosity vs. time.

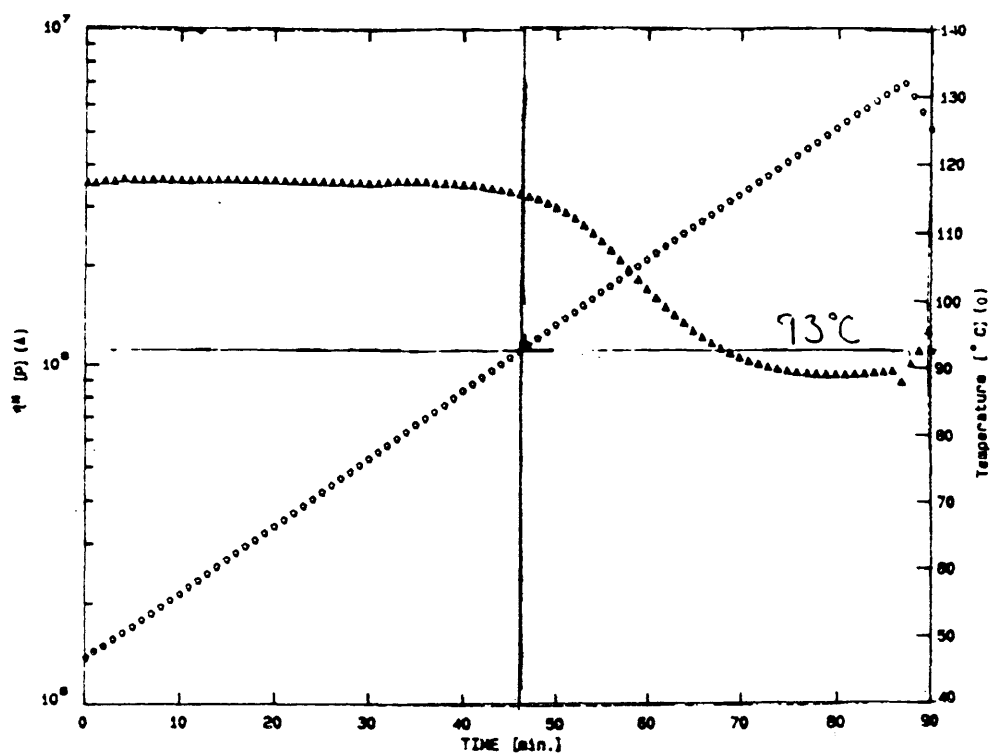


Figure 5.11: Shell at $\alpha = .7$ / viscosity vs. time.

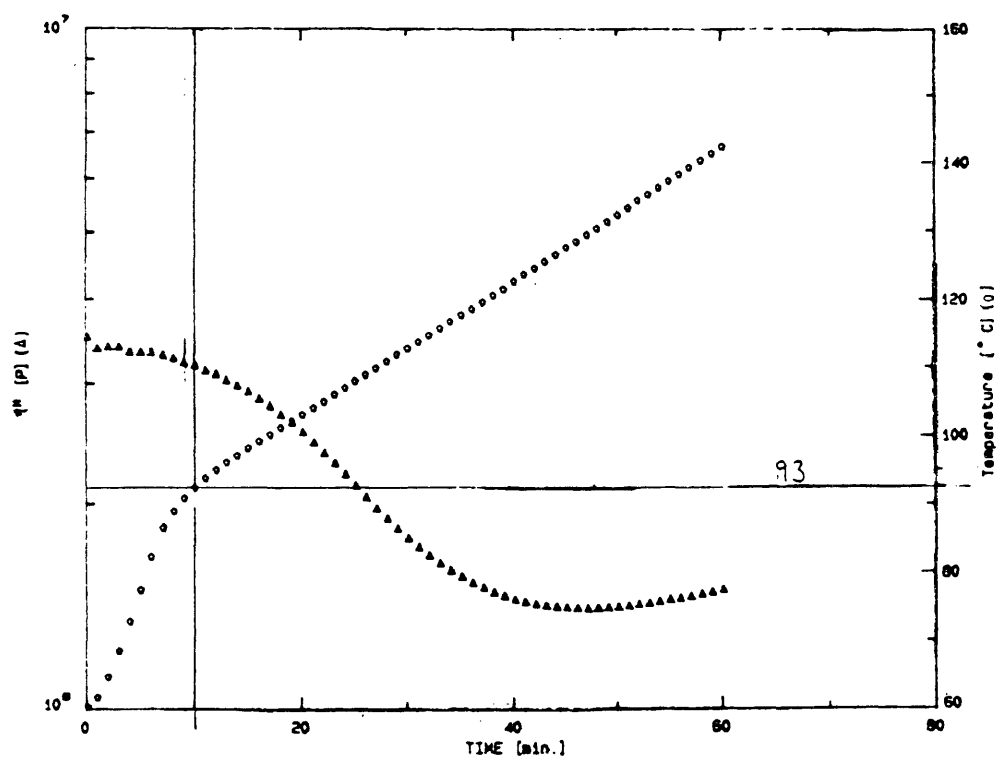


Figure 5.12: Shell at $\alpha = .8$ / viscosity vs. time.

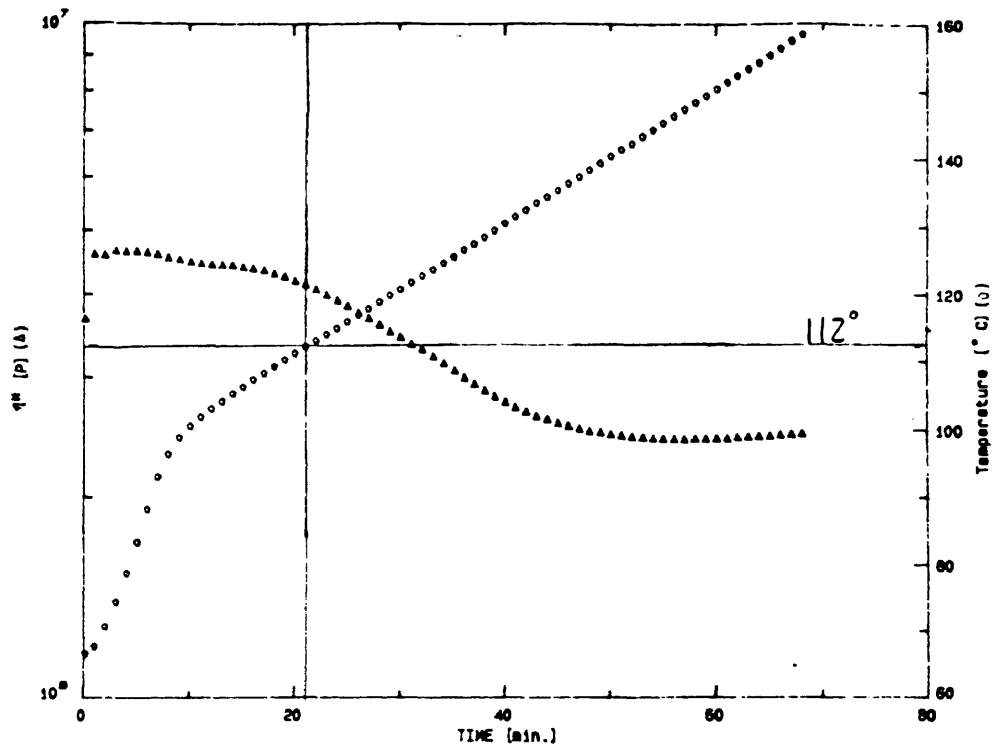


Figure 5.13: Shell at $\alpha = .9$ / viscosity vs. time.

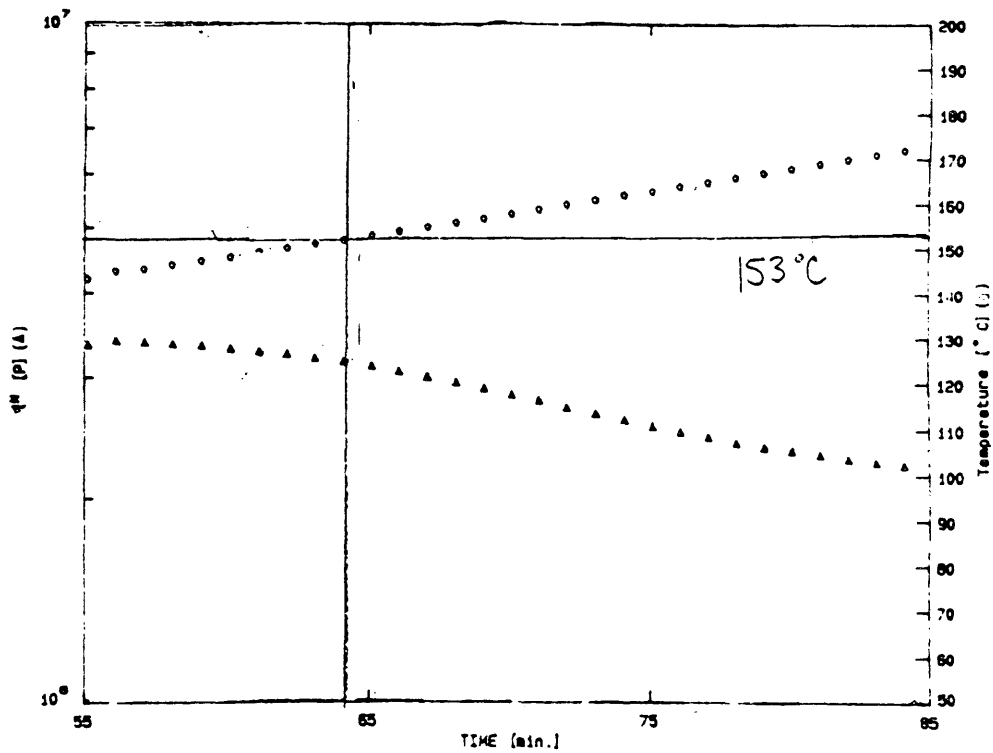


Figure 5.14: Shell at $\alpha = 1$ / viscosity vs. time.

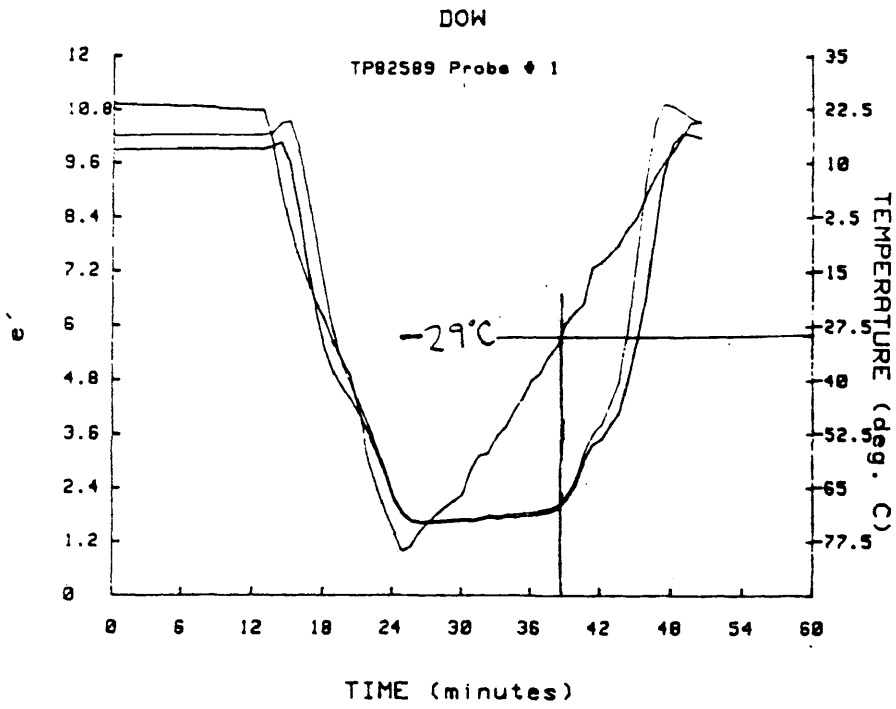


Figure 5.15: Dow at $\alpha = 0 / e'$ vs. time.

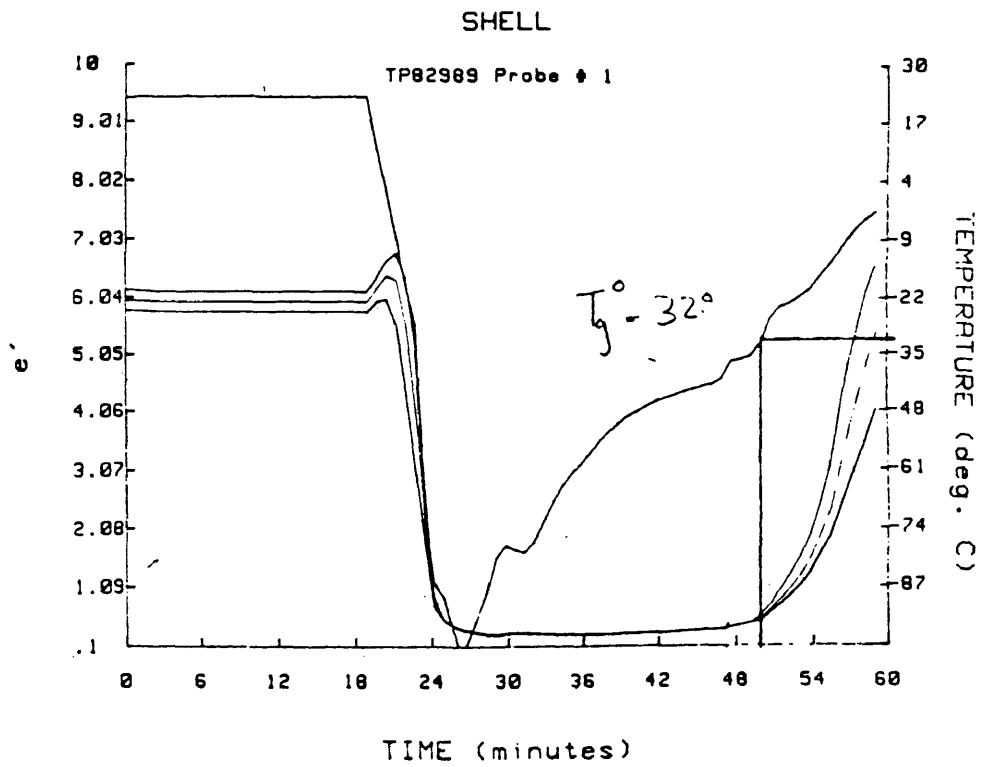
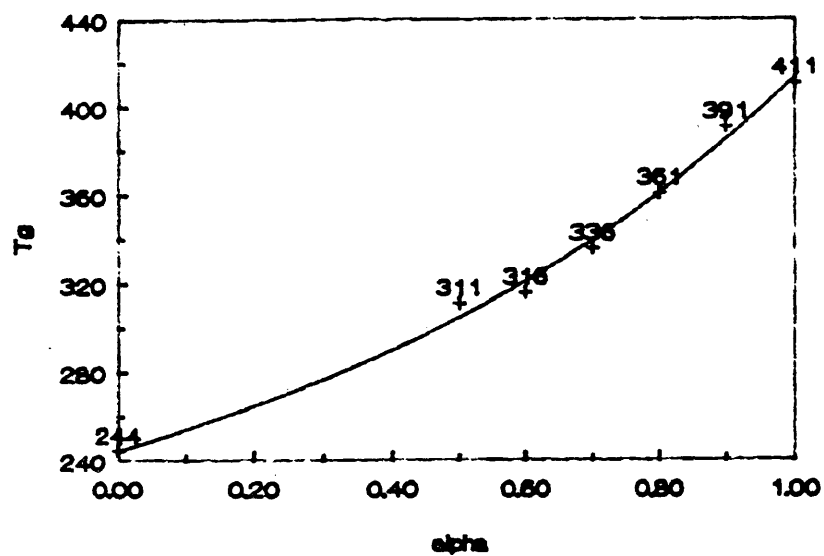
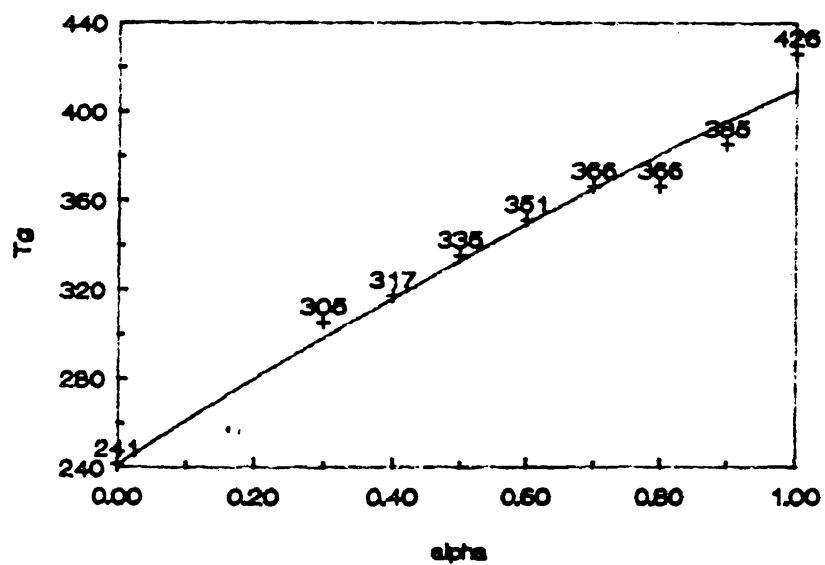


Figure 5.16: Shell at $\alpha = 0 / e'$ vs. time.

Figure 5.17: Dow: T_g vs. α .Figure 5.18: Shell: T_g vs. α .

NOTES FOR PART 2

1. D.E. Kranbuehl, Unpublished Results.
2. D.E. Kranbuehl, "Cure Monitoring", in: S.M. Lee (Ed.), Encyclopedia of Composites, New York: VCH Publishers, 1990.
3. L.E. Nielsen, J. Macromol. Sci., Rev. Macromol. Chem., C3(1), 69 (1969).
4. J.B. Enns and J.K. Gillham, J. Appl. Polym. Sci., 28, 2567, (1983).
5. H.E. Adabbo and R.J.J. Williams, J. Appl. Polym. Sci., 27, 1327 (1982).

THOMAS CLIFTON PRETTYMAN

Born October 5, 1966. Graduated from Seaford Senior High School, Seaford, Delaware, June 1984. Received Bachelor of Science from the College of William and Mary in December 1988. Entered the program for Master of Arts in Chemistry at the College of William and Mary in June 1989.